

University of St Andrews



Full metadata for this thesis is available in
St Andrews Research Repository
at:

<http://research-repository.st-andrews.ac.uk/>

This thesis is protected by original copyright

SYNTHESIS AND CHARACTERISATION OF NOVEL
CROSSLINKABLE POLYIMIDES AS MATRICES FOR
ADVANCED COMPOSITES.

A Thesis presented by William Shaw Dewar to the
University of St.Andrews for the Degree of Master of
Science.

March, 1991.



THE FRED GOSWELL
UNIVERSITY OF CALIFORNIA
LIBRARY

72 A14 15

The book is presented by William Sloan Benson to the
University of California for the Bay Area of Master of
Science.

March 1961



DECLARATION

I William Shaw Dewar hereby certify that this thesis has been composed by myself, that it is a record of my own work, and that it has not been accepted in partial or complete fulfilment of any other degree or professional qualification.

Signed Date27/3/91.....

I hereby certify that the candidate has fulfilled the conditions of the resolution and Regulations appropriate to the Degree of M.Sc.

Signature
of Supervisor Date27.3.91.....

In submitting this thesis to the University of St Andrews I understand that I am giving permission for it to be made available for use in accordance with the regulations of the University Library for the time being in force, subject to any copyright vested in the work not being affected thereby. I also understand that the title and abstract will be published, and that a copy of the work may be made and supplied to any bona fide library or research worker.

ACKNOWLEDGEMENTS

I would like to thank ICI plc for allowing me to undertake this M.Sc. degree, in particular Dr F M Willmouth and Dr P T McGrail.

I would like to thank the following people at ICI Wilton, and at St Andrews University for the valuable help they provided in this thesis:-

Dr M S Chisholm my Industrial Supervisor, providing a source of encouragement and guidance; Dr D M Smith my University Supervisor for his beneficial support especially his guidance on problematic organic reactions and NMR interpretation; Dr B Wilson (ICI) for his advice on norbornene chemistry; Dr R K Mackie (St Andrews University) for his time and effort in helping to interpret complex carbon-13 NMR spectra; Dr P N Standing for his assistance during my stay at St Andrews University.

I wish to thank the following personnel in the Analytical and Spectroscopy Department at both ICI Wilton and St Andrews University for the invaluable service they provided during this thesis: St Andrews University; Melanja Smith (NMR), and Sylvia Smith (TGA and elemental analysis). ICI Wilton; Alan Bunn and his team (NMR), Dr N J Clayden (solid state NMR), Dr J Kendrick (molecular modelling), Steve Quinn (isothermal ageing), and Andrew Broadhurst (DMTA).

CONTENTS

	Page
ABSTRACT	vii
1 INTRODUCTION	1
1.1 Thermosetting polyimides	1
1.1.1 General	1
1.1.2 The development of PMR technology	2
1.1.3 PMR-15 chemistry	6
1.1.4 Composite processing and fabrication	9
1.1.5 RDA crosslinking reaction of norbornene end-capped systems	11
1.1.6 Second generation polyimides: PMR-II	16
1.2 Objectives	18
1.2.1 Background	18
1.2.2 Aims	21
1.2.2.1 Replacement of MDA in PMR polyimides with an alternative long chain diamine.	21
1.2.2.2 Investigation of the PMR-15 polymerisation process	22
2 RESULTS AND DISCUSSION	
2.1 Dibenzoylation of durene	24
2.2 ^1H and ^{13}C NMR Analysis of 1,4-bis(4-aminobenzoyl)-2,3,5,6-tetramethylbenzene (9) and 1,4-bis(3-aminobenzoyl)-2,3,5,6-tetramethylbenzene (10).	26
2.2.1 ^1H NMR analysis of (9)	26

2.2.2	Molecular modelling of (9)	32
2.2.3	^{13}C NMR analysis of (9), (10), (14), (15) and (16)	33
2.2.3.1	^{13}C NMR analysis of (9)	37
2.2.3.2	^{13}C NMR analysis of (10)	40
2.3	^1H NMR analysis of the polyamic acid intermediates and model compounds synthesised in sections 3.5 and 3.6	41
2.3.1	Introduction	41
2.3.2	^1H NMR analysis of the model compounds synthesised in section 3.6	42
2.3.2.1	4,4'-methylenedianiline (MDA)	42
2.3.2.2	1,1'-(methylenedi-4,1-phenylene)-bismaleamic acid	42
2.3.2.3	1,1'-(methylenedi-4,1-phenylene)-bismaleimide (MDA-BMI)	42
2.3.2.4	1,1'-(methylene-4,1-phenylene)-bisnadamic acid	43
2.3.2.5	1,1'-(methylene-4,1-phenylene)-bisnadimide	43
2.3.2.6	(Mixture of) dimethyl esters of 3,3',4,4'-benzophenone-tetracarboxylic acid (BTDE)	44
2.3.2.7	Endo-5-norbornene-2,3-dicarboxylic anhydride	45
2.3.2.8	Exo-5-norbornene-2,3-dicarboxylic anhydride	45
2.3.3	^1H NMR analysis of the polyamic acid intermediates synthesised in section 3.5.	46
2.3.3.1	PAM-1 and PAM-2	46
2.3.3.2	PIN-1 (a) and PIN-2 (a) polyamic acids	53
2.3.3.3	PIN-1 and PIN-3 polyamic acids	60

2.3.4	¹ H NMR polymer interpretation summary	64
2.3.5	Number average molar mass (M _n) calculated by NMR spectroscopy	65
2.4	Thermal analysis of the imidised polymers fabricated in Section 3	69
2.4.1	Introduction	69
2.4.2	Isothermal ageing results	70
2.4.3	Thermogravimetric analysis (TGA) results	74
2.4.4	Dynamic mechanical thermal analysis (DMTA) results	79
3	EXPERIMENTAL	83
3.1	Abbreviations of monomers	83
3.2	Synthesis of (14) and (15) by Friedel-Crafts diacylation of durene	83
3.2.1	1,4-bis(4-nitrobenzoyl)-2,3,5,6-tetramethylbenzene (14)	84
3.2.2	1,4-bis(3-nitrobenzoyl)-2,3,5,6-tetramethylbenzene (15)	85
3.3	Reduction of the nitro groups in (14) and (15)	87
3.3.1	1,4-bis(4-aminobenzoyl)-2,3,5,6-tetramethylbenzene (9)	88
3.3.2	1,4-bis(3-aminobenzoyl)-2,3,5,6-tetramethylbenzene (10)	89
3.4	1,4-bis(4-maleimidobenzoyl)-2,3,5,6-tetramethylbenzene (16)	90
3.5	Polymer synthesis	92
3.5.1	PMR-15 control	94
3.5.2	Synthesis of PIN-1 formulated from the respective anhydrides	94
3.5.3	Synthesis of PIN-1(a) from PAM-1 by a Diels-Alder reaction with cyclopentadiene	95

3.5.4	Polymer fabrication	96
3.6	Model compound synthesis	97
3.6.1	1,1'-(methylene-4,1-phenylene)-bisnadidic acid	97
3.6.2	3,3',4,4'-benzophenonetetracarboxylic acid dimethyl ester	98
3.6.3	5-norbornene-2,3-dicarboxylic acid monomethyl ester	98
3.6.4	1,1'-(methylene-4,1-phenylene)-bisnadimide	99
3.6.5	1,1'-(methylenedi-4,1-phenylene)-bismaleamic acid	100
3.7	Techniques used for polymer characterisation	101
3.7.1	Thermal analysis	101
3.7.1.1	Isothermal ageing	101
3.7.1.1.1	Isothermal ageing conditions	101
3.7.1.2	Thermogravimetric analysis (TGA)	101
3.7.1.2.1	Thermogravimetric analysis conditions	102
3.7.1.3	Glass transition point (T _g) evaluation by dynamic mechanical thermal analysis (DMTA)	102
3.7.1.3.1	DMTA run conditions	102
3.7.2.1	Solution NMR	103
3.7.2.2	Solid state NMR	103
3.7.3	FTIR analysis	103
3.7.4	Differential scanning calorimetry (DSC)	103
3.8	Molecular Modelling	104
4	CONCLUSIONS	105
5	REFERENCES	109
6	APPENDICES	

ABSTRACT

The current commercial thermoset of choice for 315°C continuous use temperature applications is PMR-15, a norbornene functionalised polyimide with a formulated molecular weight (FMW) of 1500, which can be crosslinked to form a high glass transition temperature composite matrix. Developed by NASA in the late 1960s, PMR technology gave a breakthrough in terms of coupling high temperature resistance and relative ease of processing. However this technology has some major drawbacks; microcracking of PMR laminates occurs during the thermal cycling undergone by jet engines; PMR laminates are brittle in the cured state; conventional PMR prepreg contains free methylenedianiline (MDA), a potent liver toxin and suspected human carcinogen; and the batch-to-batch variability of PMR-15 resin.

This study describes: (a) the synthesis and characterisation of two diamines, 1,4-bis(4-aminobenzoyl)-2,3,5,6-tetramethylbenzene (9) and 1,4-bis(3-aminobenzoyl)-2,3,5,6-tetramethylbenzene (10), as well as (b) their incorporation into the PMR system, and the thermal properties of the resultant cross-linked polymers analysed. An investigation of the PMR-15 polymerisation process by ¹HNMR is also presented so that a consistent product can be produced from a specified polymerisation technique. ¹HNMR analysis of (9) suggests there is an electronic interaction between the amino and keto groups resulting in restricted rotation about the amine ring-to-carbonyl carbon single bond. Furthermore, ¹³CNMR evidence indicates that (9) and (10) may exist as cis and trans conformers at high temperatures.

Thermal-analysis techniques have shown that the PMR polyimides prepared from diamines (9) and (10) have inferior thermal oxidative stability to the MDA containing PMR polyimides.

The norbornene end-cap was revealed by $^1\text{HNMR}$ analysis of the polyamic acids to exist in both exo and endo isomeric forms. $^1\text{HNMR}$ also detected low levels of amine ends in the PMR polyamic acids.

Overall, 5-norbornene-2,3-dicarboxylic acid anhydride (nadic anhydride) utilised as the end-cap in the standard PMR formulation was found to be an effective end-capper, and under closely controlled reaction conditions this gave a polymer molecular weight close to its FMW and end-capped to a high degree.

1 INTRODUCTION

1.1 Thermosetting polyimides

1.1.1 General

The current commercial thermoset of choice for 315°C continuous use temperature applications is PMR-15 (in-situ Polymerisation of Monomer Reactants), a cross linkable norbornene functionalised polyimide with a formulated molecular weight (FMW) of 1500, developed by NASA in the late 1960s. Up until this time many other high temperature polymer systems had been developed but all had the crucial deficiency of being very difficult to process by conventional means.¹ PMR technology gave a breakthrough in terms of coupling high temperature resistance and relative ease of processing which had not been achieved before.

Composites based on thermosetting polyimide matrices are used primarily in the aerospace industry. For example, PMR-15 is employed in the fabrication of the US Navy F404 jet engine duct which had previously been made of titanium.² The main reason for attempting to replace metals with polymer composites in the aerospace industry is the saving in weight which can be achieved by the utilisation of these materials. This can lead to lower operational costs from using less fuel. For example, it is believed that 1kg of weight saved from a Boeing 747 is worth approximately \$450^{Per flight} in reduced fuel costs while 1kg saved on the

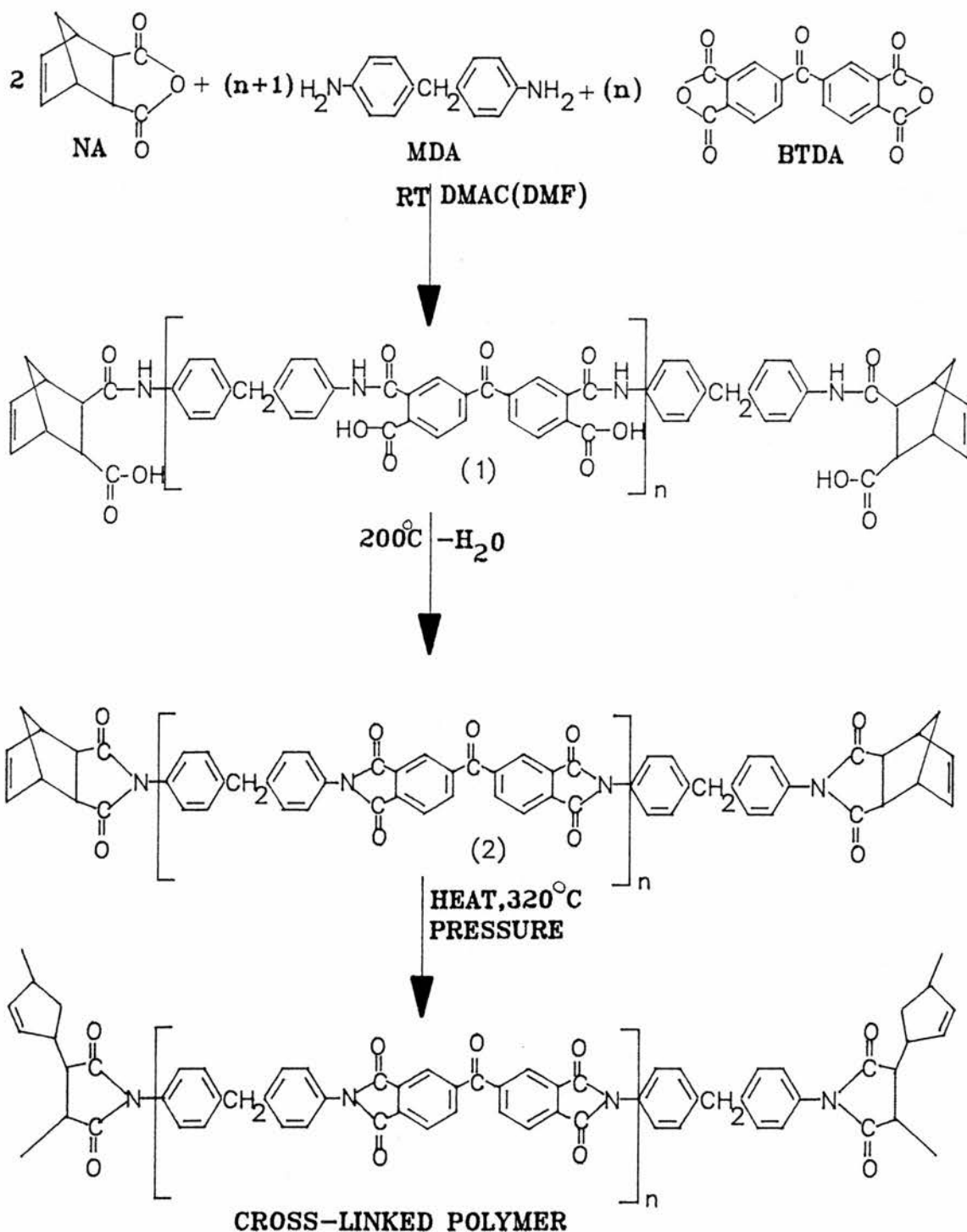
space shuttle is worth about \$30,000³. Additional weight savings are made on the body of the plane when composites are utilised in the engine as this gives a lighter engine, and it therefore needs less weight to support it.

Not only are composite materials less dense than the metals they replace, they have both a high stiffness-to-weight ratio and a high strength-to-weight ratio, making them highly desirable compared with metals. The reasons outlined above constitute the main driving force for the development of high performance composites.

1.1.2 The development of PMR technology

The benefits associated with high performance matrices were not immediately realised because of the processing difficulties associated with highly thermally stable aromatic polymers. It was not until the late 1960s that NASA developed a highly thermally stable polyimide which could be relatively easily processed : a low molecular weight norbornene-terminated polyamic acid which was applied to carbon fibres, most commonly from dimethylacetamide or dimethylformamide solution, by a solution prepregging process. The solvent is then evaporated and the polyamic acid imidised by the application of heat (200°C) into a thermally stable polyimide prepolymer^{3,4}. This is followed by the final stage of fabrication of the composite from the fully imidised prepreg by crosslinking the norbornene end-cap at elevated temperature and pressure. This technology represented a breakthrough in that the evolution of

volatiles, such as methanol or water resulting from condensation reactions, occurs before fabrication of the composite is complete thus giving a void-free composite. From Scheme 1 it can be seen that this polymer system uses three monomers; a diamine, a dianhydride, and 5-norbornene-2,3-dicarboxylic anhydride ("nadic anhydride") end-cap.



when n=2.087 then FMW =1500

Scheme 1

When $n = 1.67$, the FMW is approximately 1300, and this prepolymer thus became known as P13N⁴. P13N was a commercial system and was sold as a polyamic acid solution in dimethylformamide or N-methylpyrrolidone. The prepolymer imide formed from the polyamic acid, when melted at 200°-250°C, exhibited good melt flow characteristics, thus enabling the carbon fibres to be fully wetted and facilitating the development of well consolidated laminates.

The good melt flow characteristics, coupled with the fact that no volatiles were released during fabrication of the composite, was seen to represent a breakthrough in the area of processable thermally stable polyimides. However, in spite of this, these early systems were found to have some serious shortcomings:-

- (1) The use of high-boiling solvents such as dimethylacetamide, dimethylformamide or N-methylpyrrolidone in preparation of the polyamic-acid solution led to problems in removing the final traces of these solvents which, if left in the prepreg, resulted in voids forming in the composite laminate. Voids cause a reduction in composite strength and are thus undesirable.
- (2) Once the solvent was removed from the fully imidised prepreg, the latter lacked both tack (the ability of prepreg to stick together), and drape (the ability of prepreg to bend without springing back), both of which are serious drawbacks when attempting to fabricate complex shapes.

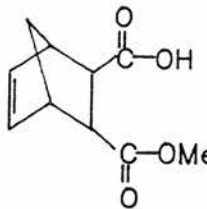
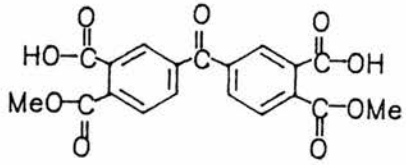
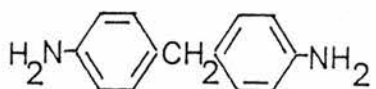
In an attempt to overcome these serious shortcomings NASA undertook further research which resulted in the production of PMR-15.³⁻⁶

1.1.3 PMR-15 chemistry

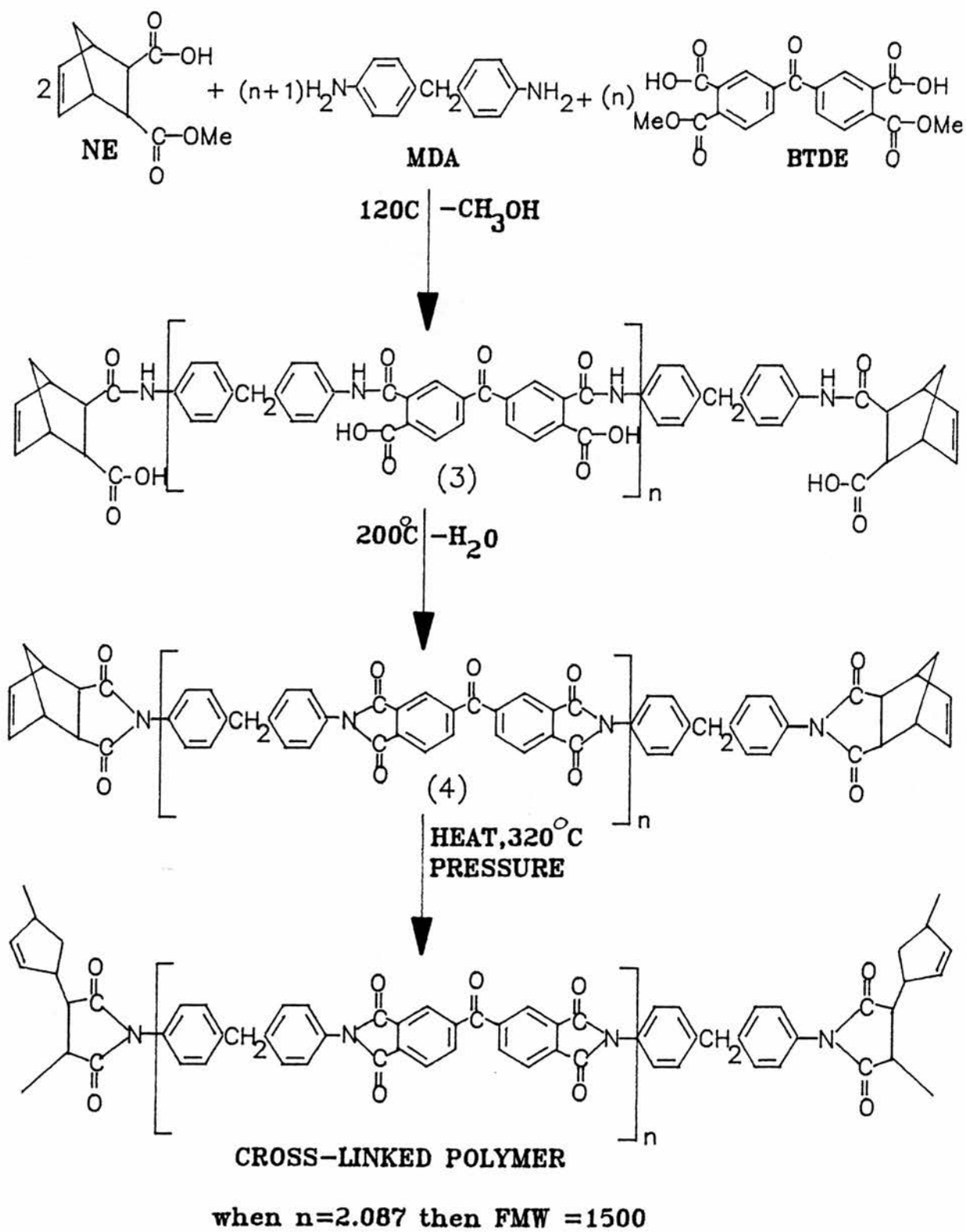
Instead of reacting an aromatic diamine with an aromatic dianhydride (and 5-norbornene-2,3-dicarboxylic anhydride as the end-cap) this approach involves the reaction of an aromatic diamine with the dialkyl ester of an aromatic dicarboxylic acid, as illustrated in Table A.⁶⁻¹⁰

Table A

Monomers utilised in the synthesis of PMR-15.

STRUCTURE	MONOMER NAME
	Monomethyl ester of 5-norbornene-2,3-dicarboxylic acid (NE)
	Dimethyl ester ^{of} 3,3', 4,4'-benzophenonetetracarboxylic acid (BTDE)
	4,4'-Methylenedianiline (MDA)

The monomers in Table A undergo firstly an amidisation followed by imidisation to form a low molecular weight prepolymer, but then importantly, these prepolymers on application of heat (<250°C) and pressure undergo a reverse Diels-Alder (RDA) reaction through the end-cap, followed by addition polymerisation of the resultant unsaturated species, leading to highly thermally stable crosslinked polyimides. As a consequence these polyimides are known as RDA addition polyimides as opposed to condensation polyimides. A generalised reaction scheme of the synthetic route to PMR-15 is given in Scheme 2.



Scheme 2

1.1.4 Composite processing and fabrication

Thermal oxidatively stable composites are processed by impregnating carbon fibres with a methanol solution containing NE, MDA and BTDE with the stoichiometry outlined in Scheme 2 (This stoichiometry was found to give the best compromise between processing characteristics, such as the viscosity of the prepolymer, and thermal oxidative stability¹¹). The methanol on the prepreg is then evaporated to approximately 10% w/w¹². This level allows the prepreg to have tack and drape which are essential when constructing laminates of complex shape. Laminates are then fabricated by stacking the prepreg pieces into piles, and heating to >200°C to form the norbornene end-capped imide prepolymer on the fibre by in-situ cyclodehydration. The final step involves the application of pressure at a temperature of 320°C resulting in an irreversible reaction of the norbornene end-cap, to give the final crosslinked matrix.

This process of fabrication has advantages over previous systems in several respects:

- (1) The use of low-boiling alcohol solvents enables the last traces of residual solvent to be removed, which is essential when attempting to fabricate void-free laminates.
- (2) The methanol solution containing the ester-acids as the prepregging solution was found to have a longer

"shelf-life" than the corresponding amic acid prepolymer solution (synthesised from the anhydrides).

This phenomenon was attributed to hydrolytic degradation of the polymer chain in solution with time, lowering the solution viscosity^{5,13}. This longer "shelf-life" in turn has meant that prepreg solutions containing 60% w/w solids can be utilised^{3,5,14}, which reduces the number of passes that the fibre has to make through the monomer solution to pick up the required weight of solids. The use of methanol solution instead of a prepolymer solution in an aprotic solvent also results in better wetting of the fibres due to the lower viscosity of the solution.

Most of the high temperature (>300°C) systems produced before the development of PMR technology were impossible to process because the thermal transitions of such polymers are too close together. That is the melting point of the polymer is too close to its decomposition point, or the polymer decomposes before it reaches its melting point. However this is not the case with PMR systems as the thermal transitions are well spaced. Differential scanning calorimetry (DSC) analysis of the monomeric PMR-15 mixture reveals four well defined thermal transitions⁶:

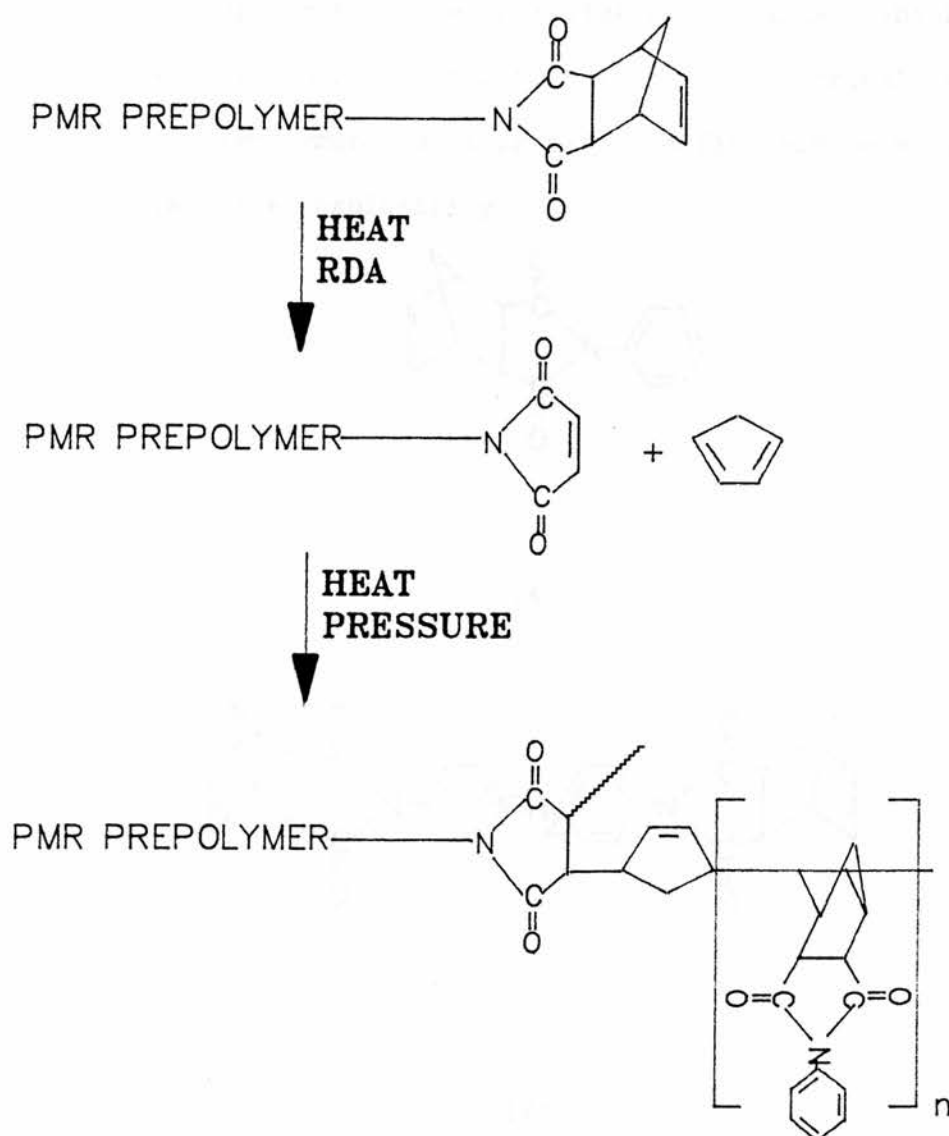
- (1) Melting of the monomer reactant mixture below 100°C.
- (2) Reaction of the monomers at approximately 140°C.

- (3) Melting of the norbornene-ended prepolymer in the range 175°-250°C.
- (4) RDA crosslinking reaction at 340°C.

Hence PMR systems can be relatively easily processed by either compression moulding or by autoclave techniques.

1.1.5 RDA crosslinking reaction of norbornene end-capped systems

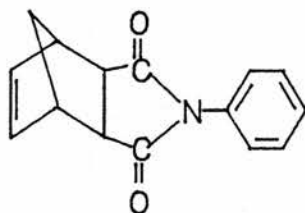
The cure mechanism of the PMR prepolymer is very complex and to date is not fully understood. However it has been postulated that the norbornene endcaps undergo a reverse Diels Alder (RDA) reaction to produce free cyclopentadiene and a maleimide end group. The cyclopentadiene then copolymerises with the maleimide end groups to give a cross-linked network, illustrated in Scheme 3. This reaction mechanism does not involve the production of side products (volatiles) which would lead to voiding in the final composite. However the cyclopentadiene which is released in the RDA reaction is a potential source of volatiles. To minimise this possibility, pressure is applied during the RDA reaction so that the cyclopentadiene is forced to react with the maleimide groups before it is lost to the atmosphere.



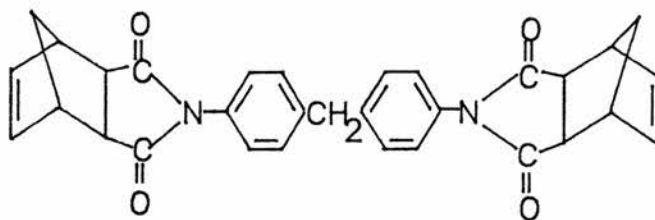
Scheme 3¹⁶

In an attempt to resolve completely the cross-linking mechanism, several studies have been carried out on model compounds¹⁵⁻¹⁷. This research has revealed that several different competing reactions take place which result in different structural crosslinks. However it must be remembered that research to date has been carried out on model compounds such as (A) and (B) overleaf due to their solubility in organic solvents, unlike the PMR-15 prepolymer.

It is proposed that the crosslinking mechanisms which occur in these model compounds probably occur in the crosslinking of the PMR-15 prepolymer, but this cannot definitely be verified due to the latter's insolubility.



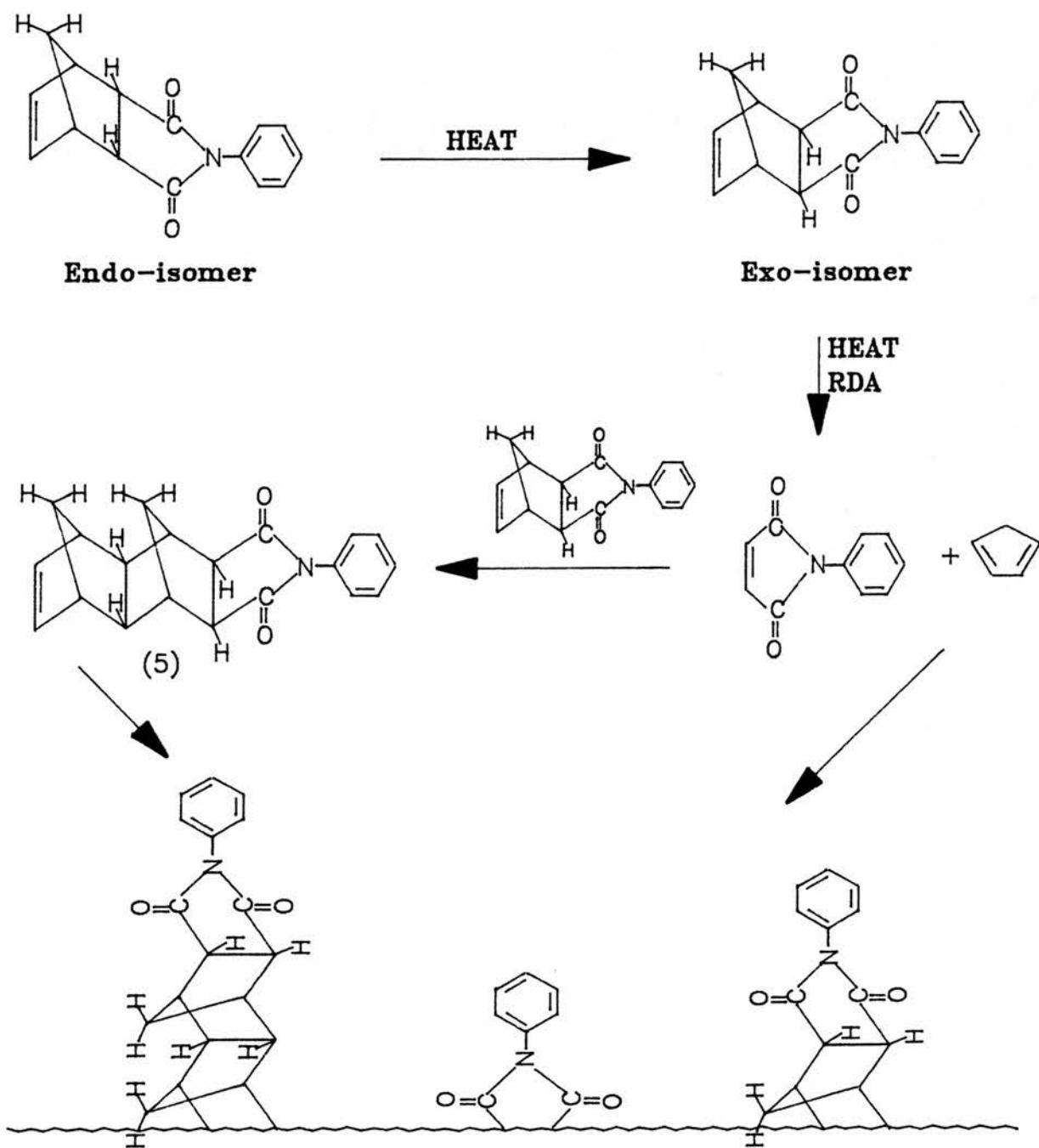
(A)



(B)

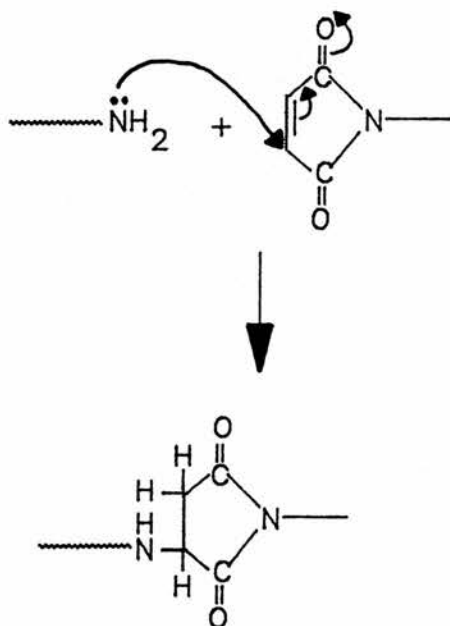
From this work¹⁵⁻¹⁷ it has been postulated that the crosslinking mechanism differs from the "conventional" mechanism (Scheme 3), in that cyclopentadiene released from the RDA reaction is not incorporated directly into the backbone of the crosslink. It is thought instead that it can recombine with a further nadimide-ended species (which tends to be the thermodynamically more stable exo-isomer) to give structure 5 (Scheme 4). Alternatives to this could be recombination with a maleimide end, to give back a nadimide end, or loss leaving a maleimide end.

As a consequence there a number of species which can undergo crosslinking illustrated for N-phenylnadimide in Scheme 4^{16,17}.



Scheme 4

Another crosslinking mechanism is possible when endcapping with 5-norbornene-2,3-dicarboxylic anhydride is incomplete. This leaves an amine end-capped species which will undergo reaction with a maleimide end group (reaction product of the RDA reaction) as outlined in Scheme 5.

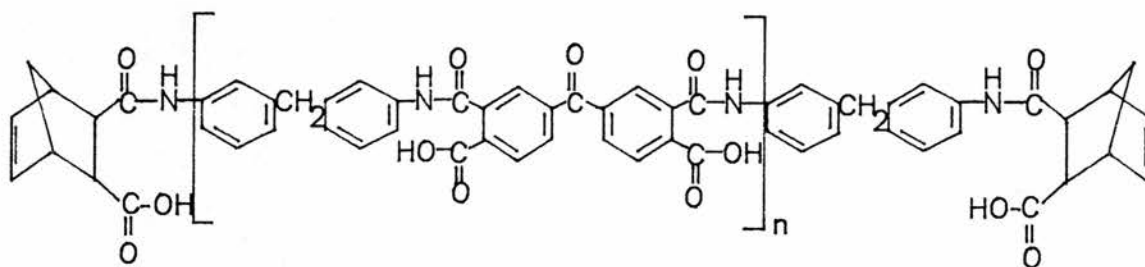


Scheme 5

This reaction is known as a Michael addition and occurs with alkenes conjugated with electron withdrawing groups. This reaction is used commercially by reacting 1,1'-(methylenedi-4,1-phenylene)-bismaleimide (MDA-BMI), with 4,4'-methylenedianiline (MDA). The MDA "chain extends" the MDA-BMI reducing the crosslink density, which results in a tougher material. The product is known commercially as Kerimid 601 and is marketed by Rhone-Poulenc.

1.1.6 Second generation polyimides: PMR-II

Since the inception of PMR polyimides, researchers have been trying to modify their properties by various methods including blending with thermoplastic polyimides¹⁸, and varying either the dianhydride (or diacid-dimethyl ester) or the diamine^{3,13,14,19-22}. One such example is the LaRC (NASA Langley Research Centre) series of resins (6) which differs from the PMR-15 resins in that their monomers are the anhydrides and not the esters, and the diamine is 3,3'-methylenedianiline and not 4,4'-methylene-dianiline. These resins are applied from solution at the amic acid stage and then heated to give the imide which is subsequently cross-linked. The main use of these resins is as high temperature adhesives.



(6)

Thermo-oxidative stability at elevated temperature is however one of the most desirable properties from any such polymer and it has been found that if MDA is replaced by p-phenylenediamine (PPDA), and BTDE replaced by the dimethyl ester of 4,4'-(hexafluoroisopropylidene)-bis(phthalic acid) (HFDE), composites made containing

this matrix have twice the lifetime of a PMR-15 composite at 316°C⁶. This has been attributed to the greater thermal stability of the F₃C - C - CF₃ link in HFDE relative to the carbonyl linkage of BTDE. The replacement of MDA by PPDA most likely plays a role in the greater thermal stability, possibly because PPDA contains no aliphatic C-H bonds which are susceptible to attack by oxygen at elevated temperatures. PMR-II was used as a name to distinguish these fluorine containing polymers (7) from first generation¹ PMR-15 systems.

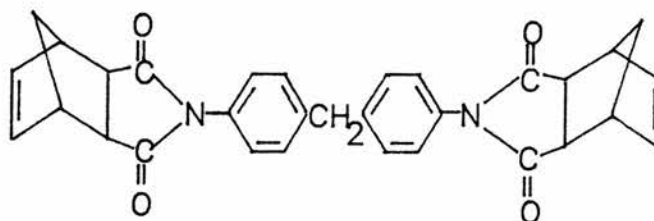
PMR-II systems were developed to meet the demand from jet engine manufacturers for a thermosetting polyimide which could survive hundreds of hours at 371°C under a pressure of 4 atm. air. The early PMR-II system was PMR-II-13 (FMW=1300); this was chosen as it could be processed similarly to PMR-15. However the full potential of PMR-II systems was not realised until it was found that higher formulated molecular weights gave increasing thermo-oxidative stability at 371°C up to a FMW of 5000, (after which the thermo-oxidative stability reaches a plateau^{1,2,23}). PMR-II-30 (FMW=3000) is the system currently receiving commercial attention as the best compromise between processability and thermal oxidative stability.

Initially these materials have not found commercial acceptability due to the expense of manufacturing HFDE. With potentially enormous financial rewards in the high temperature composite market, there is now great pressure on industry to produce a matrix which will survive high temperatures for longer periods. As a result of this several companies are now re-evaluating PMR-II systems with a view to commercialising PMR-II composites.

a consequence of this interfacial failure, microscopic cracks occur both intralaminarly and interlaminarly. The main effects of microcracking are a loss of mechanical properties (especially a fall in modulus) and, more importantly, a decrease in thermo-oxidative stability in the composite.

- (b) PMR laminates are brittle in the cured state which is attributed to their high cross-link density. Although this results in a relatively high modulus material, extensive crosslinking also gives a network which has little ductility and therefore low impact resistance.
- (c) Conventional PMR prepreg contains free methylenedianiline (MDA), a potent liver toxin and suspected human carcinogen with a permissible exposure limit of 10 ppb²⁴. This is a major problem in terms of safe prepreg handling and hence many studies have attempted to identify suitable, less toxic alternative diamines.
- (d) Before prepregging, all monomer solutions are tested by high performance liquid chromatography (HPLC). However, it is often found that solutions which have been passed by HPLC give poor quality laminates when impregnated into the fibres. It is thought that this variability can be attributed, to the preferential formation of the n=0 oligomer (8). This occurs because the monomethyl ester of 5-norbornene-2,3- dicarboxylic acid (NE) shows greater reactivity towards MDA than towards the dimethyl ester

of 3,3',4,4'-benzophenone- tetracarboxylic acid (BTDE). This reaction has the added effect of reducing the concentration of end-cap in the system and thus leading to the formation of higher molecular weight oligomers e.g. n=3, n=4, n=5. Hence this gives a broader molecular weight distribution than desired.



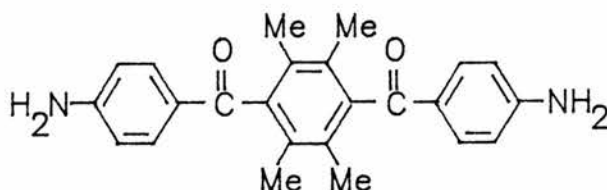
(8) n=0 oligomer

Although this problem can be solved by varying the cure schedule, this is not desirable commercially as it has to be carried out for every individual part, and is thus time-consuming and costly. The manufacturers of PMR polyimide parts are thus searching for an answer to this problem which will enable them to use the same cure schedule for every part.

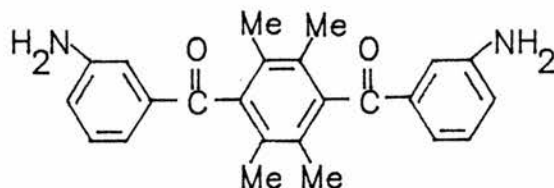
1.2.2 Aims

1.2.2.1 Replacement of MDA in PMR polyimides with an alternative long chain diamine

The diamines chosen for this study are 1,4-bis(4-aminobenzoyl)-2,3,5,6-tetramethylbenzene (9) and 1,4-bis(3-aminobenzoyl)-2,3,5,6-tetramethylbenzene (10).



(9)



(10)

The starting materials for these diamines are either 4-nitrobenzoyl chloride or 3-nitrobenzoyl chloride and durene (1,2,4,5-tetramethylbenzene) which are relatively cheap. These diamines are believed to be novel, as is the PMR system which can be made from them. Replacement of MDA by another diamine is desirable in terms of

toxicity; as previously stated, MDA is extremely toxic. It is not certain what makes one diamine more toxic than another as the relationship between biological activity and chemical structure is not well understood²⁵. It has been observed²⁵ that certain primary amines (MDA included) containing a carbon or nitrogen bridge between the two benzene rings, induce severe liver toxicity. Other amine compounds containing two conjugated benzene rings however do not affect the liver but may still induce cancer in other organs in the body eg. benzidine is a potent bladder carcinogen. The diamines with structures 9 and 10 contain three rings which are separated by carbonyl groups, and therefore such diamines probably would not be expected to be liver toxins on the basis of their structure. However even if they do not possess the toxicity of MDA, they must still be treated with caution as all known diamines possess some toxicity. It has been claimed²⁶ that a benzylic hydrogen atom (eg. a CH₂ group between benzene rings as is the case with MDA), or a -CH₃ substituent on an aromatic diamine, incorporated into the PMR formulation is important in promoting excellent thermal stability. These factors are the main driving force therefore for the synthesis and ultimately the incorporation of these long chain diamines into a PMR formulation.

1.2.2.2 Investigation of the PMR-15 polymerisation process

This investigation was initiated with the intention of identifying the problems which exist in synthesising a PMR-15 prepolymer free of unwanted oligomers such as n=0, n=1, n=3 etc, so that a

consistent product can be produced from a specified polymerisation technique.

The work undertaken involves the polymerisation of 4,4'-methylenedianiline with 3,3',4,4'-benzophenonetetracarboxylic dianhydride, and 5-norbornene-2,3-dicarboxylic anhydride (outlined in Scheme 1). This route has two advantages over the ester-acid route (outlined in Scheme 2). It allows the isolation of the relatively soluble polyamic acid ((1), Scheme 1), which can be characterised by NMR (^1H or ^{13}C). Secondly, the reaction to produce the polyamic acid ((1), Scheme 1) is homogeneous. The first stage in the ester-acid route to produce the polyamic acid ((3), Scheme 2) involves the evaporation of methanol at 120°C , giving a mixture of the polyamic acid (3) and the fully imidised product (4). This is insoluble in all low boiling solvents, and only partially soluble in dipolar aprotic solvents.

Hence it is the aim of this research to synthesise a "characterised" prepolymer (2) by Scheme 1 or by another polymerisation route, thereby gaining an understanding of the polymerisation chemistry. The cured product will then be compared with a commercial PMR-15 cured resin (synthesised via Scheme 2), by means of their respective physical properties such as glass transition temperature (T_g), dynamic weight loss and isothermal weight loss.

2 RESULTS AND DISCUSSION

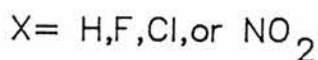
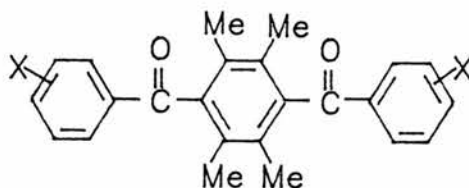
2.1 Dibenzoylation of durene

When benzene is monoacylated, the aromatic ring becomes deactivated towards further electrophilic substitution by the acylium ion, $RC\equiv O^+$. Thus diacylation of benzene is not observed. When methyl substituents are introduced they activate the benzene ring to electrophilic attack by moving electrons inductively into the ring. However, it is not until two methyl substituents are meta to each other (m-xylene) that diacylation is known to take place²⁷. The diacylation of m-xylene occurs principally at positions 4 and 6 (the 2,4-diacetyl isomer being a minor product).

Durene, which contains four methyl groups, will have an increased tendency to undergo a second diacylation reaction because:

- (a) the electronic effect of the methyl groups counteracts the electron withdrawing effect of the first acyl group, and more importantly;
- (b) the carbonyl group will be sterically hindered by the two methyl groups either side. This results in the carbonyl group being twisted out of the plane of the durene ring eliminating the mesomeric effect of the first acyl group. These properties favouring diacylation of durene led Friedel and Crafts themselves to the successful preparation of dibenzoyldurene. This synthesis

was achieved as early as 1879²⁸. Co-workers Cheng and Gore reported the preparation of dibenzoyldurene²⁹, using an excess of benzoyl chloride and aluminium chloride which gave acceptable yields. However, it was not until recently that two publications appeared on the dibenzoylation of durene in which the benzoyl chloride contained a substituent on the aromatic ring^{30,31}. These dibenzoylations of durene provided difunctional dibenzoyl durenes which in the case of Patterson³¹ were primarily synthesised as monomers to be used in PEEK (polyetheretherketone) type thermoplastic polymers. Patterson synthesised the following difunctional dibenzoyl durenes:



In particular Patterson describes the synthesis and characterisation of bis(4-chlorobenzoyl)-2,3,5,6-tetramethylbenzene. X-ray crystallography of the material gave a crystal structure shown in Appendix 1, Figure A³². From this crystal structure the carbon to carbon bond angles were found to be around 120°. Thus both the aromatic ring containing the halogen atom and the central durene ring are symmetrical and not under strain. The bonds C₂ to C₄' and C₁' to C₇ show no double bond character. The torsion angle data show the carbonyl group and the terminal phenyl

ring containing the halogen group to be in the same plane. The durene ring is twisted at an angle of 85° to this plane. The carbonyl groups are shown to be "trans" to each other.

The chemistry of durene described above opened up a novel route to the production of methyl substituted diamines, namely 1,4-bis-(4-aminobenzoyl)-2,3,5,6-tetramethylbenzene(9) and 1,4-bis(3-aminobenzoyl)-2,3,5,6-tetramethylbenzene (10), which can be utilised as monomers in the synthesis of polyimides. The route to these methyl substituted diamines involved the reaction of durene with an excess of nitrobenzoyl chloride (used as the solvent) and an excess of aluminium chloride. The resultant dinitrodibenzoyl durene product was reduced by the use of cyclohexene in dimethylformamide with a palladium/charcoal catalyst.

2.2 ^1H and ^{13}C NMR analysis of 1,4-bis(4-aminobenzoyl)-2,3,5,6-tetramethylbenzene(9) and 1,4-bis(3-aminobenzoyl)-2,3,5,6-tetramethylbenzene(10)

2.2.1 ^1H NMR analysis of 1,4-bis(4-aminobenzoyl)-2,3,5,6-tetramethylbenzene (9).

The ^1H NMR spectrum of 1,4-bis(4-nitrobenzoyl)-2,3,5,6-tetramethylbenzene(14) in CDCl_3 , outlined in Figure 1 has the following resonances: a twelve proton singlet (four methyl groups) at $\delta 2.07$ and a four proton AA'BB' pattern centered at $\delta 8.07$ and $\delta 8.39$ typical of a 1,4-disubstituted aromatic ring.

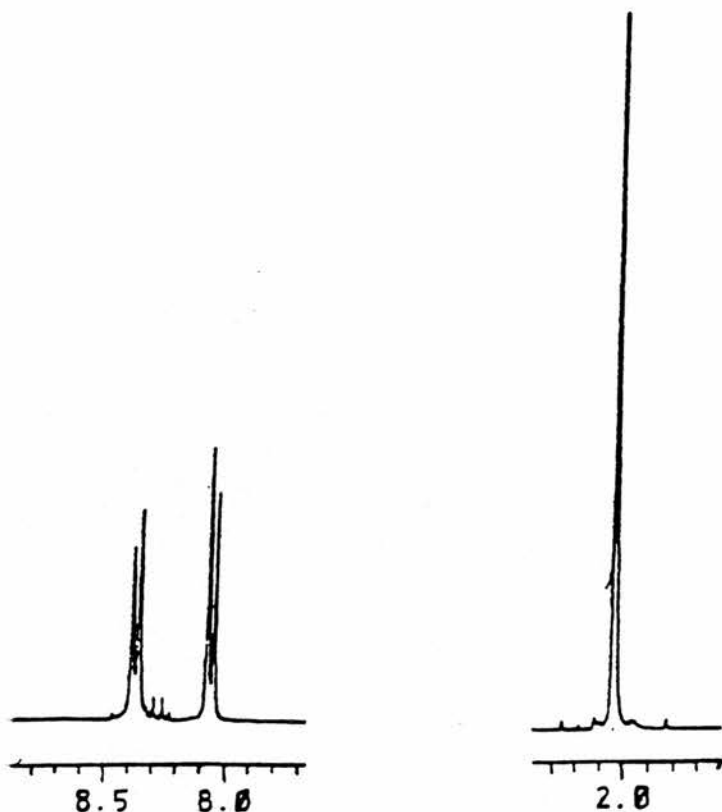


Figure 1 - ^1H NMR Resonances of 1,4-bis(4-nitrobenzoyl)-2,3,5,6-tetramethylbenzene(14) recorded in CDCl_3 at room temperature.

However, the ^1H NMR spectrum of 1,4-bis(4-aminobenzoyl)-2,3,5,6-tetramethylbenzene(9) in DMSO-d_6 at 40°C , outlined in Figure 2a, is more complex. The methyl resonance remains as a singlet at δ 1.95, but the aromatic signals are observed as a triplet (δ 6.63), and a double doublet (δ 7.51). The amino protons resonate at δ 6.18. The spectrum of (9) run in DMF-d_7 at 40°C shows the methyl singlet still at δ 1.95, the amino resonance slightly shifted to δ 6.12, the aromatic double doublet is at δ 7.48, but the triplet at δ 6.63 in DMSO-d_6 is now a double doublet at δ 6.65, shown in Figure 2b.

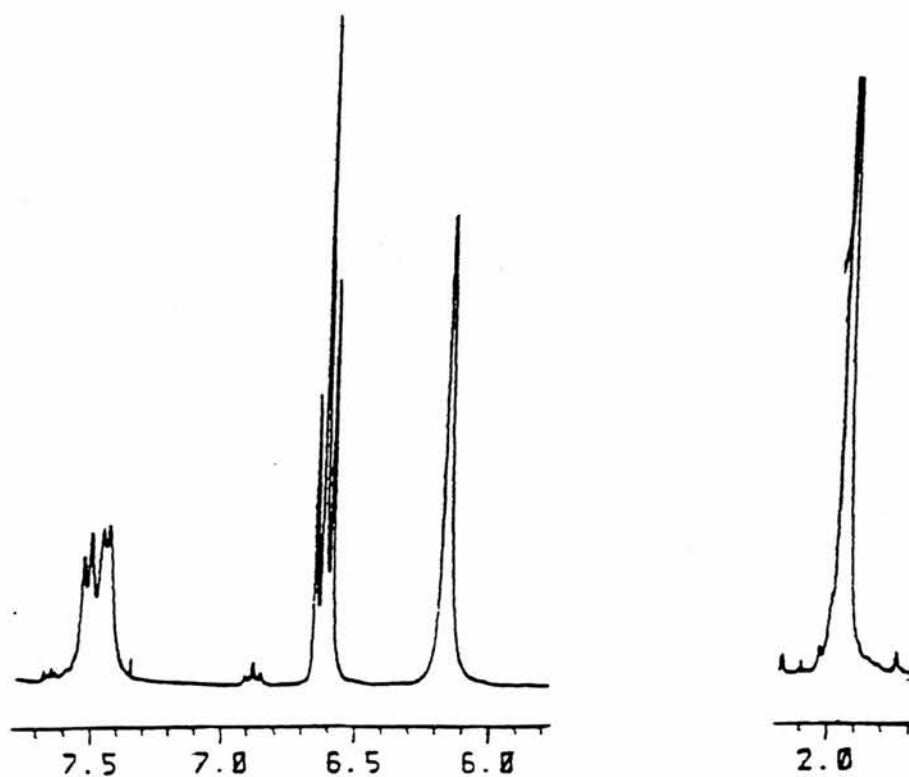


Figure 2a - ¹H NMR resonances of 1,4-bis(4-aminobenzoyl)-2,3,5,6-tetramethylbenzene(9) recorded in DMSO-d₆ at 40°C.

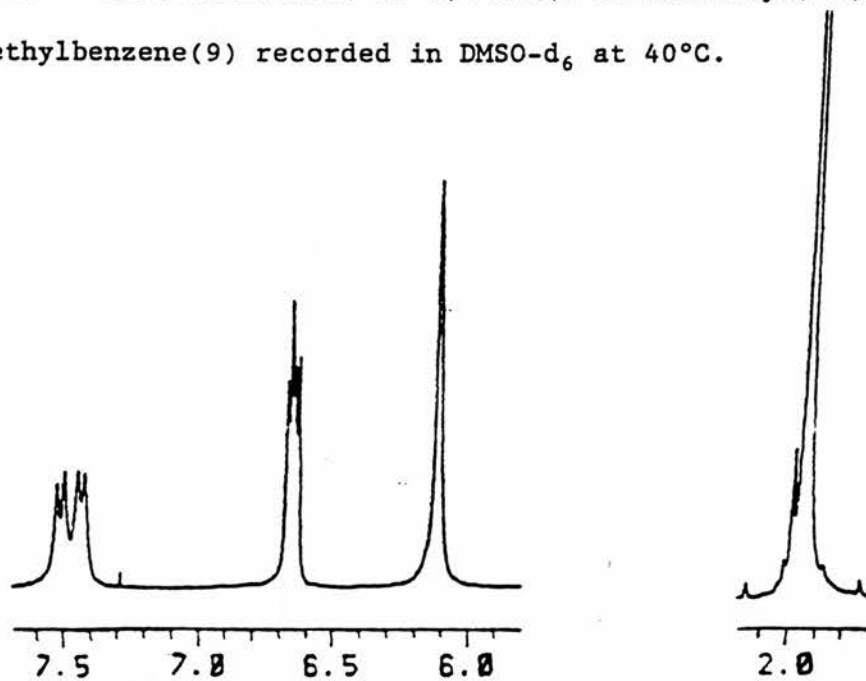
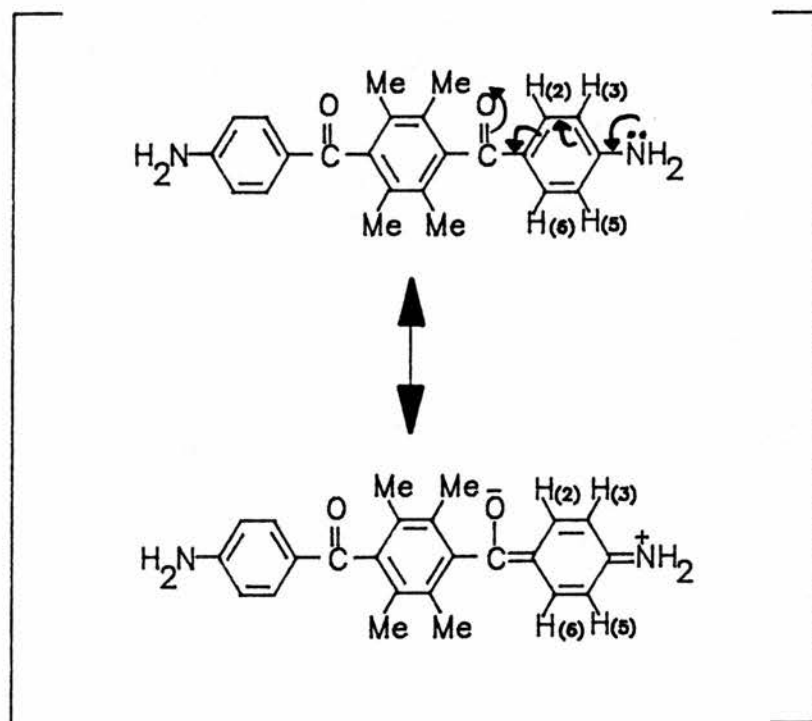


Figure 2b - ¹H NMR resonances of 1,4-bis(4-aminobenzoyl)-2,3,5,6-tetramethylbenzene(9) recorded in DMF-d₇ at 40°C.

The unusual pattern observed for the aromatic resonances implies that the two protons ortho - to the amino group are non-equivalent, and similarly that the two meta - protons are non-equivalent. Such non-equivalence is most obviously accounted for in terms of restricted rotation about the ring-to-carbonyl carbon single bond, a phenomenon which might be expected from the canonical form shown in Scheme 6.



Scheme 6

If the carbonyl group is held in the plane of the ring by overlap of the two Π -systems then one pair of ring protons ($H_{(2)}$ and $H_{(3)}$) would lie on the same side as the oxygen, and the other pair ($H_{(5)}$ and $H_{(6)}$) would lie on the opposite side. It is consistent with this theory that there is a greater chemical shift ^{difference} between $H_{(2)}$

and $H_{(6)}$ (double doublet observed in Figure 2a), than between $H_{(3)}$ and $H_{(5)}$ (double doublet overlapping to give an apparent triplet, observed in Figure 2a). In a different solvent (DMF- d_7), the spectrum was almost identical (Figure 2b), except that the $H_{(3)}$, $H_{(5)}$ signal was now resolved into a double doublet.

In order to investigate this phenomenon further, the spectra were recorded at different temperatures. In DMSO- d_6 at 90°C (Figure 3), both sets of aromatic resonances appear as simple doublets, although the resonance for $H_{(2)}$ and $H_{(6)}$ is considerably broader than the resonance for $H_{(3)}$ and $H_{(5)}$. The same is true for the spectrum in DMF- d_7 at 80°C (Figure 4); both spectra revert to

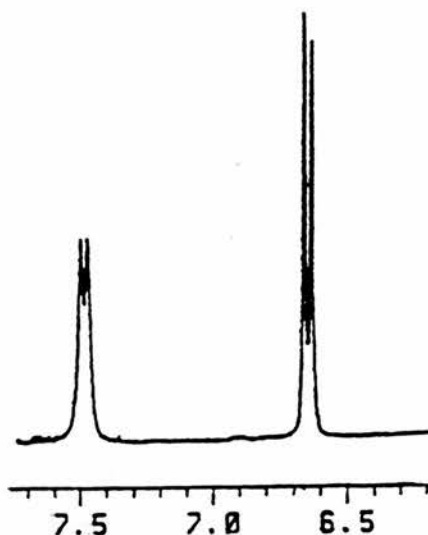


Figure 3 - ^1H NMR aromatic resonances of 1,4-bis(4-aminobenzoyl)-2,3,5,6-tetramethylbenzene (9) recorded in DMSO- d_6 at 90°C.

their original appearance when the heated samples are allowed to cool down to the original temperature (40°C).

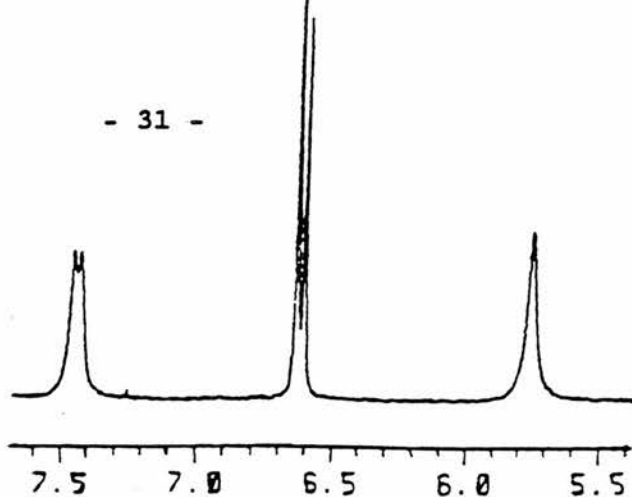


Figure 4 - ^1H NMR aromatic and amine resonances of 1,4-bis(4-amino-benzoyl)-2,3,5,6-tetramethylbenzene (9) recorded in DMF-d_7 at 80°C .

In the case of the corresponding bismaleimide (16), where the electron donating effect of the nitrogen is diminished, the aromatic proton resonances approach the "normal" AA'BB' pattern shown in Figure 5 (δ 7.55 and δ 7.98), although the former (presumably H(3) and H(5)) appear considerably broadened. In the case of the 1,4-bis(3-aminobenzoyl)-2,3,5,6-tetramethyl-

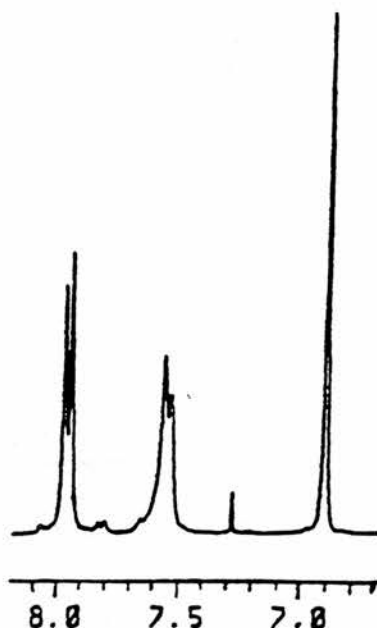


Figure 5 - ^1H -NMR aromatic and vinylic resonances of 1,4-bis-(4-maleimidobenzoyl)-2,3,5,6-tetramethylbenzene (16) recorded in CDCl_3

benzene (10) in which the amino and keto groups are not in conjugation, the aromatic resonances (Figure 6) are typical of a normal m-disubstituted aromatic ring system.

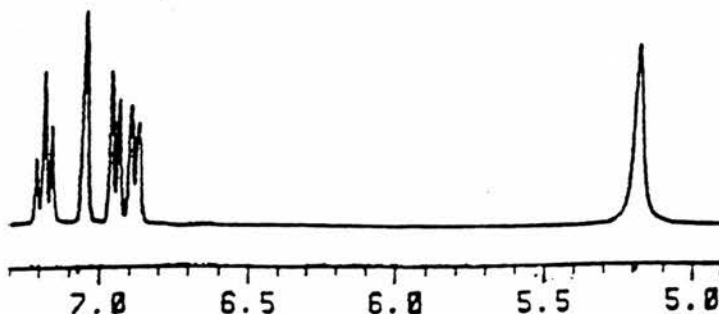


Figure 6 - ¹H NMR aromatic and amine resonances of 1,4-bis(3-aminobenzoyl)-2,3,5,6-tetramethylbenzene (10).

All of the above evidence is therefore consistent with electronic interaction between the amino and keto groups of (9) as represented by the canonical forms outlined in Scheme 6.

2.2.2 Molecular modelling of 1,4-bis(4-aminobenzoyl)-2,3,5,6-tetramethylbenzene (9).

Molecular modelling of (9) was carried out to assess the difficulty of rotation of the carbonyl group past the methyl groups. The optimised geometry of (9) (in its lowest energy conformation) is shown in Appendix 1, Figure B. The molecular modelling calculations revealed the following:

- (a) The angle of the bond between the carbonyl group and the durene ring is calculated to be 55° ie the carbonyl group is

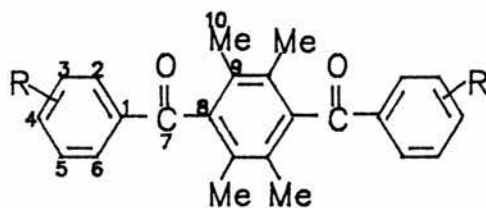
twisted at an angle of 55° to the plane containing the durene ring. This represents a large steric repulsion between the carbonyl group and the methyl groups on the durene ring. In comparison the bond angle between the phenyl ring containing the amine substituent and the carbonyl group is 16° , representing a small steric repulsion. The corresponding angle in polyetheretherketone (PEEK) is 30° ³³.

- (b) Optimised geometry calculations show that rotation about the carbonyl to durene ring bond so that the carbonyl group passes the methyl group has a rotation barrier of 118 KJmol^{-1} . This is a very high rotational barrier because free rotation about a bond is in the order of $8\text{-}12 \text{ KJmol}^{-1}$. It can thus be concluded that rotation about the carbonyl to durene ring bond will be restricted due to the steric hindrance of the methyl groups, and that the steric influence of the methyl groups pushes the durene ring out of the plane containing the carbonyl group.

2.2.3 ^{13}C NMR analysis of (9), (10), (14), (15) and (16)

The ^{13}C NMR spectra of (9), (10), (14), (15) and (16) were run in DMSO-d_6 and in DMF-d_7 at low and high temperatures. The carbon-13 chemical shifts obtained are shown in Table B below.

TABLE B



R	¹³ C chemical shift of carbons (PPM)									
	1	2	3	4	5	6	7	8	9	10
4-NO ₂ (14) 21C, CDCl ₃	140.96 (143.90)	130.50 (131.00)	124.29 (123.30)	150.83 (152.10)	/	/	199.18 (194.80)	139.94 (142.00)	130.94 (136.30)	16.12
3-NO ₂ (15) 21C, CDCl ₃	138.66 (138.70)	123.83 (125.20)	148.90 (148.10)	128.12 (127.30)	130.32 (129.10)	135.06 (136.20)	198.80 (194.80)	139.86 (142.00)	131.01 (136.30)	16.66
4-NH ₂ (9) DMSO-D ₆ 40C	125.01 124.91 (125.30)	131.47 (130.60)	112.91 (113.90)	154.32 (152.90)	/	/	198.96 198.87 (194.80)	140.72 140.65 (142.00)	129.32 (136.30)	16.12
4-NH ₂ (9) DMSO-D ₆ 90C	125.23 (125.30)	131.10 130.92 (130.60)	112.95 112.88 (113.90)	153.79 (152.90)	/	/	196.62 (194.80)	140.60 (142.00)	129.02 (136.30)	16.83 16.89 16.54 16.40
4-NH ₂ (9) DMF-D ₇ 40C	124.84 124.62 (125.30)	130.27 (130.60)	111.82 (113.90)	153.43 (152.90)	/	/	195.96 (194.80)	139.91 (142.00)	128.41 (136.30)	14.52
4-NH ₂ (9) DMF-D ₇ 80C	125.18 (125.30)	130.28 130.18 (130.60)	112.07 112.03 (113.90)	153.21 (152.90)	/	/	196.02 (194.80)	140.18 (142.00)	128.48 (136.30)	14.48 14.39
3-NH ₂ (10) DMSO-D ₆ 80C	137.63 (138.30)	113.50 113.37 (115.80)	148.93 (148.90)	119.22 118.99 (117.90)	129.20 129.00 (128.70)	116.53 116.29 (117.60)	200.01 (194.80)	140.49 (142.00)	129.28 (136.30)	15.03 15.00
3-NH ₂ (10) DMF-D ₇ 40C	136.99 (138.30)	112.45 (115.80)	148.54 (148.90)	115.83 (117.90)	128.16 (128.70)	118.18 (117.60)	199.31 (194.80)	139.78 (142.00)	128.57 (136.30)	14.52
3-NH ₂ (10) DMF-D ₇ 80C	137.34 (138.30)	112.81 112.71 (115.80)	148.40 (148.90)	116.08 (117.90)	128.14 (128.70)	118.27 (117.60)	199.21 (194.80)	140.04 (142.00)	128.66 (136.30)	14.48 14.40
4-Maleimido (16) 21C, CDCl ₃	136.18 (139.10)	130.85 (131.00)	125.68 (127.50)	135.63 (135.40)	/	/	200.16 (194.80)	140.25 (142.00)	130.92 (136.30)	16.64

The figures in brackets in Table B are the carbon-13 chemical shifts calculated from correlation data³⁴⁻³⁶ as follows:

(a) 1,4-bis(4-aminobenzoyl)-2,3,5,6-tetramethylbenzene (9)

Carbon No	Substituent effect on ¹³ C-chemical shift(PPM)			calculated chemical shift (PPM)
	-NH ₂	O = C-Ph	Ph-CH ₃	
1	-12.50	+9.30	/	125.30
2	+0.50	+1.60	/	130.60
3	-14.30	-0.30	/	113.90
4	+20.70	+3.70	/	152.90
5	/	/	/	/
6	/	/	/	/
7	/	/	/	194.80 ³³
8	/	+9.30,+3.70	+0.60,-0.10	142.00
9	/	+1.60,-0.30	+9.00,+0.60 -3.00,-0.10	136.30

128.50ppm was used as the reference carbon-13 shift for a benzene carbon in these calculations³⁶.

(b) 1,4-bis(4-nitrobenzoyl)-2,3,5,6-tetramethylbenzene(14)

Carbons 7,8,9 and 10 will remain essentially unchanged from the calculations above, however, carbons 1,2,3 and 4 will be shifted by the nitro substituent as follows:

Carbon No	Substituent effect on ¹³ C-chemical shift(PPM)		calculated chemical shift (PPM)
	-NO ₂	O = C-Ph	
1	+6.10	+9.30	143.90
2	+0.90	+1.60	131.00
3	-4.90	-0.30	123.30
4	+19.90	+3.70	152.10

(c) 1,4-bis(3-aminobenzoyl)-2,3,5,6-tetramethylbenzene(10)

Carbons 7,8,9 and 10 will remain unchanged from the calculations in (a) but carbons 1,2,3,4,5 and 6 will be shifted as follows:

Carbon No	Substituent effect on ¹³ C-chemical shift(PPM)		calculated chemical shift (PPM)
	-NH ₂	O = C-Ph	
1	+0.50	+9.30	138.30
2	-14.30	+1.60	115.80
3	+20.70	-0.30	148.90
4	-14.30	+3.70	117.90
5	+0.50	-0.30	128.70
6	-12.50	+1.60	117.60

(d) 1,4-bis(3-nitrobenzoyl)-2,3,5,6-tetramethylbenzene(15)

Carbons 1,2,3,4,5 and 6 will be shifted as follows:

Carbon No	Substituent effect on ¹³ C-chemical shift(PPM)		calculated chemical shift (PPM)
	-NO ₂	O = C-Ph	
1	+0.90	+9.30	138.70
2	-4.90	+1.60	125.20
3	+19.90	-0.30	148.10
4	-4.90	+3.70	127.30
5	+0.90	-0.30	129.10
6	+6.10	+1.60	136.20

(e) 1,4-bis(4-maleimidobenzoyl)-2,3,5,6-tetramethylbenzene(16)

Carbons 1,2,3 and 4 will be shifted as follows:

Carbon No	Substituent effect on ¹³ C-chemical shift(PPM)		calculated chemical shift (PPM)
	^a $\begin{array}{c} \text{CO}-\text{C}-\text{Cl} \\ \text{CO}-\text{C}-\text{Cl} \end{array}$	$\text{O}=\text{C}-\text{Ph}$	
1	+1.30	+9.30	139.10
2	+0.90	+1.60	131.00
3	-0.70	-0.30	127.50
4	+3.20	+3.70	135.40

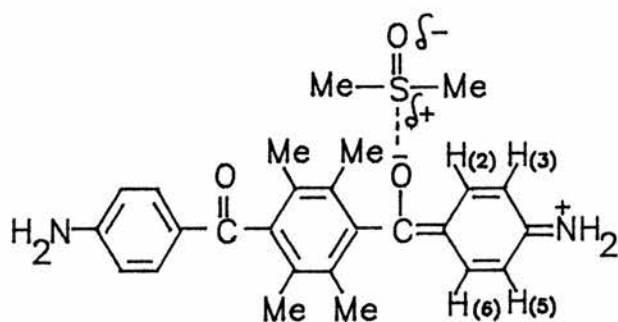
a - The substituent $\begin{array}{c} \text{CO}-\text{C}-\text{Cl} \\ \text{CO}-\text{C}-\text{Cl} \end{array}$ was used as a close approximation to $\begin{array}{c} \text{CO}-\text{C}-\text{H} \\ \text{CO}-\text{C}-\text{H} \end{array}$ as the data for this substituent was not available.

2.2.3.1 ¹³C NMR analysis of 1,4-bis(4-aminobenzoyl)-2,3,5,6-tetramethylbenzene (9)

Having run the ¹H NMR spectrum of (9) and finding it to be anomalous it was not unexpected the the ¹³C spectrum was also anomalous, although the nature of the anomalies cannot easily be explained. In DMSO-d₆ at low temperatures (40°C) three of the resonances (C1, C=O and C8) appear as split peaks, whereas there is no obvious non-equivalence of either C2 and C6 or C3 and C5. On the other hand at elevated temperature (90°C) C1, C10 and C8 give single lines whereas the C2 and C3 signals are now split; also four methyl resonances are now observed (C10). In DMF-d₇, only C1 gives a split peak at 40°C, whereas at 80°C C1 gives a single line, and C2, C3 and the methyl carbons (C10) each give two lines. In both solvents, the samples when cooled again to 40°C,

returned to the original spectrum. There is no obvious simple explanation which fits all of the above experimental information, however, the following three explanations go some of the way towards explaining the experimental data:

- (1) The fact that carbon 1 in DMF-d₇ at 40°C is split into two lines, while in DMSO-d₆ at 40°C C1, C7 and C8 are split, suggests that C7 and C8 split because of some sort of interaction of (9) with the latter solvent. Table B also highlights that when R=nitro or maleimido, no splitting of any carbon occurs. This is further evidence that the amino group through electron donation alters the structural conformation giving the canonical forms outlined in Scheme 6. If these canonical forms are indeed present then the DMSO-d₆ may interact with (9) as follows:



- (2) If the preferred conformation of (9) is the same as indicated in the crystal structure of 1,4-bis(4-chlorobenzoyl)-2,3,5,6-tetramethylbenzene (Appendix 1, Figure A), ie the outer rings and the C=O groups are orthogonal to

the central ring, it is obvious why $H_{(2)}$ and $H_{(6)}$ are non-equivalent at ordinary temperatures. One is over the central ring and is therefore influenced by the Π -system, whereas the other is adjacent to the oxygen. The corresponding carbons (C_2 and C_6) are less obviously influenced by these through-space interactions, but still give rise to a broadened single peak at 40°C .

- (3) As the sample is heated and restricted rotation about the C_1 to carbonyl bond is lessened, it is possible for this part of the molecule to adopt a conformation in which rotation (albeit still restricted) about the C_8 to $C=O$ bond also becomes possible, and the outer phenyl rings may pass the methyl groups. This may lead to two conformers which could be regarded as a "cis/trans" pair (Figure 7), one with both oxygens on the same face of the central ring plane and the other with one on either side.

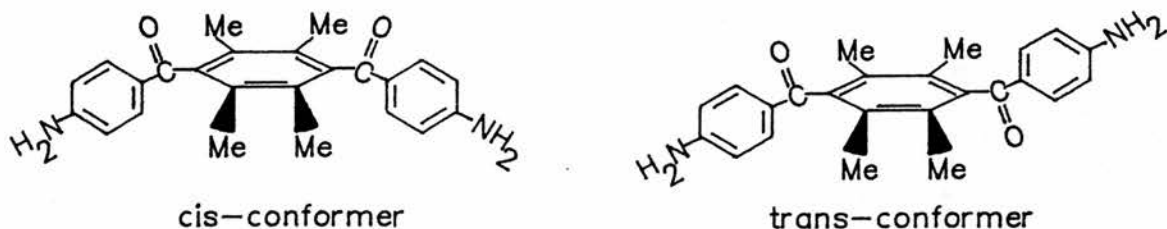


Figure 7

Thus the C2, C3 and methyl resonances of the two conformers would not necessarily be identical. However, there is no satisfactory explanation for the split resonance observed for C1 at 40°C in both DMF-d₇ and DMSO-d₆, nor for the four methyl resonances observed in DMSO-d₆ at 90°C.

2.2.3.2 ¹³C NMR analysis of 1,4-bis(3-aminobenzoyl)-2,3,5,6-tetramethylbenzene(10)

The ¹³C NMR spectra for 1,4-bis(3-aminobenzoyl)-2,3,5,6-tetramethyl benzene run in both DMSO-d₆ and DMF-d₇ at 80°C; C2 and the methyl resonance both show two lines in DMF-d₇ at 80°C, while C2, C4, C5, C6 and the methyl resonances are split in DMSO-d₆ and therefore because C4, C5 and C6 are not split in DMF-d₇ then they are most probably interacting in some way with the DMSO-d₆. These interactions must be different than the suggested interactions for (9) with DMSO-d₆, because the amine is now on position 3, and therefore the amino and keto groups are not in conjugation. The ¹³C spectrum for (10) in DMF-d₇ at 40°C appears normal, ie no splitting of any peak occurs hence the splitting of C2 and the methyl substituents in DMF-d₇ at 80°C must be a direct result of heating, and because C2 and the methyl substituents in (9) are both split similarly in DMF-d₇ at 80°C then explanation (3) in section 2.2.3.1 that cis and Trans conformers are formed at higher temperatures may hold true in this case as well.

2.3 ^1H NMR analysis of the polyamic acid intermediates and model compounds synthesised in Sections 3.5 and 3.6.

2.3.1 Introduction

The ^1H NMR spectra of the norbornene end-capped polyamic acid intermediates derived from the diamines 4,4'-methylenedianiline (MDA), 1,4-bis(4-aminobenzoyl)-2,3,5,6-tetramethylbenzene(9) and 1,4-bis(3-aminobenzoyl)-2,3,5,6-tetramethylbenzene(10) were obtained and subsequently studied to provide the following data:

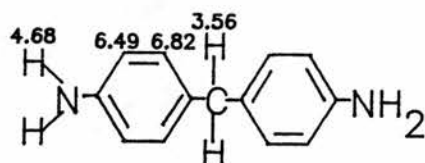
- (a) structural information on the polymers (e.g. the extent of end-capping)
- (b) the efficiency of the three diamines, MDA,(9) and (10), in the polymerisation process, and
- (c) the approximate degree of polymerisation, ie the value of \bar{n} and thus the number average molar mass M_n .

The following model compounds were synthesised (if not already commercially available) and their ^1H NMR spectra studied to provide a basis for the assignment of the complex substitution patterns in the ^1H NMR spectra of the polyamic acids. Each model compound represents a different section of the overall polymer molecule. Thus the ^1H NMR spectra of the model compounds provide information on the ^1H NMR signals expected from the different sections of the polymer structure.

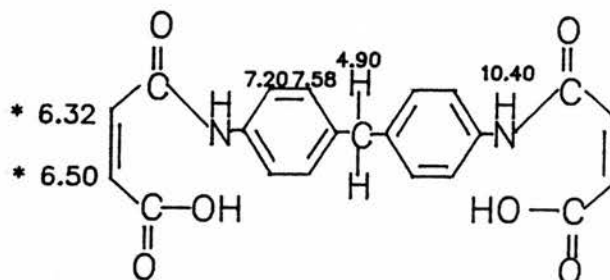
2.3.2 ^1H NMR analysis of the model compounds synthesised in Section 3.6

Chemical shifts in this section are expressed in δ

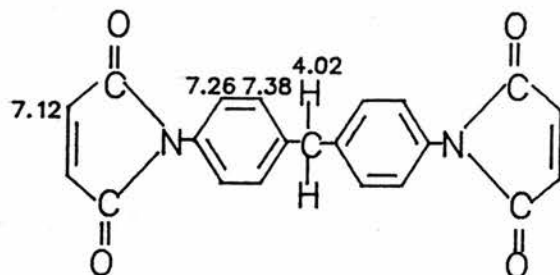
2.3.2.1 4,4'-Methylenedianiline (MDA)



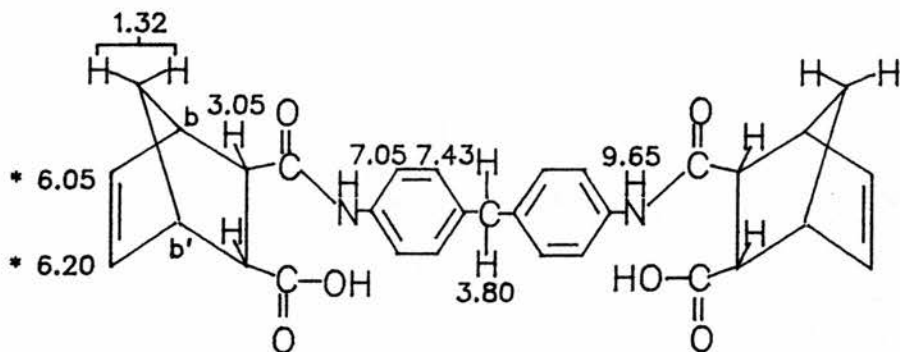
2.3.2.2 1,1'-(Methylenedi-4,1-phenylene)-bismaleamic acid



2.3.2.3 1,1'-(Methylenedi-4,1-phenylene)-bismaleimide (MDA-BMI)



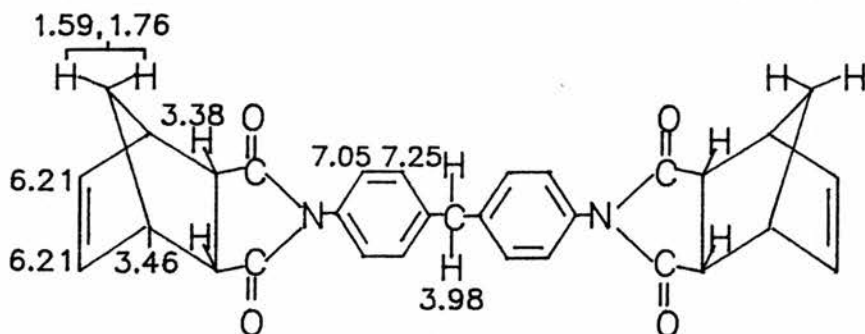
2.3.2.4 1,1'-(Methylene-4,1-phenylene)-bisnadidic acid



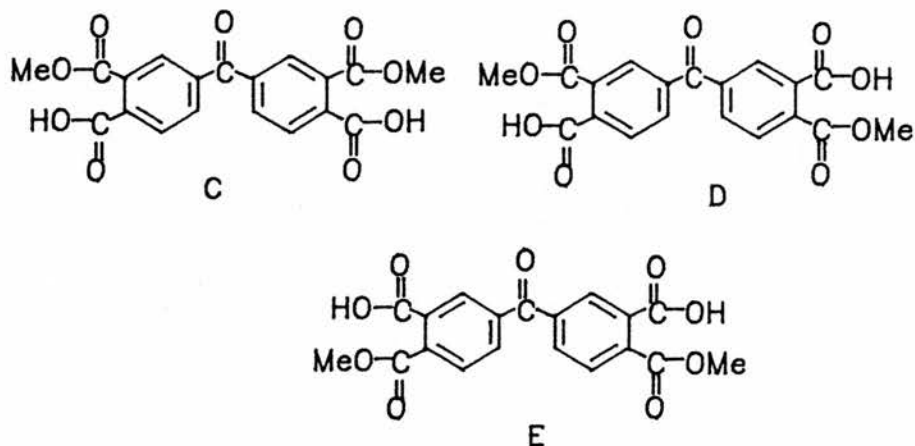
The aliphatic bridgehead hydrogens b and b¹ resonate at δ 3.20 and δ 3.36.

* The assignments for the individual hydrogens are provisional.

2.3.2.5 1,1'-(Methylene-4,1-phenylene)-bisnadimide

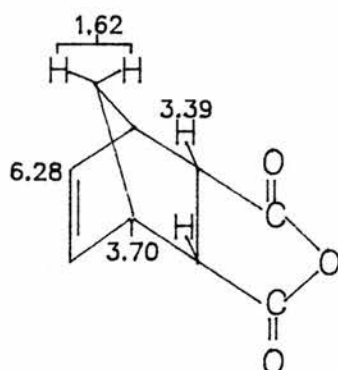


2.3.2.6 (Mixture of) dimethyl esters of 3,3',4,4'-benzophenonetetra-carboxylic acid (BTDE)



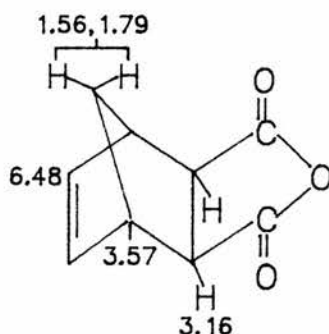
HPLC analysis showed the sample of BTDE submitted for NMR analysis to consist of three isomers (C, D and E), all present in significant amounts. The aromatic hydrogen resonances resulting from the different isomers are very complex and thus no individual aromatic hydrogen can be assigned to a particular resonance. However, the following aromatic resonances were observed: a singlet at δ 8.33; a singlet at δ 8.16; a multiplet at δ 7.95- δ 8.10; and a doublet centred at δ 7.80. The relative integrals of these signals are approximately 1:1:3:1. The methyl protons give two singlets at δ 3.95 and δ 3.98.

2.3.2.7 Endo-5-norbornene-2,3-dicarboxylic anhydride



The vinylic hydrogen resonance appears as a two proton triplet. The aliphatic bridgehead hydrogen resonance centred at δ 3.70 is a triplet, which integrates to two hydrogens. The aliphatic hydrogens resonating at δ 3.39 gave a multiplet. The methylene bridge hydrogen resonances are almost equivalent and thus the AB quartet cannot be resolved.

2.3.2.8 Exo-5-norbornene-2,3-dicarboxylic anhydride



The vinylic hydrogen resonance shows a triplet which integrates to two hydrogens. The aliphatic bridgehead hydrogen resonance centred at δ 3.57 shows a triplet also integrating to two hydrogens, whereas the aliphatic hydrogens centred at δ 3.16 give a doublet. The methylene bridge hydrogen resonance gives a doublet of doublets, with the doublet centred at δ 1.79 further split into

two triplets. This splitting could be due to one of the methylene bridge hydrogens being coupled to the neighbouring aliphatic bridgehead hydrogen. The methylene bridge signal integrates to two hydrogens.

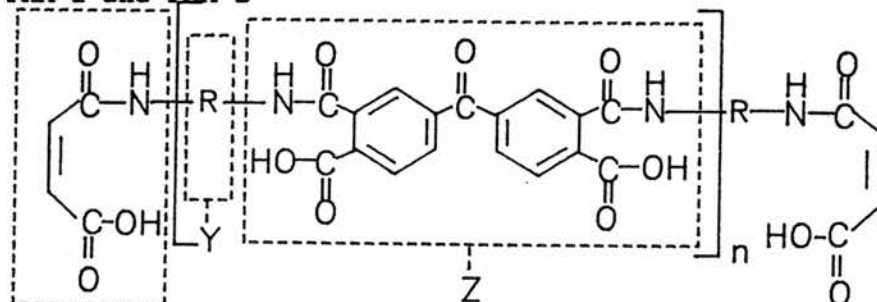
2.3.3 ¹HNMR analysis of the polyamic acid intermediates synthesised in 3.5

The polyamic acid intermediates were analysed in preference to the fully imidised products, because they were found to be more soluble in common NMR solvents such as DMSO-d₆.

The ¹HNMR spectra of the polyamic acids were interpreted by dividing the respective polymer structures into sections which correspond to the model compound structures. Thus each section of the polymer structure was assigned to a particular region in the ¹HNMR spectrum.

2.3.3.1

PAM-1 and PAM-2



X

When : R = then polymer = PAM-1

R = then polymer = PAM-2

PAM-1 and PAM-2 are maleimide ended polyamic acids, with compositions $[MA]_2[BTDA]_n[MDA]_{n+1}$ and $[MA]_2[BTDA]_n[(9)]_{n+1}$ respectively; the spectra of these are shown in Appendix 2 and in detail in Figures 8-10 below.

Maleic anhydride was utilised as the end-capper for the following reasons:

- (a) Previous work had indicated that 5-norbornene-2,3-dicarboxylic anhydride (nadic anhydride) did not give complete end-capping, thus leaving a few amine ends. At the same time co-workers in ICI had difficulty in functionalising amine-ended thermoplastics with nadic anhydride even at elevated temperatures, but functionalisation with maleic anhydride was straightforward at room temperature³⁷. Maleic anhydride was therefore utilised as an end-cap to compare its reactivity with nadic anhydride, and to investigate whether maleic anhydride used in this way gives a better control of polymer molecular weight.
- (b) Maleic anhydride as an end-cap will not introduce aliphatic hydrogens into the ¹HNMR spectrum, such as those in 1,1'-(Methylenedi-4,1-phenylene)bismadimide (2.3.2.5). Thus when the ¹HNMR spectrum of a norbornene-ended polymer is compared with the ¹HNMR spectrum of the respective maleimide ended polymer, the additional peaks due to the aliphatic hydrogens can be identified. The N-H NMR signal in Section X of the

polymers (next to the end-cap), is known from model compounds to appear upfield from the N-H signal in Section Z (between the two aromatic components of the polymer).

For most of the $^1\text{HNMR}$ spectrum studied, the N-H NMR signal in Section X of the polymer appears reduced or is missing, presumably due to deuterium exchange stemming from the presence of D_2O in the NMR solvent. Reduction in the amide signal may also result from the end-cap undergoing a small amount of imidisation. This effect is described in detail below. Such a phenomenon holds true for the $^1\text{HNMR}$ spectrum of PAM-1; only the amide hydrogen resonance in Section Z appears at $\delta 10.41$ (shown in Figure 8), but for the $^1\text{HNMR}$ spectrum of PAM-2 the amide hydrogen ($\delta 10.90$) in Section Z and the amide hydrogen resonance in Section X ($\delta 10.69$) have integrals in the correct ratio of 2:1, illustrated in Figure 9.

Section Y of PAM-1 contains the 4,4'-methylenedianiline (MDA) aromatic hydrogens and the benzophenone aromatic hydrogens are contained in Section Z. These aromatic hydrogen resonances combined are observed to resonate over the region $\delta 6.68$ - $\delta 8.23$ (shown in Figure 8).

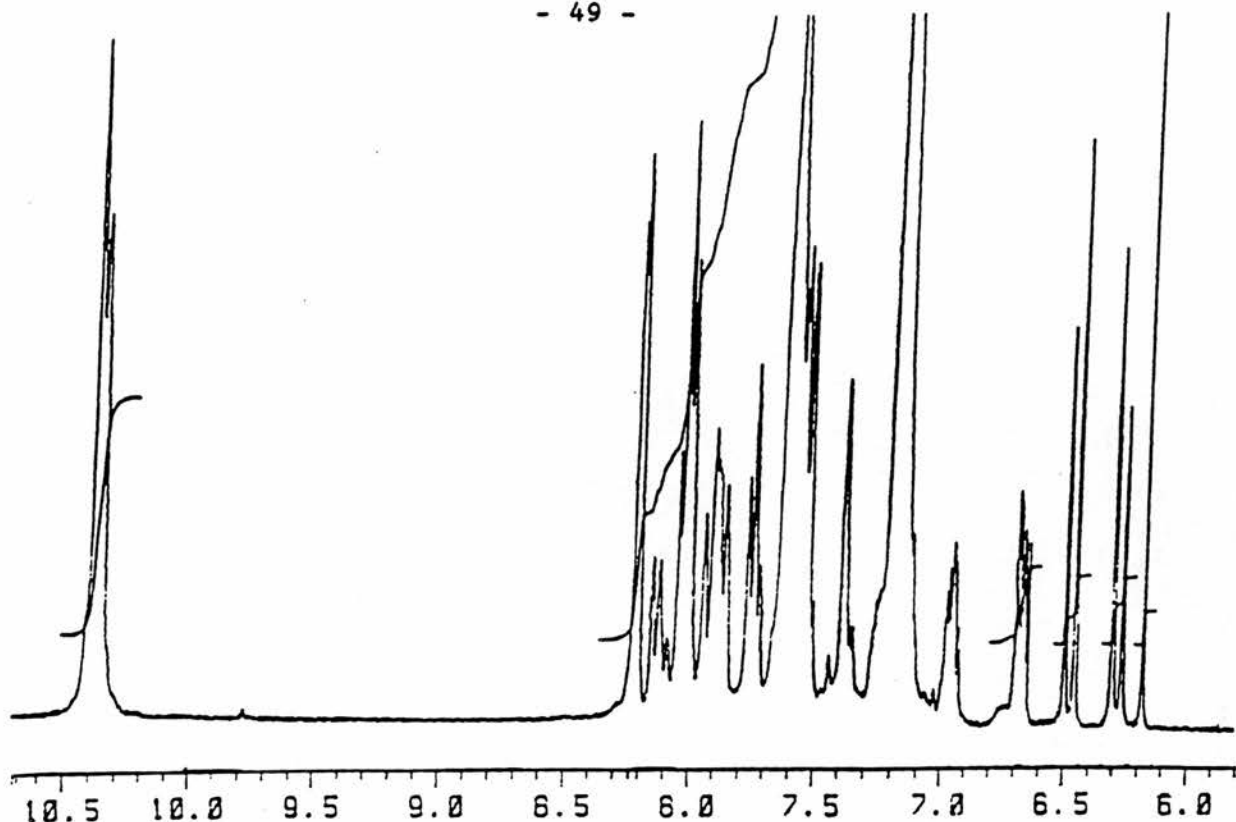


Figure 8 - The vinylic, aromatic and amide hydrogen ^1H NMR signals of PAM-1 recorded in DMSO-d_6 at 40°C .

The model compounds in Sections 2.3.2.1-2.3.2.5 show aromatic resonances over a range from δ 6.49 to δ 7.58, while the benzophenone aromatic signals in Section 2.3.2.6 resonate in the region δ 7.80 to δ 8.33. Thus it is evident that the aromatic hydrogens on the MDA component in Section Y appear up field from the aromatic hydrogens associated with the benzophenone component in Section Z. Furthermore it is noted from model compound studies that the 4,4'-methylenedianiline aromatics attached to an amine component resonate at the *high* field end of the aromatic region. Thus it is proposed that the two multiplets at δ 6.68 and δ 6.97 which are of equal intensity represent aromatic hydrogens next to an amine group. Hence from this evidence it is believed that PAM-1 contains amine ends. The aromatic resonance at the

Low field end of the spectrum (δ 8.23) is believed to be the aromatic hydrogen signal of the hydrogens between the two carbonyl groups in Section Z of the polymer.

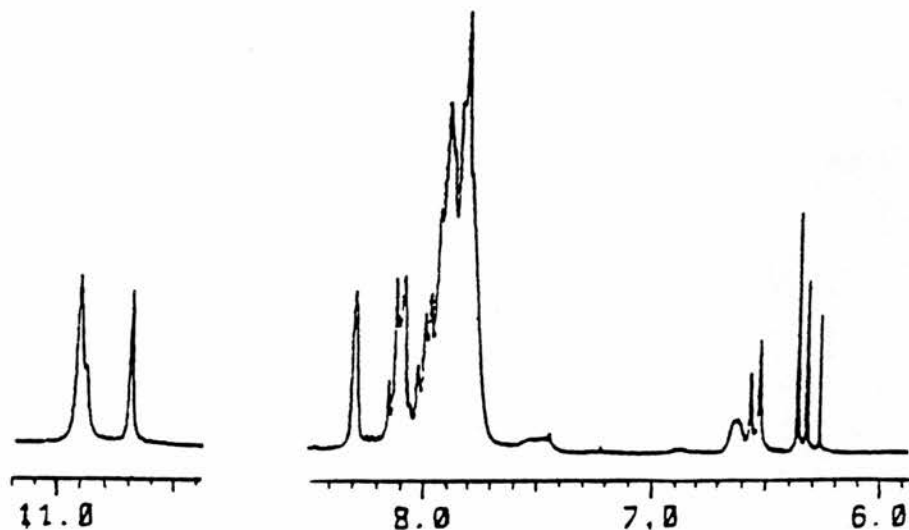
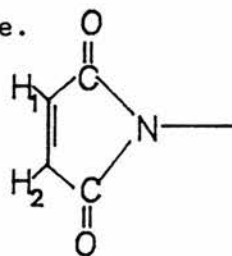


Figure 9 - The vinylic, aromatic and amide hydrogen ^1H NMR signals of PAM-2 recorded in DMSO-d_6 at 40°C .

Sections Y and Z of PAM-2 contain the combined aromatic hydrogens of the 1,4-bis(4-aminobenzoyl)-2,3,5,6-tetramethylbenzene diamine component and the benzophenone component, and are seen to resonate for PAM-2 in the range δ 7.81- δ 8.31. These aromatic resonances are more compact than those for PAM-1. The resonance at δ 8.31 is attributed to the hydrogens between the two carbonyl groups in Section Z of PAM-2. 1,4-bis(4-aminobenzoyl)-2,3,5,6-tetramethylbenzene contains aromatic resonances as low as δ 6.63, and therefore as there is no apparent evidence in the ^1H NMR spectrum of PAM-2 of aromatic resonances as low as δ 6.63, it can be assumed from this spectrum alone that there are no, or very few, amine ends in this polymer.

Section X of PAM-1 and PAM-2 contains the vinylic hydrogens of the end-cap. The ^1H NMR spectra of both PAM-1 and PAM-2 show the expected doublet of doublets in the vinylic regions. For PAM-1 the doublet of doublets is centred at δ 6.30 and δ 6.50, and for PAM-2 they are centred at δ 6.33 and δ 6.53. Both spectra also show a single peak at the low field end of the vinylic region, δ 6.20 for PAM-1 and δ 6.25 for PAM-2. This single peak has been attributed to a small amount (since the integral of the peak area is very small) of the end-cap imidising ie.



This results in H₁ and H₂ being equivalent and thus a single peak will be observed in the vinylic region.

Section Y in PAM-1 also contains a methylene group between the two phenyl rings. For the model compounds in Sections 2.3.2.1-2.3.2.5 the methylene resonance appears as a singlet as low as δ 3.56 and as high as δ 4.90.

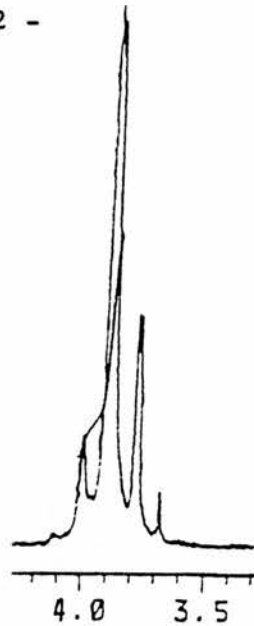


Figure 10 - The $^1\text{H-NMR}$ methylene resonances for PAM-1, recorded in DMSO-d_6 at 40°C .

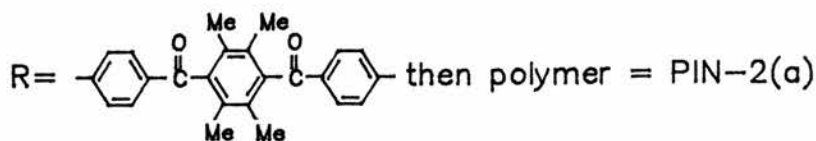
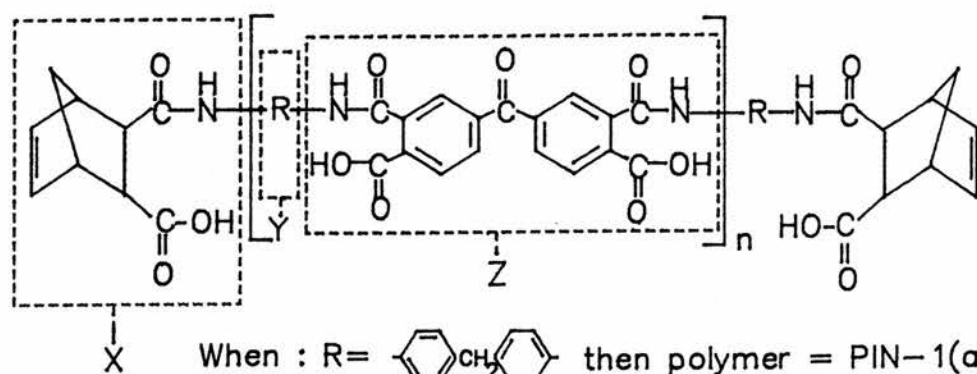
Thus the multiplet at $\delta 3.68$ - $\delta 4.00$ (four major peaks are observed for this multiplet, shown in Figure 10) in the $^1\text{H-NMR}$ spectrum of PAM-1 has been attributed to the methylene hydrogen resonances. The fact that this resonance is a multiplet and not a single peak could be due to:

- (a) the different polymer isomers formed from the reaction between the three different isomers of 3,3',4,4'-benzophenonetetracarboxylic acid dimethyl ester and 4,4'-methylenedianiline (MDA), or
- (b) as a result of the formation of oligomers with differing values of n , or

(c) as a consequence of amine ends in the polymer, hence the methylene hydrogens will be in a different environment to those with the MDA component attached to the end-cap, giving a different chemical shift for each set of methylene hydrogen resonances. This is exactly what is observed for the model compounds, the methylene hydrogen resonance has shifted from δ 3.56 in 4,4'-methylenedianiline to δ 4.90 in 1,1'-(methylenedi-4,1-phenylene)-bismaleamic acid.

Section Y in PAM-2 contains 4 methyl substituents on the central aromatic ring. These methyl hydrogens show two singlets at δ 2.04 and δ 2.06. It is not certain why two signals are observed; it may be that different oligomers ($n=1$, $n=2$, etc) result in the methyl hydrogen resonance shifting slightly up or down field, giving the appearance of a doublet.

2.3.3.2 PIN-1(a) and PIN-2(a) polyamic acids



PIN-1(a) and PIN-2(a) are the norbornene-ended polymers produced by reaction of PAM-1 and PAM-2 respectively with cyclopentadiene (reaction outlined in Scheme 12), and have compositions $[NA]_2[BTDA]_n[MDA]_{n+1}$ and $[NA]_2[BTDA]_n[(9)]_{n+1}$. The spectra of these are shown in Appendix 2 and in detail in Figures 11-15 below.

The N-H NMR signal in Section X of the polymers (next to the end-cap) resonates at δ 9.65 for PIN-1(a) (shown in Figure 11), and at δ 10.26 for PIN-2(a) (shown in Figure 12), both appearing reduced in intensity in relation to the N-H NMR signal in Section 2, which resonates at δ 10.40 for PIN-1(a) and δ 10.97 for PIN-2(a).

The backbone of the polymers PIN-1(a) and PIN-2(a) should remain unaltered from PAM-1 and PAM-2, and this is reflected in the fact that the aromatic resonance pattern for PIN-1(a) (δ 6.55- δ 8.22) is identical to that of PAM-1 (outlined in Figure 11). This is also true for the methylene resonance pattern in Section Y of PIN-1(a) (remaining unaltered from the methylene resonance pattern of PAM-1) which shows a multiplet at δ 3.60- δ 4.00 for the reasons stated in 2.3.3.1.

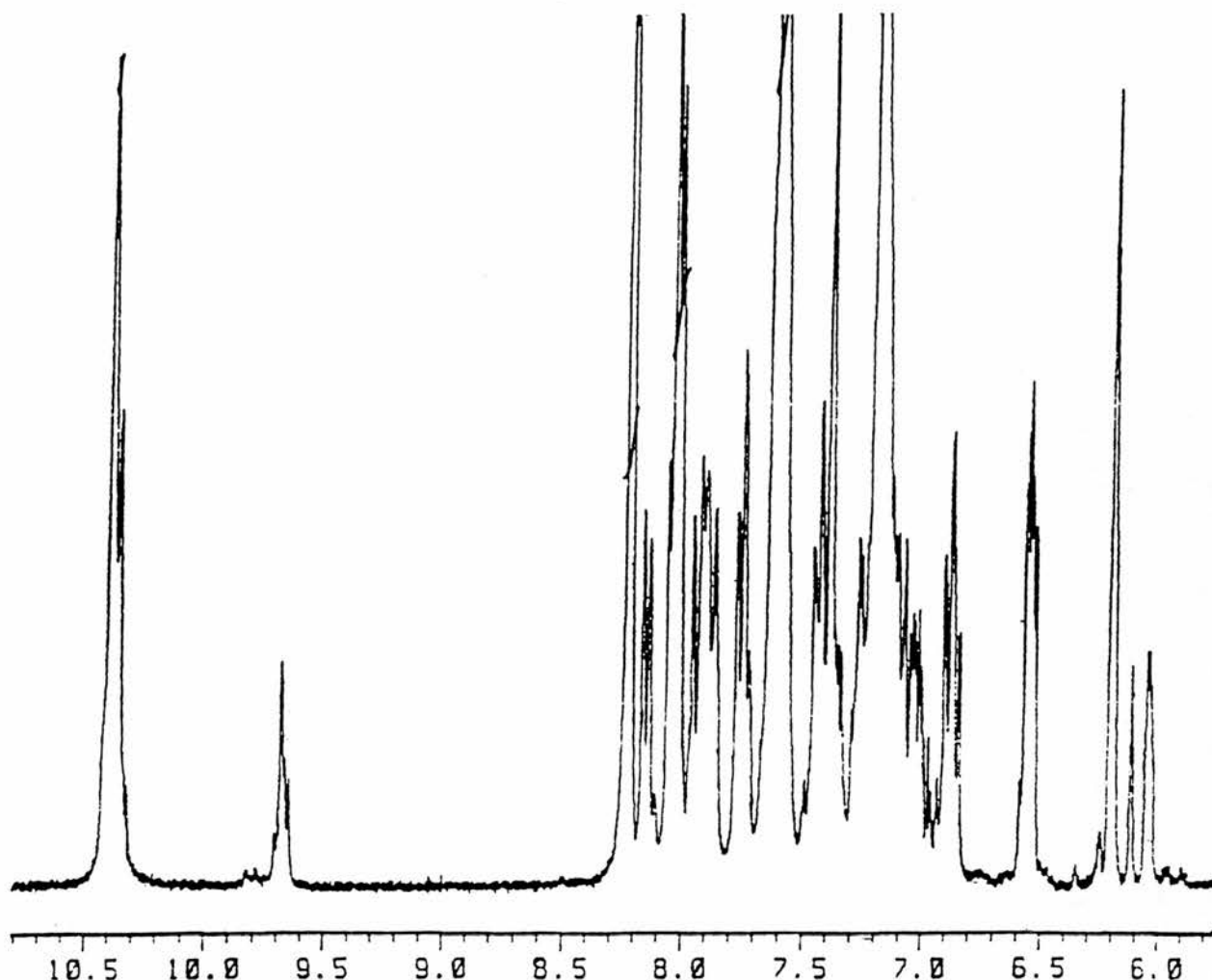


Figure 11 - The vinylic, aromatic and amide hydrogen ^1H NMR signals of PIN-1(a) recorded in DMSO-d_6 at 40°C .

However, for PIN-2(a) the main aromatic resonance pattern remains the same (δ 8.32- δ 7.46) but now a broad peak at δ 6.68 is in evidence (Figure 12). On further inspection of the ^1H NMR spectrum of PAM-2 a small broad peak adjacent to one of the doublets of the vinylic resonance can be seen at δ 6.63. These signals are at the *high* field side of the aromatics, and this suggests that both PAM-2 and PIN-2(a) contain amine ends as in the case of PIN-1 polyamic acid.

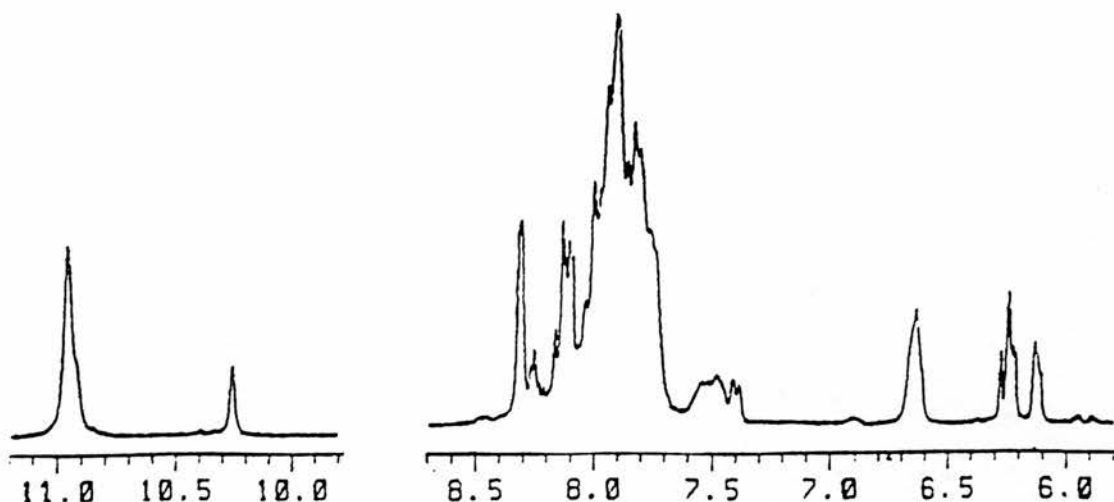


Figure 12 - The vinylic, aromatic and amide hydrogen ^1H NMR signals of PIN-2(a) recorded in DMSO-d_6 at 40°C .

From study of the model compounds it is known that the methylene bridge hydrogens (contained in Section X of the polymers) resonate the furthest upfield. Thus the signals at $\delta 1.60$ and $\delta 1.30$ in the ^1H NMR spectrum of PIN-1(a) polyamic acid have been attributed to the methylene bridge hydrogens (Figure 13).

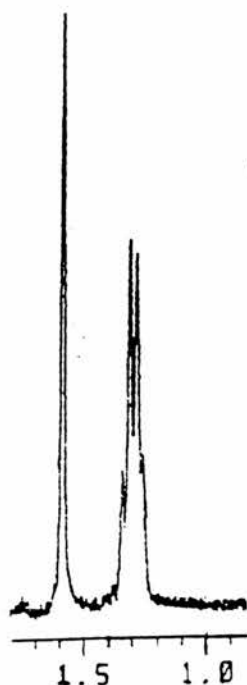
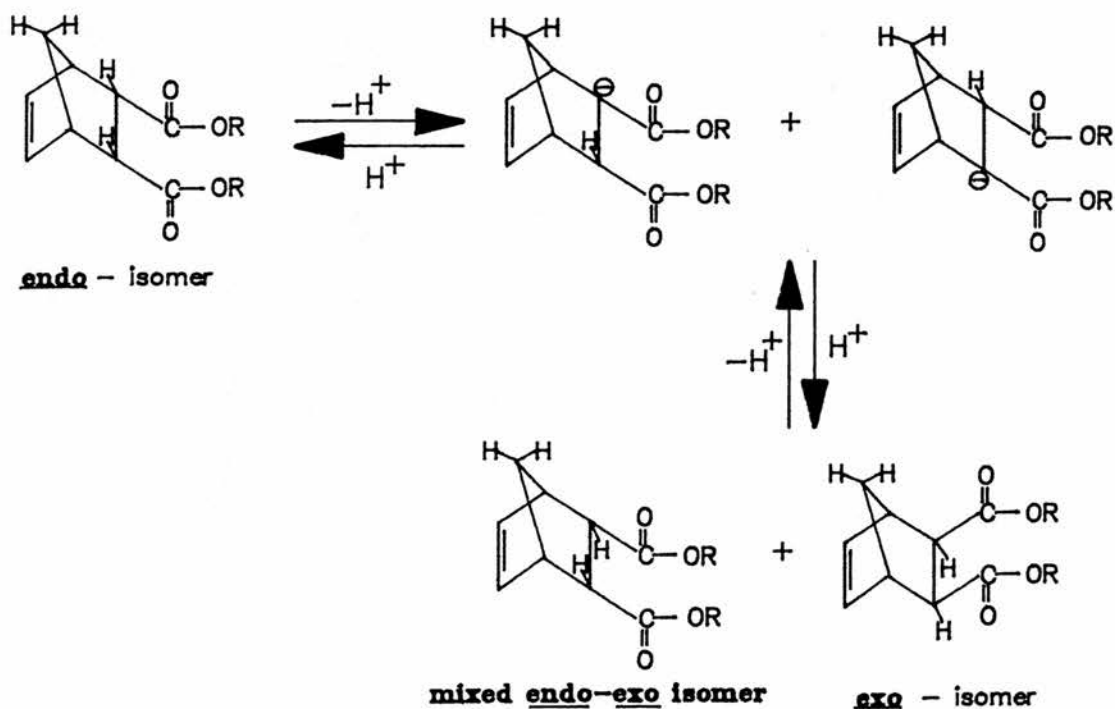


Figure 13 - The methylene bridge ^1H NMR signal of PIN-1(a) recorded in DMSO-d_6 at 40°C .

It is proposed that the low field signal is the exo isomer and the high field signal is the endo isomer. If this proposal of a mixture of endo and exo isomers is true, then this is surprising because the conversion of endo-5-norbornene-2,3-dicarboxylic anhydride (endo-nadic anhydride) into exo-5-norbornene-2,3-dicarboxylic anhydride requires high temperatures in an appropriate solvent. Thus it is proposed that some of the endo-nadic end-cap is converted to the exo-isomer in the presence of a base (such as free 4,4'-methylenedianiline (MDA)) by the formation of an enolate ion. This could happen when the hydrogens α to the carboxyl group are lost creating the enolate ion, and are subsequently replaced to give either the exo or endo forms, shown in Scheme 7.



Scheme 7

PIN-2(a) also shows two methylene bridge resonances at δ 1.60 (doublet) and δ 1.36 (multiplet) in its ^1H NMR spectrum (Figure 14), and thus for the reasons outlined above PIN-2(a) contains endo and exo-norbornene end-caps.

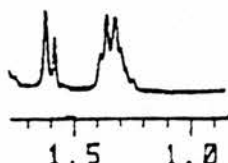
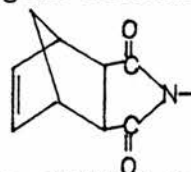


Figure 14 - The methylene bridge ^1H NMR signal of PIN-2(a) in DMSO-d_6 at 40°C .

Section X of the polymers also contains the vinylic hydrogens, which for PIN-1(a) show three split peaks at δ 6.22, δ 6.10 and δ 6.02 (Figure 11). The peak at δ 6.10 is by far the smallest in terms of peak area and is attributed to the vinylic hydrogens attached to the end-cap which has undergone imidisation. ie.



The integral of the peak area centred at δ 6.02 is similar to that of the proposed endo-methylene bridge hydrogen signal at δ 1.60, while the combined integrals of the peak areas centred at δ 6.22 and δ 6.10 are similar to the integral of the peak area of the proposed exo-methylene bridge hydrogen signal. Therefore it is suggested that the vinylic hydrogens attached to the exo-norbornene end-cap are shifted downfield from the vinylic hydrogens attached to the endo-norbornene end-cap. This hypothesis is backed up by the ^1H NMR chemical shifts of the vinylic hydrogens in exo-5-norbornene-2,3-dicarboxylic anhydride

being shifted further downfield (δ 6.48) than the vinylics in endo-5-norbornene-2,3-dicarboxylic anhydride (δ 6.28). The vinylic hydrogen resonances for PIN-2(a) show two multiplets at δ 6.13 and δ 6.24 (Figure 12). These multiplet signals are not characteristic of the vinylic signals assigned to PIN-1(a) above, but are thought to be linked to the methylene bridge hydrogen signals in the same way that the vinylics in PIN-1(a) are linked to the methylene bridge hydrogen signals. That is the two vinylic signals occur as a direct result of the presence of endo and exo norbornene isomers, with the multiplets at δ 6.24 the vinylic resonance attached to the exo-norbornene endcap. The reaction of cyclopentadiene with both PAM-1 and PAM-2 to produce PIN-1(a) and PIN-2(a) results in an increase of the aliphatic hydrogen content of the endcap (Section X). The aliphatic methylene bridge hydrogens have been discussed above which leaves the aliphatic hydrogens α and β to the carboxyl group, and by subtracting the PAM-1 $^1\text{H-NMR}$ spectrum from the PIN-1(a) $^1\text{H-NMR}$ spectrum they are found to resonate at δ 3.49 (single peak), δ 3.32 (multiplet) δ 3.21 (doublet) and δ 3.05 (doublet).

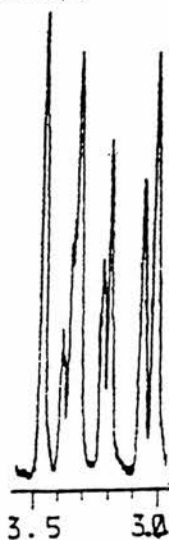
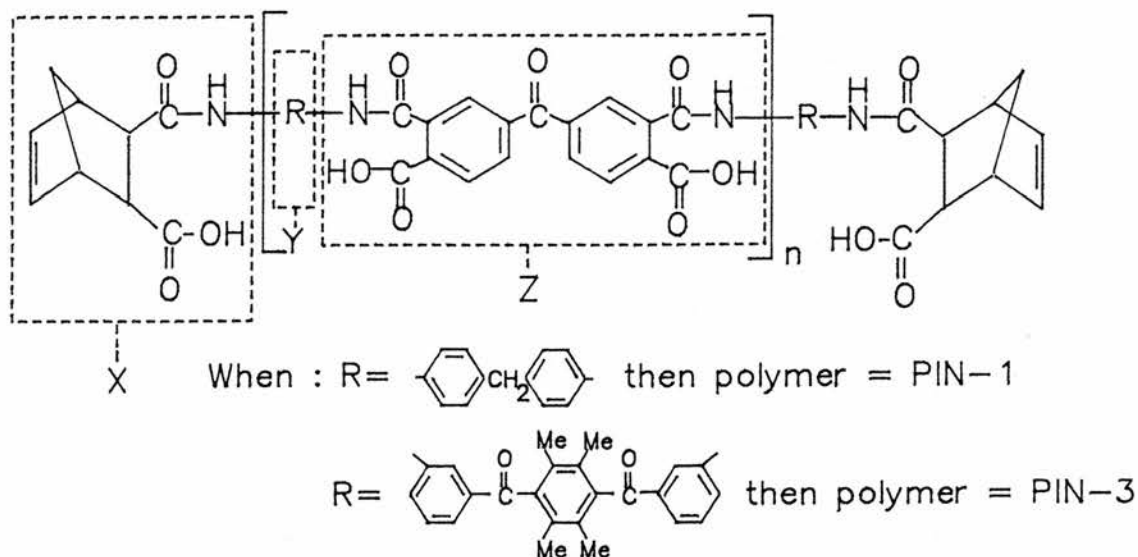


Figure 15 - The $^1\text{H-NMR}$ resonances of the aliphatic hydrogens α and β to the carboxyl group in the norbornene end-cap of PIN-1(a).

However, these signals are very complex and thus cannot be assigned to either the α or β hydrogens (Figure 15). In the same way the aliphatic hydrogens α and β to the carboxyl group in the norbornene end-cap of PIN-2(a) can be assigned to the weak resonances in the region δ 3.08- δ 3.58.

The methyl resonance pattern for PIN-2(a) remains unaltered from the one observed for PAM-2 showing two singlets at δ 1.97 and δ 2.01.

2.3.3.3 PIN-1 and PIN-3 polyamic acids



PIN-1 polyamic acid is a norbornene ended polyamic acid with composition $[NA]_2[BTDA]_n[MDA]_{n+1}$ and differs from PIN-1(a) in that norbornene-2,3-dicarboxylic anhydride was used as the endcap (rather than forming the norbornene endcap by reacting the maleimide ended polymer with cyclopentadiene, ^{as} in the case of PIN-1(a) polyamic acid).

PIN-3 is a norbornene ended polyamic acid containing 1,4-bis(3-aminobenzoyl)-2,3,5,6-tetramethylbenzene(10) with composition $[NA]_2[BTDA]_n[10]_{n+1}$. The 1H NMR spectra of these polymers is shown in Appendix 2.

The amide *hydrogen* in Section X of the polymers (next to the endcap) resonates at δ 9.70 for PIN-1 and at δ 10.07 for PIN-3, both appearing reduced in intensity in relation to the amide *hydrogen* in Section Z, which resonates at δ 10.40 for PIN-1 and δ 10.74 for PIN-3. The aromatic resonance pattern for PIN-1 (Sections Y and Z) is identical to that of PIN-1(a) and PAM-1, resonating in the region δ 8.29- δ 6.57. This contains the two multiplets of similar intensity at δ 6.57 and δ 6.88, which have been attributed earlier (see PAM-1) to amine-ended polymer, and also shows the single peak at δ 8.29 which has been assigned to the hydrogens between the two carbonyl groups in Section Z. The aromatic hydrogens in Sections Y and Z for PIN-3 resonate in the region δ 6.82- δ 8.29 (Figure 16).

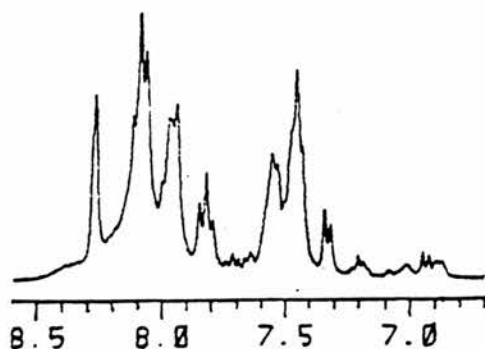


Figure 16 - The aromatic hydrogen 1H NMR signals of PIN-3 recorded in $DMSO-d_6$ at $40^\circ C$.

This aromatic resonance pattern covers a wide area of the aromatic region, and for the same reasons discussed for PIN-2(a) and PAM-1, the ^{high} field aromatic resonance signals must result from the presence of amine ends in the polymer. The multiplet centred at δ 7.50 probably results from the aromatics present in the diamine component in Section Y of the polymer, with the other broad peaks downfield resulting from the aromatic resonances in Section Z, These include the characteristic single peak at the high field end of the aromatic region (δ 8.29), due to the hydrogen resonances between the two carbonyl groups in Section Z.

The signals at δ 1.55 (single peak) and δ 1.30 (multiplet) in the ¹HNMR spectrum of PIN-1 can be attributed to the methylene bridge resonances due to the endo and exo-isomers of the norbornene endcap (described in detail for PIN-1(a)).

PIN-3 also shows two weak methylene bridge signals at δ 1.59 and δ 1.31. Section X of the polymers also contains the vinylic hydrogens which for PIN-1 show three split peaks at δ 6.22, δ 6.12 and δ 6.08, which is an identical vinylic resonance pattern to PIN-1(a). The vinylic resonance at δ 6.12 is thus attributed to vinylic hydrogens attached to imidised endcap. The integral of the peak area centred at δ 6.08 is similar to that of the proposed endo-methylene bridge hydrogen signal at δ 1.58, while the combined integrals of the peak areas centred at δ 6.22 and δ 6.12 is similar to the integral of the peak area of the proposed exo-methylene bridge hydrogen signal. Thus as in the case of PIN-1(a) it is

again proposed that the vinylic hydrogens attached to the exo-norbornene endcap resonate downfield from the vinylic hydrogens attached to the endo-norbornene endcap.

The vinylic hydrogen resonance for PIN-3 shows two multiplets at δ 6.21 and δ 6.10 similar to those shown for PIN-2(a), and are thought to be linked to the methylene bridge signals in the same way that the vinylics in PIN-1(a) and PIN-1 are linked to the methylene bridge signals. That is, the two vinylic signals occur as a direct result of the vinylic hydrogens being attached to either the endo or exo norbornene isomers. Thus the multiplet at δ 6.21 is the vinylic signal of the hydrogens attached to the exo-norbornene endcap, and the δ 6.13 vinylic resonance is the vinylic hydrogens attached to the endo-norbornene endcap.

The aliphatic hydrogens α and β to the carboxyl group in Section X for both polymers are assigned as follows; PIN-1: δ 3.46 (single peak), δ 3.34 (triplet), δ 3.22 (doublet), δ 3.04 (doublet), which is identical to the substitution pattern found for PIN-1(a) PIN-3: these only show weak resonances in the region δ 3.52- δ 3.05.

The methylene resonance in Section Y of PIN-1, gives the identical resonance pattern to PAM-1 and PIN-1(a) for the reasons suggested in 2.3.3.1 at δ 3.91.

The four methyl substituents attached to the central ring in Section Y of PIN-3, resonate to give two singlets at δ 1.97 and δ 2.05, which is identical to both PAM-2 and PIN-2(a).

2.3.4 ^1H NMR polymer interpretation summary

Table C is a summary table containing the $^1\text{HNMR}$ chemical shifts due to the various sections within the polymer backbone.

TABLE C

POLYMER	^1H NMR CHEMICAL SHIFT (PPM)							
	1 ^d	2 ^e				a,b	c	
PAM-1	10.41	/	8.23-6.68	6.30,6.50, 6.20	3.92 (multiplet)	NA	NA	NA
PIN-1(a) polyamic acid	10.40	9.65	8.22-6.55	6.22,6.10, 6.02	3.91 (multiplet)	3.49,3.32 3.21,3.05	1.60,1.30	NA
PIN-1 polyamic acid	10.40	9.70	8.29-6.57	6.22,6.12 6.08	3.91 (multiplet)	3.46,3.34 3.22,3.04	1.58,1.30	NA
PAM-2 polyamic acid	10.88	10.69	8.31-7.82	6.53,6.33 6.25	NA	NA	NA	1.95
PIN-2(a) polyamic acid	10.97	10.26	8.32-7.46	6.24,6.13	NA	3.58-3.08	1.60,1.36	2.02
PIN-3 polyamic acid	10.74	10.07	8.29-6.82	6.28,6.21 6.10	NA	3.52-3.05	1.59,1.32	2.01

* NB PIN-2 is not included in this table because the $^1\text{HNMR}$ resonances were too weak to analyse accurately.

d-1 is the amide link between the dianhydride component and the amine component of the polymer.

e-2 is the amide hydrogen attached to the amide link between the endcap and the diamine component.

The identification of the functional groups within the polymer by $^1\text{H NMR}$ allows the number average molar mass M_n to be calculated.

2.3.5 Number average molar mass (M_n) calculated by NMR spectroscopy

The number average molar masses (M_n) were determined and are shown below in Tables D and E for all the polymers outlined in Table C, by calculation of the peak area ratio of two functional groups within the polymer to give the repeat unit n from which M_n can be determined:

TABLE D

Polyamic acid	calculated n	FMW ^a	n^1	M_n^1	n^2	M_n^2	n^3	M_n^3
PIN-1	2.09	1614	2.60	1900	3.10	2100	2.47	1800
PIN-1(a)	2.09	1614	4.12	2700	3.95	2600	2.15	1600
PAM-1	2.09	1482	2.86 ^b	1900	/	/	2.14	1500

n^1 - n was calculated from the ratio of the $^1\text{H NMR}$ peak area of the methylene bridge on the norbornene endcap to the $^1\text{H NMR}$ peak area of the methylene group between the phenyl groups.

n^2 - n was calculated from the ratio of the $^1\text{H NMR}$ peak area of the methylene bridge on the norbornene endcap to the $^1\text{H NMR}$ peak area of the aromatic hydrogens.

n^3 - n was calculated from the ratio of the $^1\text{H NMR}$ peak area of the methylene group between the phenyl rings to the $^1\text{H NMR}$ peak area of the aromatic hydrogens.

- a Formulated molecular weight (FMW) of the polyamic acid.
- b This value was calculated from the ratio of the $^1\text{HNMR}$ area of the vinylic protons attached to the maleamic acid endcap, to the $^1\text{HNMR}$ peak area of the methylene group between the phenyl rings.

TABLE E

Polyamic acid	calculated n	FMW ^a	n ¹	Mn ¹	n ²	Mn ²	n ³	Mn ³
PIN-2	2.09	2153	2.35	2300	2.25	2300	2.13	2200
PIN-2(a)	2.09	2153	3.67	3300	3.43	3100	2.08	2100
PIN-3	2.09	2153	2.21	2200	2.84	2700	2.58	2500
PAM-2	2.09	2020	/	/	1.83	1800	2.07	2000

n¹-n was calculated from the ratio of the $^1\text{HNMR}$ peak area of the vinylic protons attached to the endcap to the $^1\text{HNMR}$ peak area of the methyl substituent.

n²-n was calculated from the ratio of the $^1\text{HNMR}$ peak area of the vinylic protons attached to the endcap to the $^1\text{HNMR}$ peak area of the aromatic hydrogens.

n³-n was calculated from the ratio of the $^1\text{HNMR}$ peak area of the methyl substituents to the $^1\text{HNMR}$ peak area of the aromatic hydrogens.

Table D shows three different calculated number average molar masses, Mn^1 , Mn^2 and Mn^3 for the three polyamic acids PIN-1, PIN-1(a) and PAM-1. Mn^3 for these three polymers is lower than either Mn^1 or Mn^2 . This is probably because when calculating Mn^1 and Mn^2 , the Mn is calculated from a ratio involving either the vinylic protons or the methylene bridge protons on the end-cap, and if these signals are smaller than the theoretical values in terms of peak area, then the value for Mn will be larger than both the theoretical (FMW), and any Mn value calculated from a ratio which does not involve the end-cap (eg Mn^3 Table D). Thus Mn^1 and Mn^2 are larger than Mn^3 (in Table D) and the FMW, because the polymers are not fully end-capped. Hence the comparison between Mn^3 and Mn^1 or Mn^2 gives an estimation of the degree of end-capping. It is thus proposed that Mn^3 in Table D is the most accurate measure of the number average molecular weight, with Mn^1 and Mn^2 giving an idea of how well the polymers have been end-capped. Mn^3 values in Table D for PAM-1 and PIN-1(a) are almost identical. This is to be expected as PIN-1(a) is the reaction product of PAM-1 and cyclopentadiene and, assuming no degradation of the polymer backbone, the reaction would be expected to occur without much change in Mn. Mn^3 of PIN-1 is slightly higher than those of PIN-1(a) and PAM-1, which may indicate that maleic anhydride (used as the end-capper in PAM-1) is slightly more reactive than nadic anhydride (used as the end-capper in PIN-1), and thus controls molecular weight to the desired level. The Mn^1 value for PIN-1(a) (the reaction product of PAM-1 with cyclopentadiene) is considerably higher than the Mn^1 value for

PAM-1 which indicates the Diels-Alder reaction between PAM-1 and cyclopentadiene to convert the maleimide ends of the polymer into norbornene ends has not gone to completion, thereby giving a low signal for the methylene bridge protons and thus producing a high M_n value. The M_n^1 , M_n^2 values for PIN-1 are not excessively higher than the FMW value, and therefore although nadic anhydride is less reactive than maleic anhydride, it is still an effective end-capper. Thus under closely controlled reaction conditions nadic anhydride gives a polymer close to its FMW, and end-capped to a high degree. (This keeps the amine ends to a minimum and therefore minimises the Michael addition crosslinking mechanism see 1.1.5).

Table E shows the M_n values for the polymers containing diamines (9) and (10). M_n^3 values for the four polymers are the closest to the FMW values, and because M_n^3 values are not calculated from a ratio involving the endcap, these values are taken to be the most accurate for these polymers. The M_n^1 and M_n^2 values for PIN-2(a) are a great deal higher than the M_n^3 value because M_n^1 and M_n^2 are calculated from a ratio involving the norbornene vinylic hydrogens, and thus it can be concluded that the Diels-Alder reaction of PAM-2 with cyclopentadiene to produce PIN-2(a) (ie the conversion of maleimide ends to norbornene ends) has not gone to completion. This gives a low vinylic hydrogen signal and thus produces high M_n values. The M_n^2 values for both PIN-2 and PIN-3 are higher than M_n^3 and the FMW, and since the M_n^2 value is based on a ratio involving the end-cap, then it must be concluded that these polymers are not completely norbornene endcapped.

2.4 Thermal analysis of the imidised polymers fabricated in Section 3

2.4.1 Introduction

Thermogravimetric analysis and isothermal ageing are closely related. Isothermal analysis records the change in weight of the sample at a given temperature as a function of time, while thermogravimetric analysis (TGA) measures the change in weight of the sample as a function of temperature as the temperature is increased at a given rate. Both techniques are used together because they give complementary data: TGA is used to show the temperature range over which a particular polymer is thermally stable, thus this technique ranks polymers in order of thermal oxidative stability (TOS). Polymers with suitable TOS values (obtained by TGA) are then isothermally aged to provide information on potential service temperatures and times.

In simple terms, the dynamic mechanical thermal analysis (DMTA) technique measures the modulus of a sample as the temperature is varied. For measurement of the glass transition temperature (T_g) of a material, DMTA is found to be significantly more sensitive than differential thermal analysis techniques such as DSC (Differential Scanning Calorimetry). The DMTA technique applies a sinusoidal stress to the sample under examination (the sinusoidal stress is applied by supplying a sinusoidal current to a vibrator unit in the DMTA head). If the solid is perfectly elastic, elastic deformation takes place, with the strain occurring in phase with the stress. This elastic deformation is the storage

modulus and is referred to as E' . E'' is the loss modulus. This is the viscous component of the deformation and arises when some internal molecular motion occurs in the same frequency range as the applied stress. Thus the sample behaves in a viscoelastic manner, with the strain lagging behind the stress. $\tan \delta$ is the loss tangent and is a measure of $\frac{E''}{E'}$. This term is dimensionless.

2.4.2 Isothermal ageing results

Isothermal ageing studies were carried out on the following cross-linked polymers (fabrication of which is described in 3.5.4) PMR-15 control, PIN-1, PIN-1(a), PIN-2, PIN-2(a), PIN-3, PMR-II-30 under the conditions outlined in Section 3.7.1.1.1. The results of these experiments are depicted in Figures 17 and 18.

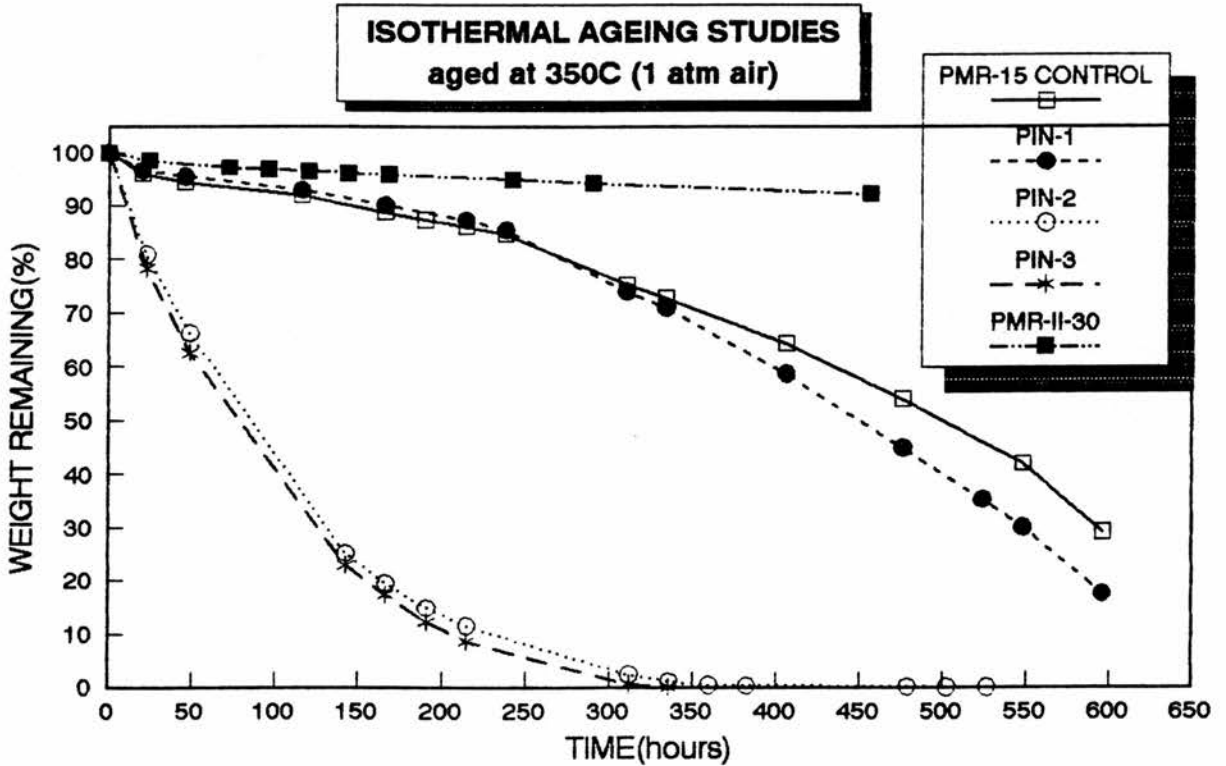


Figure 17

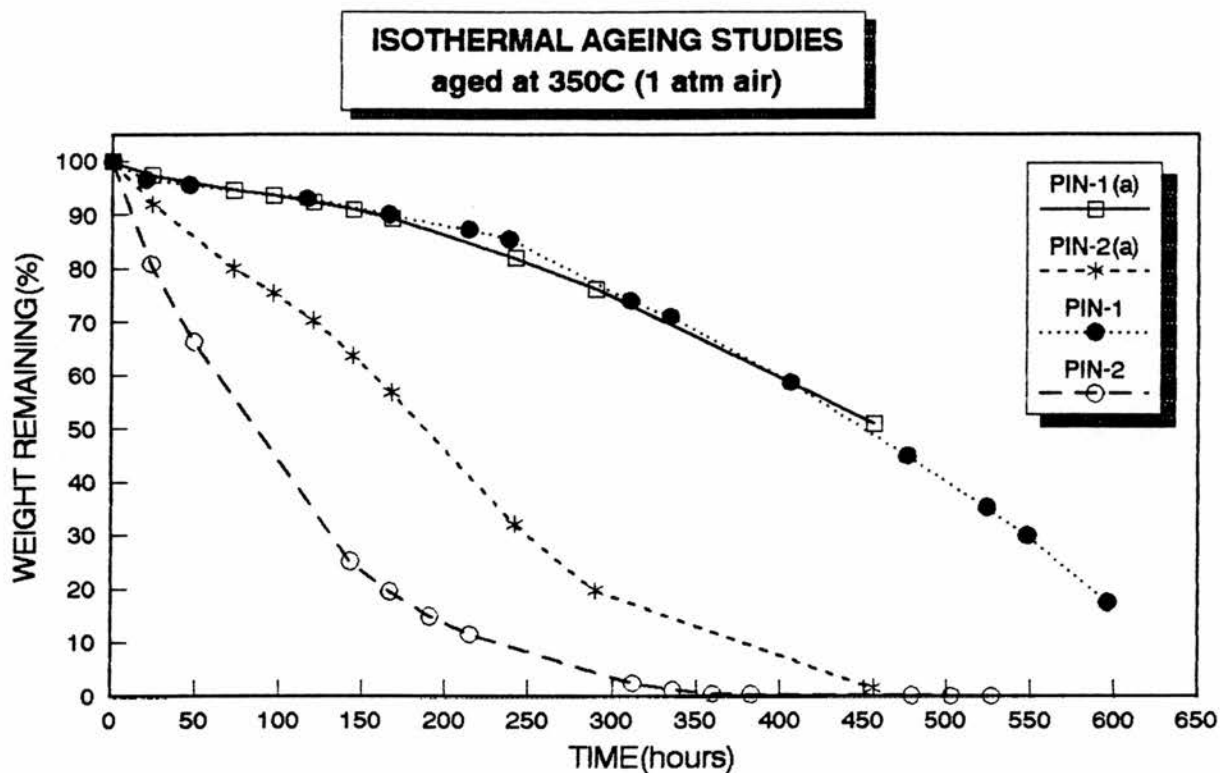
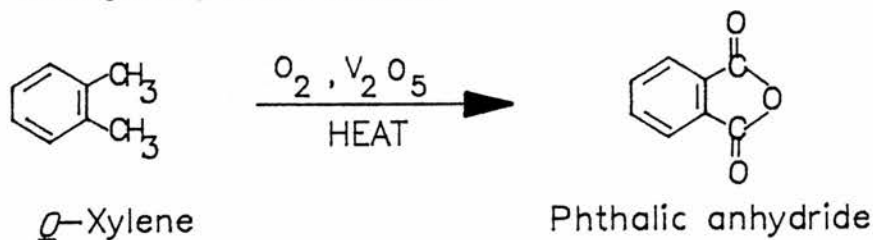


Figure 18

It must be noted that PMR-II-30 with composition $[NA]_2[HFDA]_n$ $[PPDA]_{n+1}$ has a Formulated Molecular Weight (FMW) double that of the other polymers synthesised. Thus PMR-II-30 cannot be used as a direct comparison for the other polymer systems fabricated because an increase in molecular weight of these norbornene-ended thermosetting polymers results in an increase in thermal stability upto a FMW of 5000^{1,2}. (This is due to the decreasing aliphatic content of the end-cap). PMR-II-30 also contains the more thermally stable dianhydride, HFDA. However, PMR-II-30 was included in these studies to illustrate the excellent thermal oxidative properties of a processable high temperature thermosetting polymer (<10% weight loss after 500 hrs at 350°C). Figure 17 shows the results of ageing PMR-15 control, PIN-1, PIN-2 and PIN-3 at 350°C.

It can be seen that PIN-2 and PIN-3 with compositions, $[NA]_2[BTDA]_n[(9)]_{n+1}$ and $[NA]_2[BTDA]_n[(10)]_{n+1}$ respectively, show inferior thermal oxidative stability (TOS) properties to those observed for the PMR-15 control and PIN-1 both with composition $[NA]_2[BTDA]_n[MDA]_{n+1}$. Thus since the only variable in the compositions of these polymers is the diamine, it must be assumed that the loss in the thermal stability of polymers PIN-2 and PIN-3 is a consequence of the diamine component within these polymers undergoing thermal oxidation. PIN-2 contains the diamine, 1,4-bis(4-aminobenzoyl)-2,3,5,6-tetramethylbenzene(9) and PIN-3 contains the diamine, 1,4-bis(3-aminobenzoyl)-2,3,5,6-tetramethylbenzene(10). Both these diamines contain four methyl substituents on the central phenyl ring (the structures of diamines (9) and (10) are shown in Section 1.2.2). It was hoped that the methyl substituents would cross-link into the polymer network²⁶ (although methyl substituents are well known to undergo oxidation, the industrial production of phthalic anhydride in Scheme 8 is an example). Such an effect would increase the number of crosslinks per repeat unit in the polymer, thus enhancing its thermal stability. However, from Figure 17 it is evident that the methyl substituents are probably not taking part in a crosslinking mechanism, but are most likely undergoing oxidation at elevated temperatures, a process which results in the poor oxidative stability of the polymers, PIN-2 and PIN-3. The molecular weights of PIN-2 and PIN-3 are not factors in their poor oxidative thermal stability because the measured number average molar masses M_n of the polyamic acids (measured by ¹H-NMR) are higher than the PIN-1 polyamic acid measured M_n (see Section 2.3.5). This shows

good thermal oxidative stability when it is imidised and subsequently cross-linked.



Scheme 8

PIN-1 and PMR-15 control fabricated polymers show almost identical ageing curves (Figure 17); they only differ in the methods of their synthesis; Both polymers have the same compositions and FMWs, and hence would be expected to have similar ageing characteristics. Furthermore, it can be assumed that because the PMR-15 control polymer has a similar thermal oxidative stability to that of the PIN-1 polymer, the number average molar masses (M_n) of the two polymers must be similar.

Figure 18 compares polymer PIN-1 with PIN-1(a) (both having compositions $[\text{NA}]_2[\text{BTDA}]_n[\text{MDA}]_{n+1}$), and polymer PIN-2 with PIN-2(a) (with compositions $[\text{NA}]_2[\text{BTDA}]_n[(9)]_{n+1}$). PIN-1(a) and PIN-2(a) were synthesised from the respective maleimide ended polymers, PAM-1 and PAM-2 by a Diels-Alder reaction with cyclopentadiene. Figure 18 shows PIN-2 and PIN-2(a) to have very poor thermal oxidative stability, believed to be caused by the methyl substituents attached to the respective diamines undergoing oxidation at elevated temperatures as discussed above. Interestingly PIN-2(a) is shown to exhibit better thermal

oxidative stability than PIN-2 (shown in Figure 18), even though they both have similar Mns (measured by $^1\text{H-NMR}$). A possible explanation could be that PIN-2(a) contains maleimide ends as well as nadimide ends,^{as} concluded from the $^1\text{H-NMR}$ evidence in Section 2.3.5 (due to incomplete reaction of PAM-2 with cyclopentadiene). Thus PIN-2(a) will contain a reduced concentration of aliphatic hydrogen endcap resulting in an increase in the thermal oxidative stability of the polymer compared to the fully nadimide-ended polymer. PIN-1 and PIN-1(a) give similar ageing curves, even though the NMR interpretation revealed the presence of a small amount of maleimide in PIN-1(a). Figures 17 and 18 also reveal that the polymers PMR-15 control, PIN-1 and PIN-1(a) have isothermal ageing curves with relatively gentle gradients, which indicates that these resin matrices will survive temperatures of 350°C for short periods of time (about 200 hrs) without a significant weight loss (which correlates with a loss in mechanical properties for the resin).

2.4.3 Thermogravimetric analysis (TGA) results

Thermogravimetric analysis was undertaken on the following cross-linked polymer resins (fabrication of which is described in 3.5.4): PMR-15 control, PIN-1, PIN-1(a), PIN-2, PIN-2(a) and PIN-3, under the conditions described in Section 3.7.1.2.1. The results are shown in Figures 19, 20, 21 and 22.

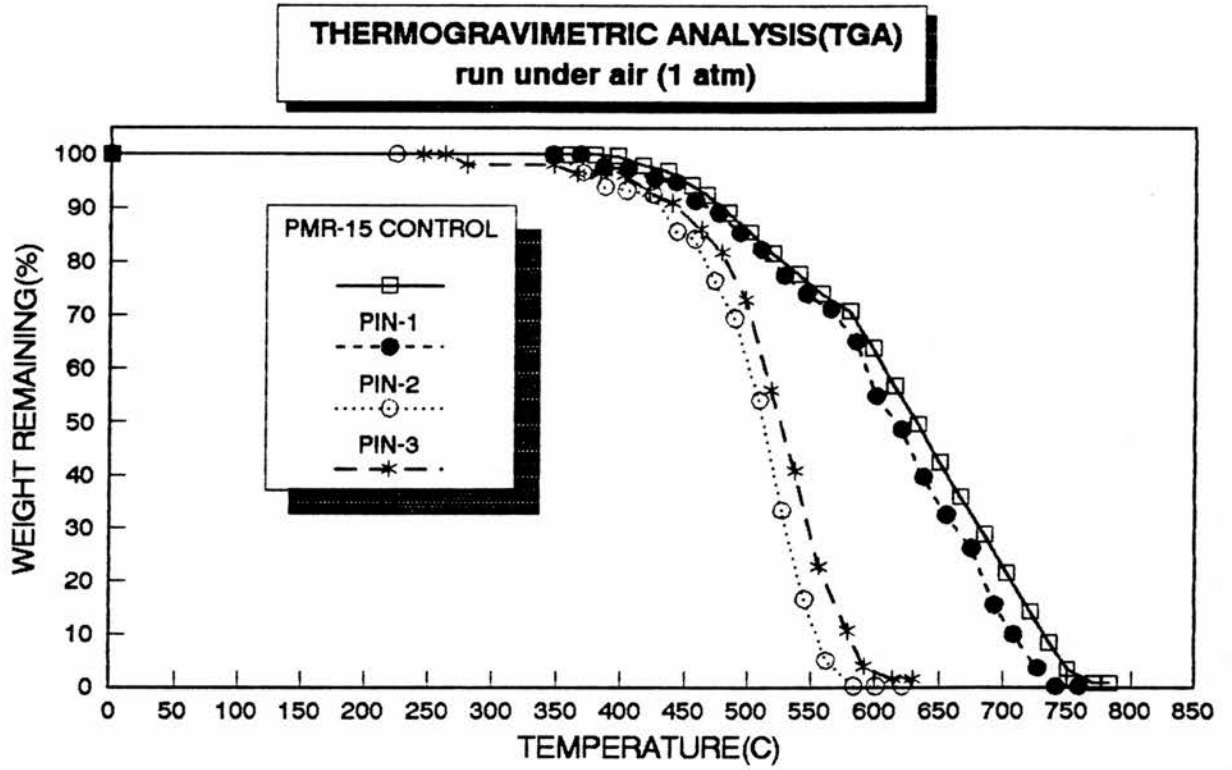


Figure 19

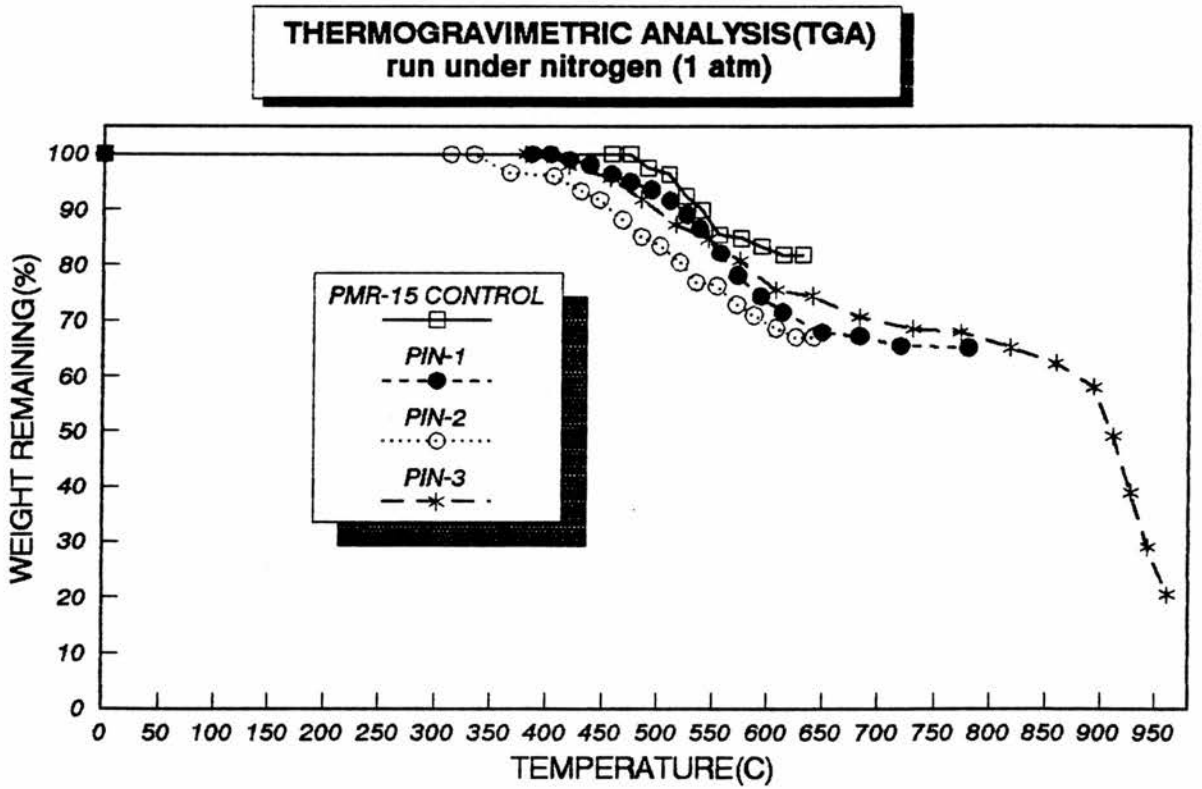


Figure 20

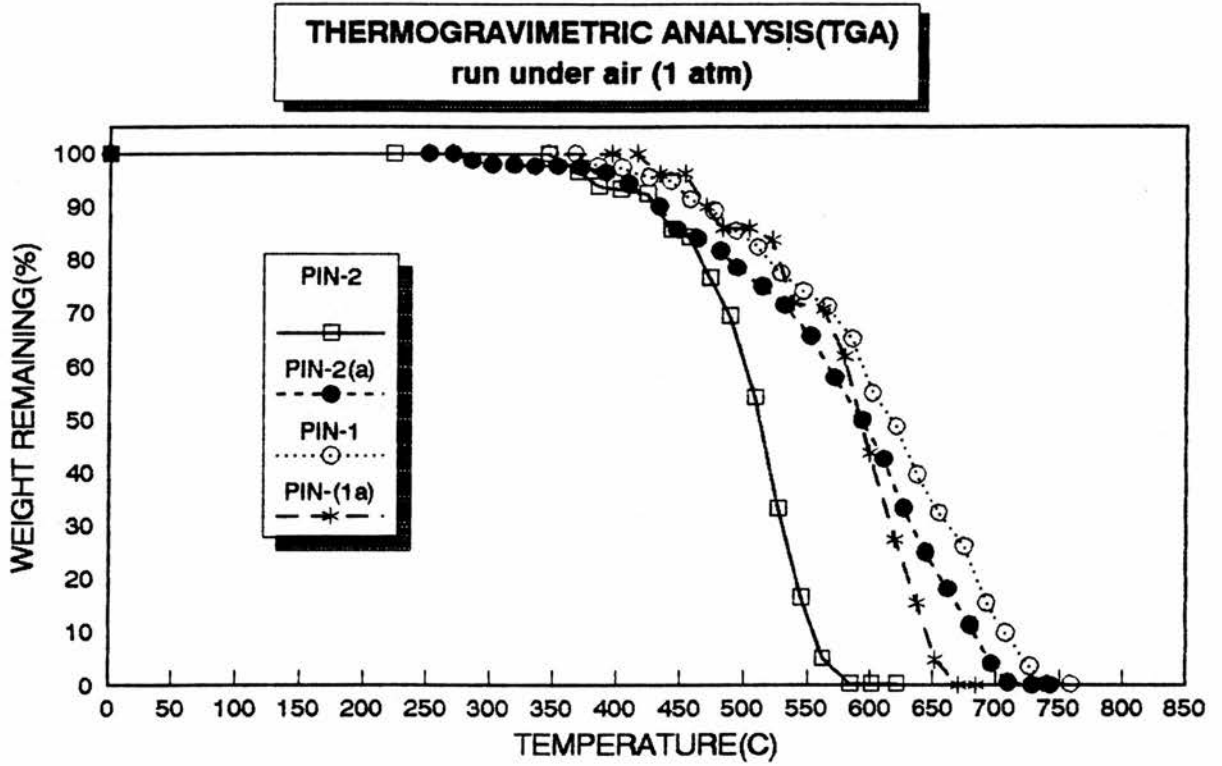


Figure 21

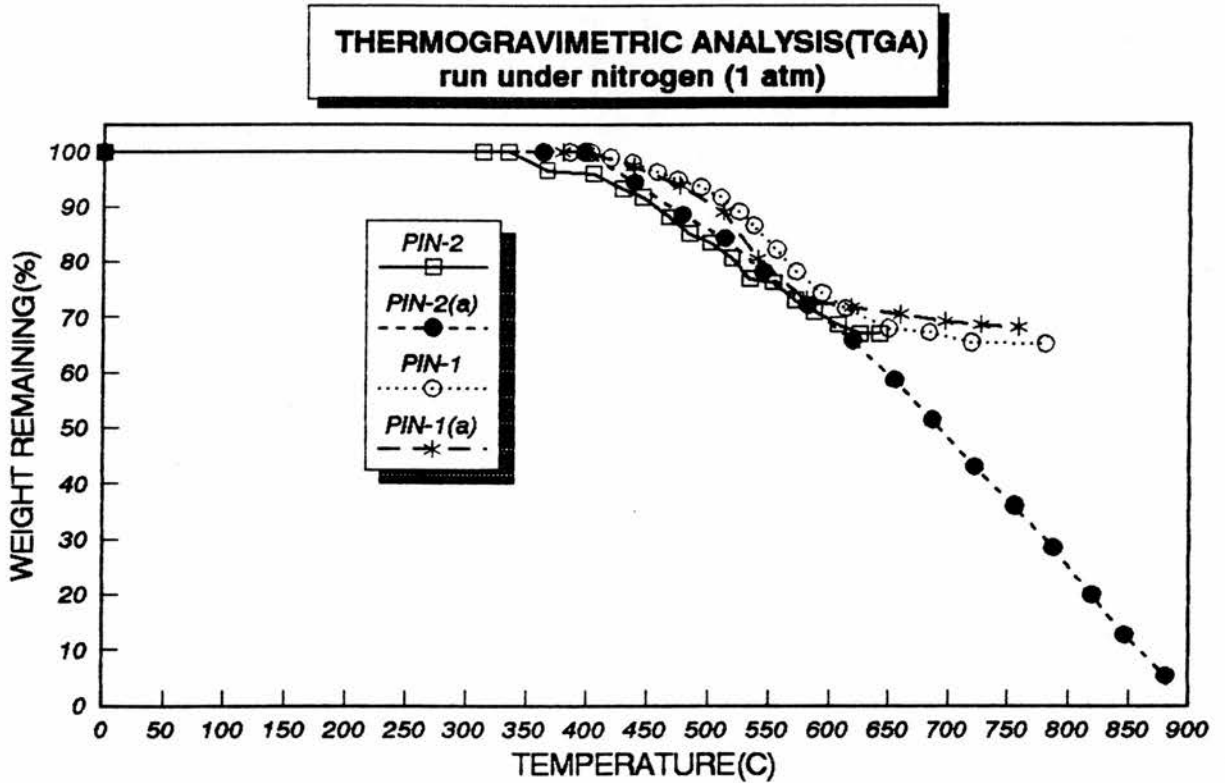


Figure 22

Figures 19 and 20 compare the TGA traces of PMR-15 control, PIN-1, PIN-2 and PIN-3 run under 1 atmosphere of air with those run under 1 atmosphere of nitrogen.

This comparison illustrates the contribution of thermal oxidative degradation towards the overall degradation of the polymer, as well as illustrating over what temperature ranges these polymers are thermally stable (both under nitrogen and air).

Figures 19 and 20 reveal that:

- (a) with the exception of PIN-2, polymers PMR-15 control, PIN-1 and PIN-3 have higher degradation onset temperatures under nitrogen than under air. (ie. PMR-15 control, 474°C (N₂), 378°C (air); PIN-1, 402°C (N₂), 367°C (air); PIN-3, 399°C (N₂), 262°C (air)), and
- (b) the degradation curves of the four polymers under nitrogen show plateaus at approximately 600°C corresponding to residual char, >60% yield (ie carbon and nitrogen). This effect differs from the TGA curves run under air, where the polymers degrade completely, presumably releasing CO₂, H₂O and nitrogen oxides. Thus from the comparison of Figures 19 and 20 the major role of oxidation in the degradation of these polymers at elevated temperatures can be clearly seen.

The relatively low onset temperatures of degradation for PIN-2 and PIN-3 under air (Figure 19) and the steep gradient of the subsequent degradation curves, show the lack of thermal oxidative stability of these polymers in comparison with the 4,4'-methylenedianiline (MDA) containing polymers viz PIN-1 and the PMR-15 control.

Figures 21 and 22 compare PIN-1 with PIN-1(a) (the reaction product of PAM-1 with cyclopentadiene) and PIN-2 with PIN-2(a) (the reaction product of PAM-2 with cyclopentadiene) under both air and nitrogen. The following observations were made:

- (a) Polymers PIN-1 and PIN-2(a) show higher degradation onset temperatures under nitrogen than under air (e.g. PIN-1, 402°C (N₂), 367°C (air); PIN-2(a), 397°C (N₂), 270°C (air)).
- (b) Even though polymers PIN-2 and PIN-1(a) show higher degradation onset temperatures under air than under nitrogen (e.g. PIN-2, 346°C (air), 334°C (N₂); PIN-1(a), 410°C (air), 399°C (N₂)), the rate at which both polymers lose weight (degrade) is faster when run under air than under nitrogen (e.g. PIN-2 has 54.1% weight remaining in air at 509°C, but has 83.5% weight remaining in nitrogen at 501°C. PIN-1(a) has 61.7% weight remaining in air at 579°C, but has 73.1% weight remaining in nitrogen at 580°C).
- (c) Figure 22 clearly shows that under nitrogen, degradation of the polymers is markedly reduced, with PIN-1, PIN-1(a) and PIN-2 showing a significant char yield (>60% yield) at approximately 600°C.

(d) The crosslinked polymer resin PIN-2(a) shows a lower degradation onset temperature in comparison to PIN-2, but thereafter PIN-2 degrades more rapidly than PIN-2(a) (from 450°C upwards), clearly illustrated in Figure 21. This observation was made in the isothermal section and was explained in terms of the reduced aliphatic hydrogen endcap content increasing the thermo-oxidative stability of PIN-2(a).

PIN-1 and PIN-1(a) give similar degradation curves (and degrade at a slower rate than either PIN-2 and PIN-2(a) for the reasons discussed in Section 2.4.2). This result is consistent with polymers of similar average number molecular weights (M_n) (measured by NMR in Section 2.3.5) and with the same compositions.

2.4.4 Dynamic mechanical thermal analysis (DMTA) results

DMTA was performed to ascertain the T_g values of the following crosslinked polymers; PMR-15 control, PIN-1, PIN-1(a), PIN-2, PIN-2(a), PIN-3 and PMR-II-30. The T_g for each individual system was measured from three different plots:

- (a) the storage modulus, E' versus temperature
- (b) the loss modulus E'' versus temperature

(c) Tan δ versus temperature

The Tgs obtained for these crosslinked polymer resins are detailed below in Table F.

TABLE F

CROSS-LINKED POLYMER RESIN	Measured Tgs from DMTA curves		
	T _g ¹ (°C)	T _g ² (°C)	T _g ³ (°C)
PIN-1	318	Not observed	Not observed
PMR-15 control	312	Not observed	Not observed
PIN-1(a)	306	331	344.5
PIN-2	Not observed ^a	Not observed	Not observed
PIN-2(a)	305	359	317
PIN-3	283	Not observed	Not observed
PMR-II-30	320	332	364.5

T_g¹ is measured by taking a tangent to the curve produced from a plot of E' versus temperature.

T_g² is measured from the maximum peak height of the curve produced from a plot of E'' versus temperature.

T_g³ is calculated from the plot of Tan δ versus temperature.

a - No Tg was observed for PIN-2 due to slippage of the sample in the DMTA unit.

In the case of thermosetting polymers (such as those in Table F) the T_g of the polymer can be related to the degree of crosslinking. The crosslink sites in the polymers outlined in Table F are situated at the ends of the polymers (illustrated in Schemes 1 and 2, Section 1.1.2). Thus by increasing the polymer molecular weight, a decrease in the crosslinking sites will result, thereby decreasing the T_g of the resultant crosslinked system. However this trend is counterbalanced to a certain extent by the increase of the polymer T_g in proportion to its molecular weight.

Table F provides the following observations:

- (a) With the exception of PIN-3 all the polymers have T_g s (T_g^1) in excess of 300°C . These high T_g s can be credited to the stiff aromatic backbone, and in particular the imide rings contained within the backbone.

- (b) PIN-1 and PIN-1(a) have similar T_g^1 values (318°C and 306°C respectively). This is consistent with the fact that they have similar M_n values (Section 2.3.5). These T_g values are slightly lower than corresponding values in the literature (eg Ref 9). However, these differences may result from the method of measurement. For example it is known that when measuring T_g by DMTA, a variance in heating rate and/or frequency will result in a variation of the T_g^{38} .

- (c) The T_g^1 values of the PMR-15 control and PIN-1 are similar. This suggests that the PMR-15 control has a comparable molecular weight and degree of norbornene end-capping to PIN-1.
- (d) PIN-3 has a lower T_g (T_g^1) than PIN-2(a). This effect probably stems from the difference in the respective diamine components (9) and (10) (assuming that they both have a similar number of crosslink sites). The presence of the meta-diamine (10) in PIN-3 will produce a kink in the polymer chain. Thus the polymer chains are unable to pack as closely together as the para system. Hence the onset of molecular motion occurs at lower temperatures with PIN-3 compared to PIN-2(a).

The complementary thermal-analysis techniques, TGA and isothermal ageing have shown polymers PIN-2, PIN-2(a) and PIN-3 (containing diamines (9) and (10) respectively) to have inferior thermal oxidative stability to the MDA containing polymers, PMR-15 control, PIN-1 and PIN-1(a). In particular, isothermal ageing under 1 atm air reveals that the MDA containing polymers can survive temperatures of 350°C for short periods of time (200 hrs), but the polymers containing diamines (9) and (10) have almost completely degraded (approximately 10% weight remaining) after 200 hrs at 350°C. Hence polymers PIN-2, PIN-2(a) and PIN-3 cannot survive the high temperatures required of these type of matrix.

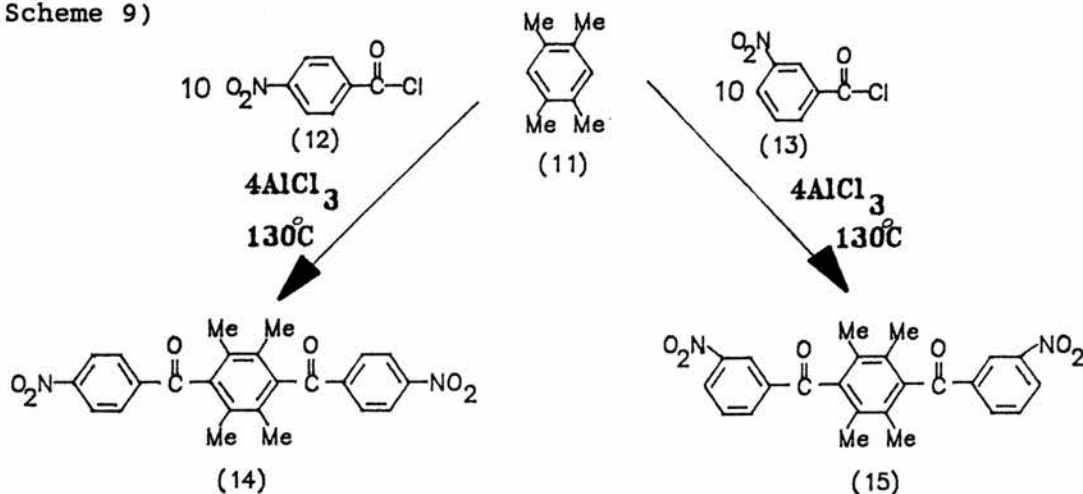
3 EXPERIMENTAL

3.1 Abbreviations of Monomers

Monomethyl ester of 5-norbornene-2,3-dicarboxylic acid	NE
Dimethyl ester of 3,3',4,4'-benzophenonetetracarboxylic acid	BTDE
5-norbornene-2,3-dicarboxylic acid anhydride	NA
3,3',4,4'-benzophenonetetracarboxylic acid dianhydride	BTDA
4,4'-methylenedianiline	MDA
1,1'-(methylenedi-4,1-phenylene)-bismaleimide	MDA-BMI
1,4-bis(4-aminobenzoyl)-2,3,5,6-tetramethylbenzene	(9)
1,4-bis(3-aminobenzoyl)-2,3,5,6-tetramethylbenzene	(10)
Durene; (1,2,4,5-tetramethylbenzene)	(11)
4-nitrobenzoyl chloride	(12)
3-nitrobenzoyl chloride	(13)
1,4-bis(4-nitrobenzoyl)-2,3,5,6-tetramethylbenzene	(14)
1,4-bis(3-nitrobenzoyl)-2,3,5,6-tetramethylbenzene	(15)

3.2 Synthesis of (14) and (15) by Friedel-Crafts diacylation of durene

(Scheme 9)



Scheme 9

Although the syntheses of (14) and (9) have been described previously³⁰, significant alterations have been made to the method (Schemes 9 and 10) in order to optimise yields and to simplify the process. This improved method is also used for the syntheses of (15) and (10). In both cases the acid chloride ((12), (13)) used for the Friedel-Crafts reaction is present in vast excess because, as well as being a reactant, it is also used as the solvent. There is a slight complication in the case of p-nitrobenzoyl chloride (12) as the solvent in that it is a solid with melting point 73°C. This problem is overcome by heating the acid chloride until it melts and then adding the aluminium chloride to form the so-called Perrier complex. Before adding the durene the final temperature of the reaction mixture is raised to 130°C in order to ensure that the reaction goes completely through to the diacylated product (14) and (15) and does not stop at the monoacylated stage.

3.2.1 1,4-bis(4-nitrobenzoyl)-2,3,5,6-tetramethylbenzene(14)

The reaction flask, equipped with a paddle stirrer, nitrogen inlet, thermometer and condenser, was charged with 4-nitrobenzoyl chloride (185.57g, 1.00 mol). The temperature was raised to 85°C to melt the 4-nitrobenzoyl chloride. To this molten material was added slowly aluminium chloride (53.34g, 0.40 mol) and the mixture stirred for 15 minutes to form the Perrier complex. Durene (13.42g, 0.10 mol) was then added in small portions to the reaction flask, resulting in a reasonably viscous medium. The temperature of the reaction was then raised to 130°C and stirred

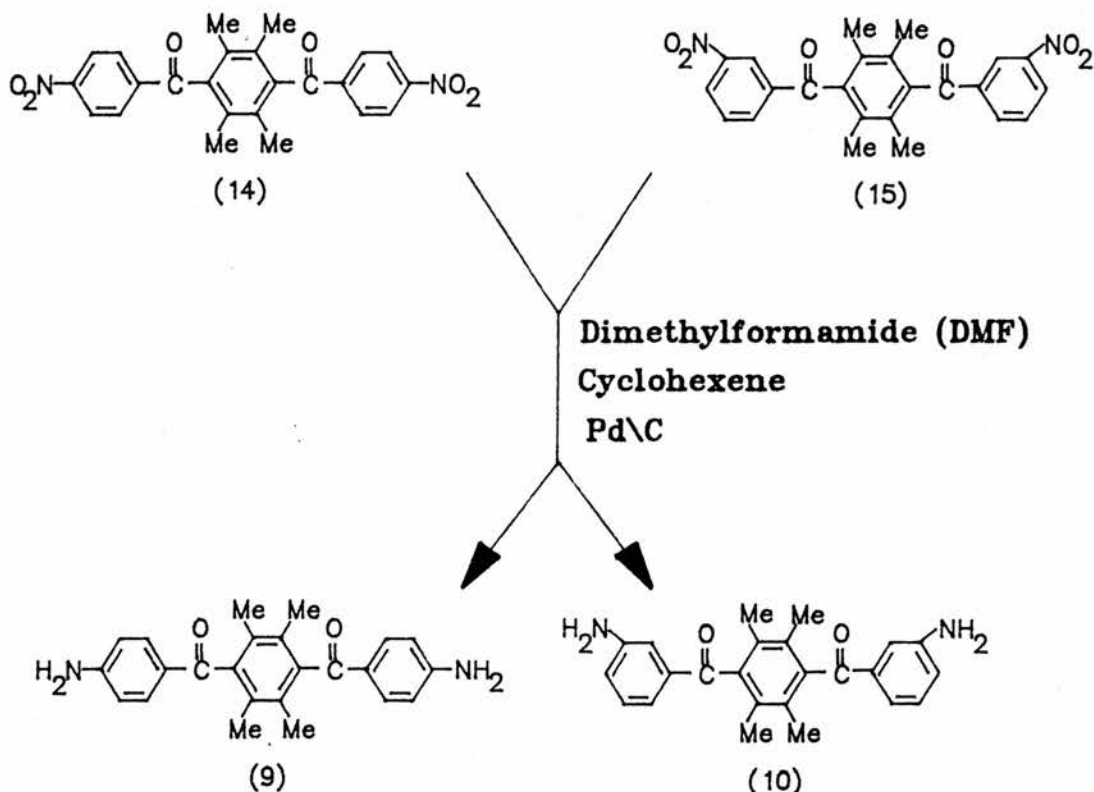
at this temperature under nitrogen for 4 hours. The temperature of the reaction was then lowered to 90°C and chloroform added to dissolve the reaction mixture, which prevented the molten reaction mixture from solidifying on cooling. The chloroform solution was then poured on to crushed ice with vigorous stirring. Concentrated hydrochloric acid was then added to break up the remaining Perrier complex. The dark chloroform layer was then separated from the aqueous layer and insoluble material. An equivalent quantity of 2M NaOH was then added to the chloroform solution and the mixture heated under reflux with vigorous stirring in a warm water-bath for 15 minutes. This extraction was repeated three times to complete the hydrolysis of unreacted acid chloride. The chloroform layer was then washed several times with water, dried over magnesium sulphate and evaporated leaving a dark brown crude product. This was further purified by redissolution in the minimum amount of chloroform and then slowly pouring this solution into petroleum (bp 80°-100°C). The final product was dried in a vacuum oven at 80°C. Yield, 32.41g (75%); found: C,66.6%; H,4.8%; N,6.4%. Calc for $C_{24}H_{20}N_2O_6$: C,66.7%; H,4.7%; N,6.5%. DSC: a sharp melting endotherm was observed at 262°C (lit mpt³⁰ 262-263°C). ¹H and ¹³C NMR spectra are interpreted in Section 2.

3.2.2 1,4-bis-(3-nitrobenzoyl)-2,3,5,6-tetramethylbenzene (15)

The reaction flask, equipped with a link stirrer, nitrogen inlet, thermometer and condenser, was charged with 3-nitrobenzoyl chloride (98.35g, 0.530 mol) and the temperature raised to 50°C. The aluminium chloride (28.27g, 0.212 mol) was then added, and this

mixture was stirred for 15 minutes to allow the Perrier complex to form. The temperature was increased to 85°C, at which point durene (7.11g, 0.53 mol) was added. Once this addition was complete the temperature of the reaction flask was further increased to 130°C, and maintained at this temperature for 4 hrs, with stirring, under nitrogen. The mixture was then cooled to 90°C and chloroform (200 ml) was added, and the chloroform solution was then poured on to crushed ice with vigorous stirring. Concentrated hydrochloric acid was then added with further stirring. The dark chloroform layer was then separated from the aqueous layer after which an equivalent quantity of 2M sodium hydroxide was added to the chloroform. This mixture was heated under reflux, with stirring, on a warm water bath for 15 minutes. The extraction with base was repeated twice. The chloroform layer was then washed several times with distilled water, dried over magnesium sulphate and evaporated, leaving a brown solid which was dried in a vacuum oven at 60°C. Yield, 21.40g (93%). Found: C, 64.7%; H, 4.6%; N, 6.4%; Calc for $C_{24}H_{20}N_2O_6$: C, 66.7%; H, 4.7%; N, 6.5%. DSC : a sharp melting endotherm was observed at 303°C. 1H and ^{13}C spectra are interpreted in the discussion section.

3.3 Reduction of the nitro groups in (14) and (15) (Scheme 10)



Scheme 10

Orthodox methods of reducing nitro groups on a laboratory scale involve the use of metals in acid, such as Sn/HCl or SnCl₂/CH₃-COOH. However, this technique relies on the nitro compound being at least partly soluble in the aforementioned media, which is often not the case (as here). A further drawback when using tin or a tin salt is that insoluble tin-containing residues are frequently left in the final product which in the present cases could cause problems during polymerisation involving the diamines.

There is a less well known technique, but one which is well documented³⁹⁻⁴², which solves the above problems and gives a pure product, without the need for recrystallisation in many cases. This technique (catalytic transfer hydrogenation) involves the use of cyclohexane (hydrogen donor) in the presence of a palladium/charcoal catalyst. The advantage of this method is that the hydrogen donor releases hydrogen to the catalyst under mild conditions, and therefore there is no need for high pressures or temperatures to reduce the nitro groups. One added advantage of this method is that it allows the use of highly polar solvents such as dimethylformamide, in which (14) and (15) are partially soluble. Since (9) and (10) are completely soluble in the reaction medium, product isolation simply involves filtration of the catalyst and then precipitation of the diamine. This process utilises a relatively large amount of catalyst; however, it can be re-used up to six times⁴⁰.

3.3.1 1,4-bis(4-aminobenzoyl)-2,3,5,6-tetramethylbenzene(9)

The reaction flask equipped with a link stirrer, nitrogen inlet, thermometer and condenser was charged with 1,4-bis(4-nitrobenzoyl)-2,3,5,6-tetramethylbenzene (31.00g, 0.072 mol) and dimethylformamide (DMF) (310 ml). This mixture was heated to 50°C giving a partial solution. The 10% palladium on carbon catalyst (7.70g, 0.1 mol equiv) and cyclohexene (73.0 ml, 0.72 mols) were added into the reaction flask. The temperature of the mixture was further increased to 90°-95°C and held at this temperature for 5 hrs. The reaction mixture was then allowed to cool to room

temperature, the palladium catalyst was filtered off and the filtrate then slowly poured on to crushed ice with stirring giving a light brown precipitate, which was filtered and then slurried several times in warm distilled water. The product was finally washed on the filter and then dried in a vacuum oven at 80°C; Yield, 24.62g (92%); found: C, 77.1%; H, 6.5%; N, 7.5%. Calc for $C_{24}H_{24}N_2O_2$: C, 77.4%; H, 6.5%; N, 7.5%. DSC a sharp melting endotherm was observed at 340°C (No lit mpt recorded). 1H and ^{13}C spectra are in the Discussion Section.

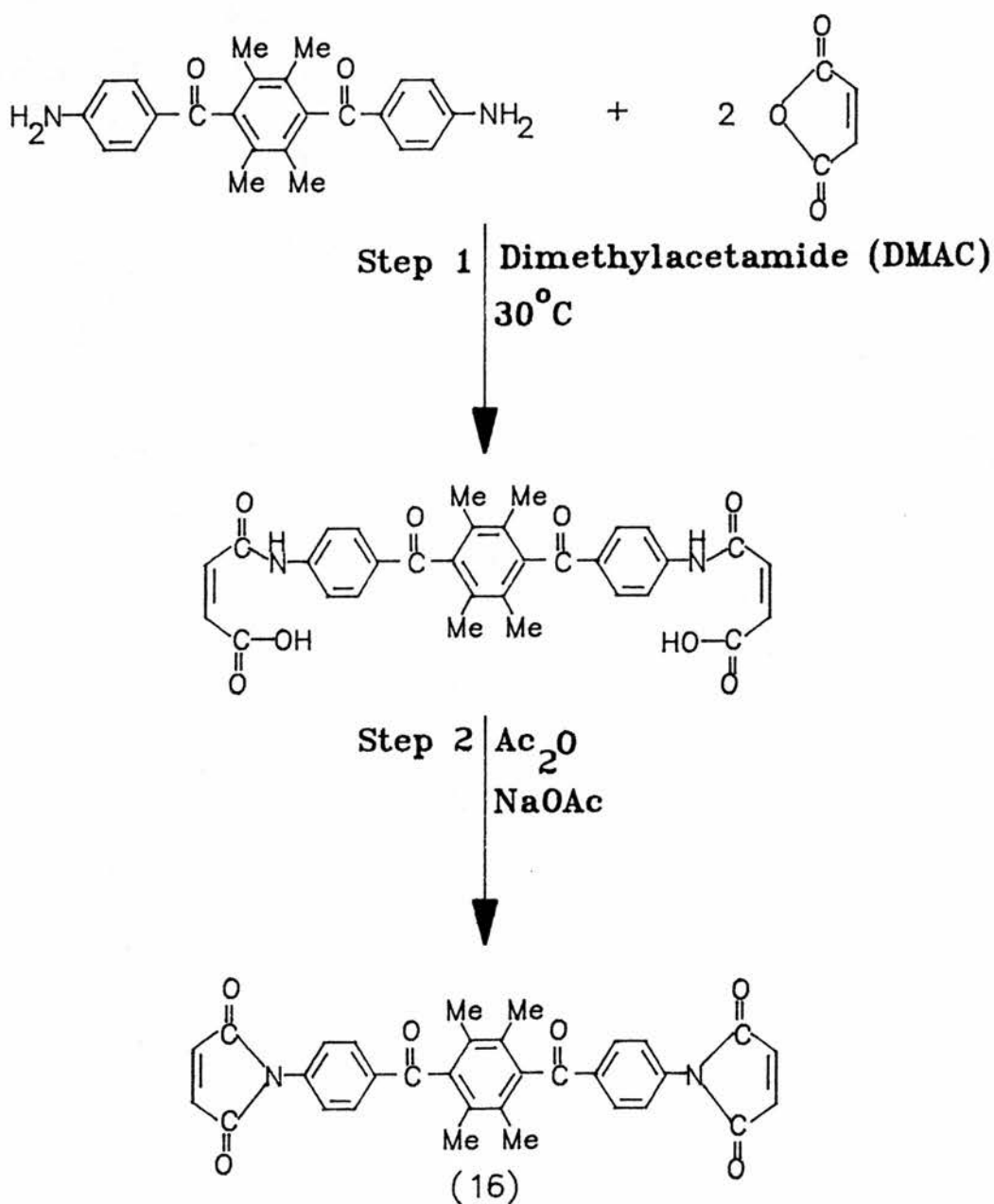
3.3.2 1,4-bis(3-aminobenzoyl)-2,3,5,6-tetramethylbenzene (10)

The reaction flask equipped with a link stirrer, thermometer and condenser was charged with 1,4-bis(3-nitrobenzoyl)-2,3,4,6-tetramethylbenzene (16.00g, 0.037 mol) and DMF (150 ml). This mixture was heated to 60°C giving a partial solution at which time the 10% palladium on carbon catalyst (3.90g, 0.1 mol equiv) and cyclohexene (37.6 ml, 0.370 mol) were added. The temperature of the reaction flask was increased to 90°-95°C, and held at this level for 4 hrs. The reaction mixture was then allowed to cool to room temperature, the palladium catalyst was filtered off, and the filtrate was then slowly poured on to crushed ice with stirring giving an off-white precipitate. This was then filtered off and washed on the filter with distilled water. The product was then slurried several times in warm distilled water, re-filtered and finally washed on the filter with distilled water, then dried in a vacuum oven at 80°C, Yield, 11.33g (82%). found: C, 76.9%; H,

6.5%; N, 7.4%. Calc for $C_{24}H_{24}N_2O_2$: C, 77.4; H, 6.5%; N, 7.5%.

DSC: a sharp melting endotherm was observed at 298°C. 1H and ^{13}C spectra are discussed in Section 2.

3.4 1,4-bis(4-maleimidobenzoyl)-2,3,5,6-tetramethylbenzene (16)
(Scheme 11)



Scheme 11

Step 1 - The reaction flask, equipped with a magnetic follower, nitrogen inlet and thermometer, was charged with 1,4-bis(4-aminobenzoyl)-2,3,5,6-tetramethylbenzene (9) (2.00g, 0.0054 mol) and dimethylacetamide (20ml). The temperature was raised to 30°C and stirring continued under nitrogen until solution was complete. To this solution was added maleic anhydride (1.17g, 0.0119 mol) in one portion as a solid. The reaction mixture was maintained at 30°C for a further 4 hrs, after which the reaction flask was cooled to room temperature, and the solution was then slowly poured into a vigorously stirred ice/water mixture. The resultant light yellow precipitate was filtered off, then slurried in distilled water for several hours. The maleamic acid was finally filtered off and dried in a vacuum oven at 55°C. Yield, 2.15g (71%). Found: C, 67.5%; H, 4.9%; N, 5.1%. Calc for $C_{32}H_{28}N_2O_8$: C, 67.6%; H, 5.0%; N, 4.9%. DSC : a sharp melting endotherm was observed at 280°C.

Step 2 - The maleamic acid (1.80g, 0.0032 mol), synthesised above, and DMAC (20 ml) were charged into a reaction flask equipped with a magnetic follower, nitrogen inlet, thermometer and condenser. To this stirred solution were added sodium acetate (2.44g, 0.0298 mol) and acetic anhydride (11.0 ml, 0.119 mol). The mixture was heated to 40°C and held at this temperature for 2.5 hrs; then further heated at 65°C for 1.5 hrs and cooled to room temperature. The precipitated solid was filtered, slurried in warm water, followed by slurrying in acetone, and finally dried in a vacuum oven at 50°C. Yield, 0.71g (42%). Found : C, 71.1%; H, 4.7%; N, 5.2%.

Calc for $C_{32}H_{24}N_2O_6$: C, 72.2% H, 4.5%; N, 5.3%. DSC :
Exotherm observed at 300°C (crosslinking or decomposition).

3.5 Polymer synthesis

The monomer reactants utilised in this investigation (illustrated in Table G) were purchased from commercial sources (diamines (9) and (10) were synthesised in Section 3.2 and 3.3); the anhydrides were recrystallised from acetic anhydride.

TABLE G

<u>Structure</u>	<u>Monomer Name</u>
	5-norbornene-2,3-dicarboxylic anhydride (Nadic anhydride, NA)
	Maleic anhydride
	3,3',4,4'-benzophenonetetracarboxylic dianhydride (BTDA)
	4,4'-(hexafluoroisopropylidene)-diphthalic anhydride (HFDA)
	4,4'-methylenedianiline (MDA)
	p-phenylenediamine (PPDA)
	1,4-bis(4-aminobenzoyl)-2,3,5,6-tetramethylbenzene (9)
	1,4-bis(3-aminobenzoyl)-2,3,5,6-tetramethylbenzene (10)

A number of polymers were synthesised in this study, the compositions of which (end-capped polymers, before cross-linking is initiated) are detailed in Table H.

TABLE H

<u>Polymer</u>	<u>Composition</u>	<u>n</u>	<u>FMW</u>
PMR-15 (CONTROL) ^a	[NE] ₂ [BTDE] _n [MDA] _{n+1}	2.09	1500
PMR-II-30	[NA] ₂ [HFDA] _n [PPDA] _{n+1}	5	2982
PIN-1	[NA] ₂ [BTDA] _n [MDA] _{n+1}	2.09	1500
PIN-2	[NA] ₂ [BTDA] _n [(9)] _{n+1}	2.09	2040
PIN-3	[NA] ₂ [BTDA] _n [(10)] _{n+1}	2.09	2040
PAM-1	[MA] ₂ [BTDA] _n [MDA] _{n+1}	2.09	1481
PAM-2	[MA] ₂ [BTDA] _n [(9)] _{n+1}	2.09	2018
PIN-1(a) ^b	[NA] ₂ [BTDA] _n [MDA] _{n+1}	2.09	1500
PIN-2(a) ^b	[NA] ₂ [BTDA] _n [(9)] _{n+1}	2.09	2040

a - The PMR-15 control was synthesised (synthesis outlined in 3.5.1) from a commercial methanol solution of NE, BTDE and MDA, present in a 50% w/w concentration.

b - PIN-1(a) and PIN-2(a) were synthesised from the respective maleimide ended polymers, PAM-1 and PAM-2 by a Diels-Adler reaction with cyclopentadiene shown in Scheme 12 and described in 3.5.3.

Where: PIN = Polyimide nadimide ended

PAM = Polyamic acid maleimide ended

3.5.1 PMR-15 control

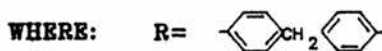
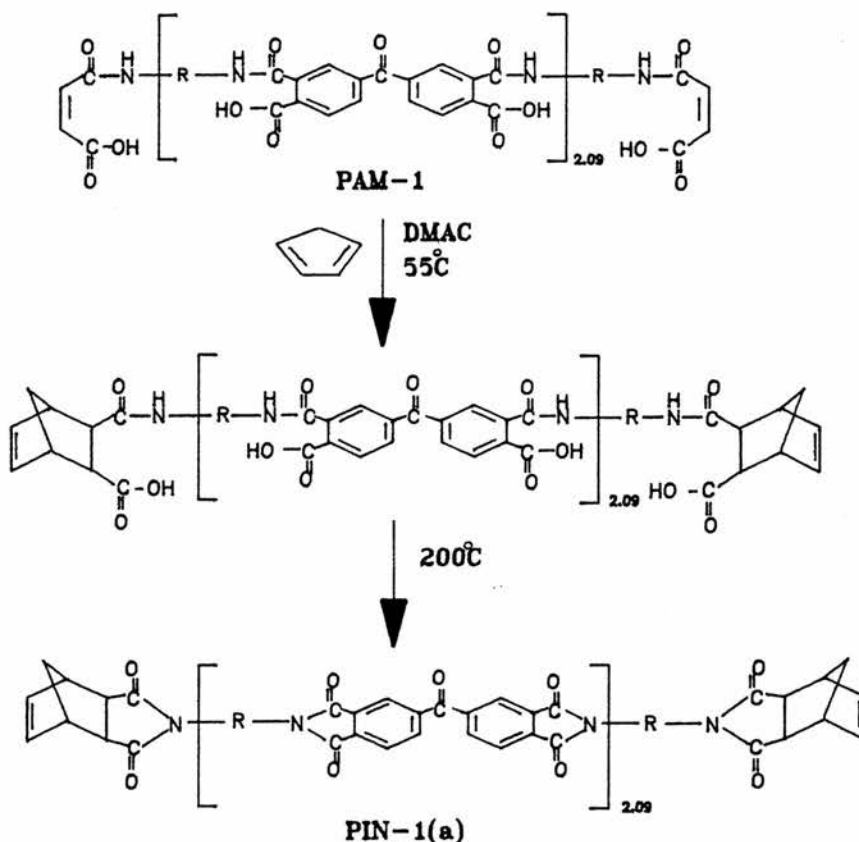
The reaction vessel containing 200 mls of a 50% w/w commercial monomer solution of NE, BTDE and MDA in methanol, (the stoichiometric ratio of monomers was 2 moles NE, 2.09 moles BTDE and 3.09 moles MDA), was heated to 120°C and held at this temperature until all the methanol had evaporated, leaving a brick red solid in the reaction vessel. This solid was crushed into a fine powder and then placed into an air circulating oven set at 200°C for 2 hrs, giving a deep brick red solid, which had been imidised to the prepolymer as shown by a strong sharp band at 1780cm⁻¹ in the FTIR spectrum. The band at 1780cm⁻¹ and a further band at 1720cm⁻¹ have been attributed to the symmetric and asymmetric stretches of the carboxyl groups coupled through the five-membered imide ring⁴³.

3.5.2 Synthesis of PIN-1 formulated from the respective anhydrides (Scheme 1).

The reaction flask equipped with a magnetic follower, thermometer and nitrogen inlet was charged with 4,4'-methylenedianiline (3.06g, 0.0154 mol) and dimethylacetamide (25 ml). Once solution was complete 3,3',4,4'-benzophenonetetracarboxylic dianhydride (3.36g, 0.0104 mol) was added as a solid followed by the addition of 5-norbornene-2,3-dicarboxylic anhydride (1.64g, 0.01 moles) as a solid. The resultant solution was stirred under nitrogen at room temperature for 16.5 hrs. The reaction solution was then

slowly poured into an ice/water mixture with vigorous stirring. This produced an off-white polymeric solid precipitate, which was then filtered off, slurried in distilled water for several hours, and then re-filtered. This process was repeated twice. The polyamic acid was dried in a vacuum oven at 55°C and then imidised in an air circulating oven set at 200°C for 2 hrs. The imidised material was moulded according to the technique described in 3.5.4. PIN-2 and PIN-3 were synthesised by a similar route as was PMR-II-30, PAM-1 and PAM-2.

3.5.3 Synthesis of PIN-1(a) from PAM-1 by a Diels-Alder reaction with Cyclopentadiene (Scheme 12)



Scheme 12

The reaction flask equipped with a magnetic follower, thermometer, dropping funnel and condenser was charged with PAM-1 (11.00g, 0.0074 mol), synthesised by the method described in 3.5.2, and dimethylacetamide (35 ml). This mixture was stirred under nitrogen until solution was complete. Freshly distilled cyclopentadiene (3.47g, 0.0525 mol) was then added slowly under nitrogen with stirring. The solution was stirred for 2 hrs at room temperature, then at 55°C for 1.5 hrs; it was cooled to room temperature, and then poured slowly into an ice/water mixture with vigorous stirring, giving a light yellow precipitate. This was filtered off, slurried in distilled water for 1 hr, re-filtered, then slurried again in distilled water for several hours before being filtered and dried in a vacuum oven at 50°C. The product was then imidised in an air circulating oven set at 200°C for 2 hrs. The imidised material was moulded according to the procedure described in 3.5.4. PIN-2(a) was synthesised similarly.

3.5.4 Polymer fabrication

The imidised powder (2.50g) was poured into a matched metal mould (4cm x 1cm) which in turn was inserted into an air-circulating oven set at 280°C-300°C and left at this temperature for 5-10 mins. The pre-heated mould, complete with contents, was then placed into a press pre-heated to 320°C. Pressure was then applied slowly over a period of 15-30 mins (upto 570 psi). The cure temperature (320°C) and pressure were held constant for 2 hrs after which the mould was cooled under pressure to 150°C and then removed from the press.

The moulding, once removed from the mould, was postcured in an air circulating oven set at 340°C for 24 hrs.

3.6 Model compound synthesis

In order to interpret the complex NMR spectra obtained from the polyamic acid intermediates of the polymers outlined in Table H, a number of model compounds were synthesised, all of which are described in this section.

3.6.1 1,1'-(methylenedi-4,1-phenylene)-bisnadac acid (cf 2.3.2.4)

The reaction flask equipped with a glass link stirrer, thermometer, condenser and pressure-compensating funnel was charged with 4,4'-methylenedianiline (MDA) (39.65g, 0.2 mol) and acetone (40 ml). Once the MDA had completely dissolved, the solution was cooled to <10° by means of an ice-bath. 5-norbornene-2,3-dicarboxylic anhydride (65.66g, 0.4 mol) dissolved in acetone (150 ml) was added dropwise, the temperature being maintained below 10°C. After the addition was complete the resultant solution was allowed to warm up to room temperature. During this time the bisnadac acid precipitated out of the solution resulting in a viscous suspension. Further acetone (40 ml) was added to enable the stirring of the reaction mixture to continue. Stirring under nitrogen at room temperature was continued overnight. The off-white solid was then filtered off, slurried in acetone for 0.5 hr, re-filtered, washed on the filter with acetone, and finally dried in a vacuum oven at 60°C; yield, 91.97g (87%) mp,

127.5°-129.5°C; Found: C, 69.9%; H, 5.9%; N, 5.2%. Calc for $C_{31}H_{30}N_2O_6$: C, 70.7%; H, 5.7%; N, 5.3%.

3.6.2 3,3',4,4'-benzophenonetetracarboxylic acid dimethyl ester (cf 2.3.2.6)

A quickfit conical flask equipped with a condenser was charged with 3,3',4,4'-benzophenonetetracarboxylic dianhydride (32.22g, 0.10 mol) and methanol (45g). This mixture was heated under reflux with stirring, until all the solid was in solution, and then for an additional 2 hrs. The resultant solution was then evaporated under reduced pressure. The viscous resin which remained was then placed into a vacuum oven set at 80°C. This procedure gave an orange glassy solid which when crushed gave an off-white solid; yield, 24.30g (63%), mp, 68°-70°C; Found: C, 58.1%; H, 3.7%. Calc for $C_{19}H_{14}O_9$: C, 59.1%; H, 3.7%. HPLC analysis showed the presence of three main isomers.

3.6.3 5-norbornene-2,3-dicarboxylic acid monomethyl ester (cf 1.1.3)

A quickfit conical flask equipped with a condenser was charged with 5-norbornene-2,3-dicarboxylic anhydride (32.83g, 0.20 mol) and methanol (46g). This mixture was heated under reflux with stirring, until all the solid was in solution and then for an additional 2 hrs. The excess methanol was then distilled off leaving a viscous solution. On standing overnight the product crystallised out. These fine white crystals were filtered off,

then slurried in diisopropyl ether, re-filtered and washed on the filter with diisopropyl ether. The product was finally dried in a vacuum oven at 60°C; yield, 26.49g (68%) mp, 94°-96°C; Found: C, 61.5%; H, 6.1%. Calc for $C_{10}H_{12}O_4$; C, 61.2%; H, 6.2%.

3.6.4 1,1'-(methylene-4,1-phenylene)-bisnadimide (cf 2.3.2.5)

3.6.4.1 Method 1

5-norbornene-2,3-dicarboxylic acid monomethyl ester (9.81g, 0.05 mol) and 4,4'-methylenedianiline (4.96g, 0.025 mol) were dissolved in methanol (30 ml). The solution was then heated under reflux with stirring for 2 hrs. The majority of the methanol was then distilled off, leaving a viscous gel which was then oven dried at 150°C for 2hrs: yield, 10.90g (89%) mp, 239.5°-240.5°C; Found : C, 75.1%; H, 5.5%; N, 5.7%. Calc for $C_{31}H_{26}N_2O_4$; C, 75.9%; H, 5.3%; N, 5.7%.

3.6.4.2 Method 2

The reaction flask, equipped with a pressure-equalising funnel, thermometer, magnetic follower, nitrogen inlet and condenser was charged with 1,1'-(methylenedi-4,1-phenylene)-bismaleimide (MDA BMI) (25g, 0.0698 mol) and dimethylformamide (100 ml) then stirred until solution was complete. Freshly distilled cyclopentadiene (11.51g, 0.174 mol) was then added dropwise under nitrogen to the stirred MDA-BMI solution. There was a noticeable exotherm with a

maximum temperature of 52°C being reached. Towards the end of the addition the product precipitated from solution. DMF (25 ml) was added to the reaction vessel to produce a mobile reaction slurry. The temperature of the reaction flask was increased to 40°C and maintained at this value for 1.5 hrs. The reaction flask was cooled and the white solid was filtered off, slurried twice in acetone for several hours, re-filtered, and dried in a vacuum oven at 50°C. Yield, 25.15g (73%) mp 243.5°-244.5°C. Found: C, 75.3%; H, 5.5%; N, 5.9%. Calc for $C_{31}H_{26}N_2O_4$: C, 75.9%; H, 5.3%; N, 5.7%.

3.6.5 1,1'-(methylenedi-4,1-phenylene)-bismaleamic acid (cf 2.3.2.2)

The reaction flask equipped with a magnetic follower, thermometer, nitrogen inlet, condenser and pressure-compensating funnel was charged with 4,4'-methylenedianiline (MDA) (9.91g, 0.05 mol) and acetone (100 mls). Once solution was complete maleic anhydride (10.79g, 0.11 mol) dissolved in acetone (20 mls) was added dropwise; the reaction temperature was maintained below 10°C. Soon after the start of the addition a yellow precipitate was observed. On completion of the addition the yellow slurry was stirred under nitrogen at room temperature for a further 2 hrs. The yellow solid was then filtered off, washed on the filter with acetone, then slurried twice in acetone for several hours, re-filtered and then dried in a vacuum oven at 50°C. Yield, 18.35g (93%); mp, 194°-196°C; Found: C, 63.3%; H, 4.6%; N, 7.0%. Calc for $C_{21}H_{18}N_2O_6$: C, 64.0%; H, 4.6%; N, 7.1%.

3.7 Techniques used for polymer characterisation

3.7.1 Thermal analysis

3.7.1.1 Isothermal ageing

The isothermal ageing studies were undertaken to determine whether the cross-linked polymers could withstand long-term ageing at elevated temperatures, thus providing information on potential service temperatures. This test is used as a first screening test, because the equipment needed is relatively simple and cheap. If the isothermal ageing data then seem promising further complex analysis testing can be undertaken.

3.7.1.1.1 Isothermal ageing conditions

Isothermal weight loss measurements were carried out on the postcured neat resin mouldings (fabrication described in 3.5.4). The neat resin samples were inserted into an air circulating oven set at 350°C and aged for 500 hrs under 1 atmosphere of air.

3.7.1.2 Thermogravimetric analysis (TGA)

TGA provides a plot of weight loss versus temperature i.e. a weight loss is observed as the polymer begins to degrade. TGA can provide information on the nature of decomposition but importantly it shows the temperature range over which a particular polymer is

thermally stable, and this ranks polymers in order of thermal stability.

3.7.1.2.1 Thermogravimetric analysis conditions

TGA analysis of the neat resin samples was undertaken on a Stanton Redcroft thermo-recording balance with a heating rate of 10°C/min under 1 atmosphere of air or under nitrogen.

3.7.1.3 Glass transition point (T_g) evaluation by dynamic mechanical thermal analysis (DMTA)

The T_g of a polymer is an important property because it controls the mechanical properties at elevated temperatures and, in the case of a thermosetting polymer, T_g can be related to the extent of physical and chemical crosslinks in the network structure.

DMTA measures the change in dimensional properties of a sample as a function of temperature; thus the softening point of the polymer (T_g) can be obtained.

3.7.1.3.1 DMTA run conditions

The neat resin samples were run on a power head, P1 DMTA under nitrogen with a heating rate of 2°C/min. A single cantilever method was employed whereby the sample is clamped at one end and allowed to oscillate at the other end with a frequency of 10 Hz.

3.7.2.1 Solution NMR

Solutions were run on a Bruker AM 300 NMR; Proton Spectra were run at 300 MHz and ^{13}C were run at 75.47 MHz. Deuterated solvents used were either CDCl_3 , DMSO-d_6 or DMF-d_7 . The spectra of DMSO-d_6 solutions were run at 40°C.

3.7.2.2 Solid state NMR

^{13}C spectra were run at 50.3 MHz on a Bruker MSL 200 solid state NMR at ambient temperature.

3.7.3 FTIR Analysis

The polymer spectra were obtained from solid spectra by means of KBr discs run on a Perkin-Elmer 1600 series FTIR. The KBr sample discs were prepared by grinding the sample (1% by weight) with KBr and compressing this mixture into a transparent disc with the use of a SPECAC KBr disc press.

3.7.4 Differential scanning calorimetry (DSC)

The DSC thermograms were obtained using a METTLER TC10A cell attached to a METTLER TA 3000 processor. The samples were contained in aluminium pans. Each pan had a hole in the lid to allow for expansion of the sample or evolution of gas. Each sample was scanned from 50°C-500°C at a rate of 10°/min under a

steady flow of nitrogen. The reference port contained an empty sealed aluminium pan.

3.8 Molecular Modelling

1,4-bis(4-nitrobenzoyl)-2,3,5,6-tetramethylbenzene (14) and 1,4-bis(4-aminobenzoyl)-2,3,5,6-tetramethylbenzene (9) were modelled on the following system:

Software : POLYGRAF, Biodesign Inc, California

Hardware : Silicon Graphics 4D/20

4 CONCLUSIONS

4.1 Replacement of MDA in PMR Polyimide with an Alternative Long Chain Diamine

The successful synthesis of 1,4-bis(4-aminobenzoyl)-2,3,5,6-tetramethylbenzene (9) and 1,4-bis(3-aminobenzoyl)-2,3,5,6-tetramethylbenzene (10) provided the opportunity to utilise these novel diamines in the PMR formulation.

4.1.1 ^1H and ^{13}C NMR analysis of (9)

Both the ^1H and ^{13}C NMR spectra of 1,4-bis(4-aminobenzoyl)-2,3,5,6-tetramethylbenzene (9) shows unexpected anomalies. These anomalies have been accounted for in terms of electronic interaction between the amino and keto groups of (9), resulting in restricted rotation about the amino ring-to-carbonyl carbon single bond, represented by the canonical forms outlined in Scheme 6. Furthermore the ^{13}C NMR evidence suggests that (9) may exist as a "cis/trans" pair (Figure 7) at elevated temperatures.

The ^1H NMR spectrum of (10) was typical of a normal m-disubstituted aromatic ring system. However the ^{13}C NMR data indicate that (10) may also exist as cis and trans conformers at high temperatures.

Further work should include the elucidation of the crystal

structure of (9). This will confirm whether the canonical forms outlined in Scheme 6 exist by providing bond lengths and thus demonstrating if bonds NH₂ to C4 and C1 to C7 are shortened (ie. the possession of double bond character), as in the case for the two canonical forms in Scheme 6.

4.1.2 Thermal oxidative stability (TOS) of (9) and (10) containing PMR polyimides versus the TOS of MDA PMR polyimides

The thermal analysis techniques, TGA and isothermal ageing have shown the PMR polyimides containing diamines (9) and (10) to have inferior thermal oxidative stability to the MDA containing polyimides. Thus it can be concluded from this evidence that the polyimides containing diamines (9) and (10) cannot survive the high temperatures required of these type of matrices. However PIN-2(a) containing diamine (9), which is believed to contain maleimide ends as well as nadimide ends (concluded from the ¹HNMR evidence) shows an increase in TOS over its nadimide ended counterpart, PIN-2. This increase in TOS is accounted for in terms of a reduced aliphatic hydrogen end-cap content.

4.2 Investigation of the PMR-15 Polymerisation Process

¹HNMR spectroscopy was undertaken on the various polyamic acids synthesised in this study to provide conclusions on: (a) polymer structure and (b) the degree of polymerisation.

- (a) Incomplete end-capping of the polymers was indicated by two multiplets at the low field end of the aromatic region. Thus some amine ends are present in the polymer, which will lead to further complications in the cross-linking mechanism (illustrated in Scheme 5).

A third signal (in addition to the two other vinylic resonances) was observed in the $^1\text{HNMR}$ vinylic regions of all the polyamic acids studied. This signal was attributed to the vinylic hydrogens attached to a small amount of imidised endcap (maleimide and nadimide).

The polyamic acids end-capped with 5-norbornene-2,3-dicarboxylic anhydride gave $^1\text{HNMR}$ spectra containing two methylene bridge hydrogen resonances. From these observations it was proposed that the norbornene end-cap exists as both the endo- and exo- isomers, by conversion of the endo- isomer into the exo-isomer through formation of an intermediate enolate ion (shown in Scheme 7).

- (b) Calculation of three different number average molar masses (M_n^1 , M_n^2 and M_n^3) for each polymer from the $^1\text{HNMR}$ spectra, gave the following information;

Nadic anhydride, although slightly less reactive than maleic anhydride, is still an effective end-capper, and under closely controlled reaction conditions gives a polymer close

to its FMW and end-capped to a high degree. Although maleic anhydride gives a slightly better control of molecular weight than nadic anhydride, the Diels-Alder reaction of the maleic ended polymer (PAM-1 and PAM-2) with cyclopentadiene to give the corresponding nadic ended polymer (PIN-1(a) and PIN-2(a)) was shown to be incomplete. Thus this particular route did not generate a highly norbornene end-capped polyimide.

REFERENCES

- 1 C S Marvel, J Macromol Sci., 1975, Part C, 13, 219.
- 2 J. Baker-Counsell, Plastics & Rubber Weekly, Jan 9, 1988, 9.
- 3 D Wilson, Brit. Polym. J., 1988, 20, 405.
- 4 S J Shaw, Mat. Sci. & Technology., 1987, 3, 589.
- 5 T T Serafini, P Delvigs, G R Lightsey, J. Appl. Polym. Sci., 1972, 16, 905.
- 6 T T Serafini, ACS Symp. Series, 1980, 132, 15.
- 7 P J Dynes, T T Lino, C L Hammermesh, E F Witucki, Polyimides: Synth. Charact. Appl., (proc. tech. Conf. Polyimides), 1982, 1, 311.
- 8 D Garcia, T T Serafini, J. Polym. Sci. Polym. Phys., 1987, 25, 2275.
- 9 D A Scola, J H Vontell, Chemtech., Feb 1989, 112.
- 10 T T Serafini (ed), "Characterisation Methodology for PMR-15", High Temperature Polymer Matrix Composites, 1987, Noyes Data Corporation, New Jersey, p149-154.

- 11 T T Serafini, Proc. of the 5th Int. Conf. on Composite Materials, Metal Soc., 1985, 1007.
- 12 R D Vannucci, Sampe Quarterly, 1987, 19, 31.
- 13 T T Serafini, P Delvigs, Applied Polymer Symposium, 1973, 89.
- 14 H Stenzenberger, Brit. Polym. J., 1988, 20, 383.
- 15 J N Hay, J D Boyle, S F Parker, D Wilson, Polymer, 1989, 30, 1032.
- 16 A C Wong, W M Ritchey, Macromolecules, 1981, 14, 825.
- 17 A C Wong, A N Garroway, W M Ritchey, Macromolecules, 1981, 14, 832.
- 18 R H Pater, C D Morgan, Sampe Journal, 1988, 24, 25.
- 19 W B Alston, ACS Polymer Preprints, 1986, 27, 410.
- 20 G Green, Adv. Comp. Eng., Autumn 1988, 20.
- 21 I Goldfarb, High Temperature Crosslinked Polymers, Chapter III, Section A, Materials Laboratory, Air Force Wright Aeronautical Laboratories, Wright-Patterson, AFB, Ohio p9-10.
- 22 T T Serafini, (Ed), "Replacement of MDA with more oxidatively stable diamines in PMR-Polyimides", High temperature polymer matrix composites, 1987, Noyes Data Corporation, New Jersey, p186-197.

- 23 R D Vannucci, Int. Sampe Tech. Conf. - Eng, 1988, 20, 562.
- 24 Composites Adhes. Newsletter, Feb/March 1989, 5, 5.
- 25 J L Radomski, Ann. Rev. Pharmacol. Toxicol, 1979, 19, 129.
- 26 W B Alston, National Aeronautics and Space Administration, Lewis Research Centre, Private Communication.
- 27 G Marrino and H C Brown, J. Am. Chem. Soc., 1959, 81, 5929.
- 28 C Friedel, J M Crafts and E Ador, C R hebd. Seanc, Acad. Sci., Paris, 1879, 88, 880.
- 29 C L Cheng, P H Gore, G L D Ritchie, Aust. J Chem., 1973, 26, 867.
- 30 G G Barclay, PhD Thesis, 1988, University of Strathclyde.
- 31 K Patterson, PhD Thesis, 1990, University of St Andrews.
- 32 G Ferguson, University of Guelph, Canada, Private Communication.
- 33 J Kendrick, ICI Wilton, Private Communication.
- 34 G Ievy and G L Nelson, "Carbon-13 Nuclear Magnetic Resonance for Organic Chemists", New York, Wiley-Interscience, 1972, p114.

- 35 L F Johnson and W C Jankowski, "Carbon-13 Nuclear Magnetic Resonance Spectra", New York, Wiley-Interscience, 1972, p351.
- 36 D F Ewing, Org. Mag. Res., 1979, 12, 499.
- 37 A C Street, ICI Wilton, Private Communication.
- 38 S W Hill, Rolls-Royce plc, Alferton Rd, Derby, Private Communication.
- 39 E A Braude, R P Linstead, K R H Wooldridge, J. Chem. Soc., 1954, 3586.
- 40 I D Entwistle, R A W Johnstone, T J Povall, J. Chem. Soc. Perkin Trans. 2, 1975, 1300.
- 41 H Imai, T Nishiguchi, K Fukuzumi, J. Org. Chem., 1977, 42, 431.
- 42 R A W Johnstone, A H Wilby, Chem Rev., 1985, 85, 129.
- 43 C A Pryde, J. Polym. Sci., Polym. Chem., 1989, (A), 27, 711.

APPENDIX 1

Figure A - The crystal structure of
1,4-bis(4-chlorobenzoyl)-2,3,5,6-tetramethylbenzene

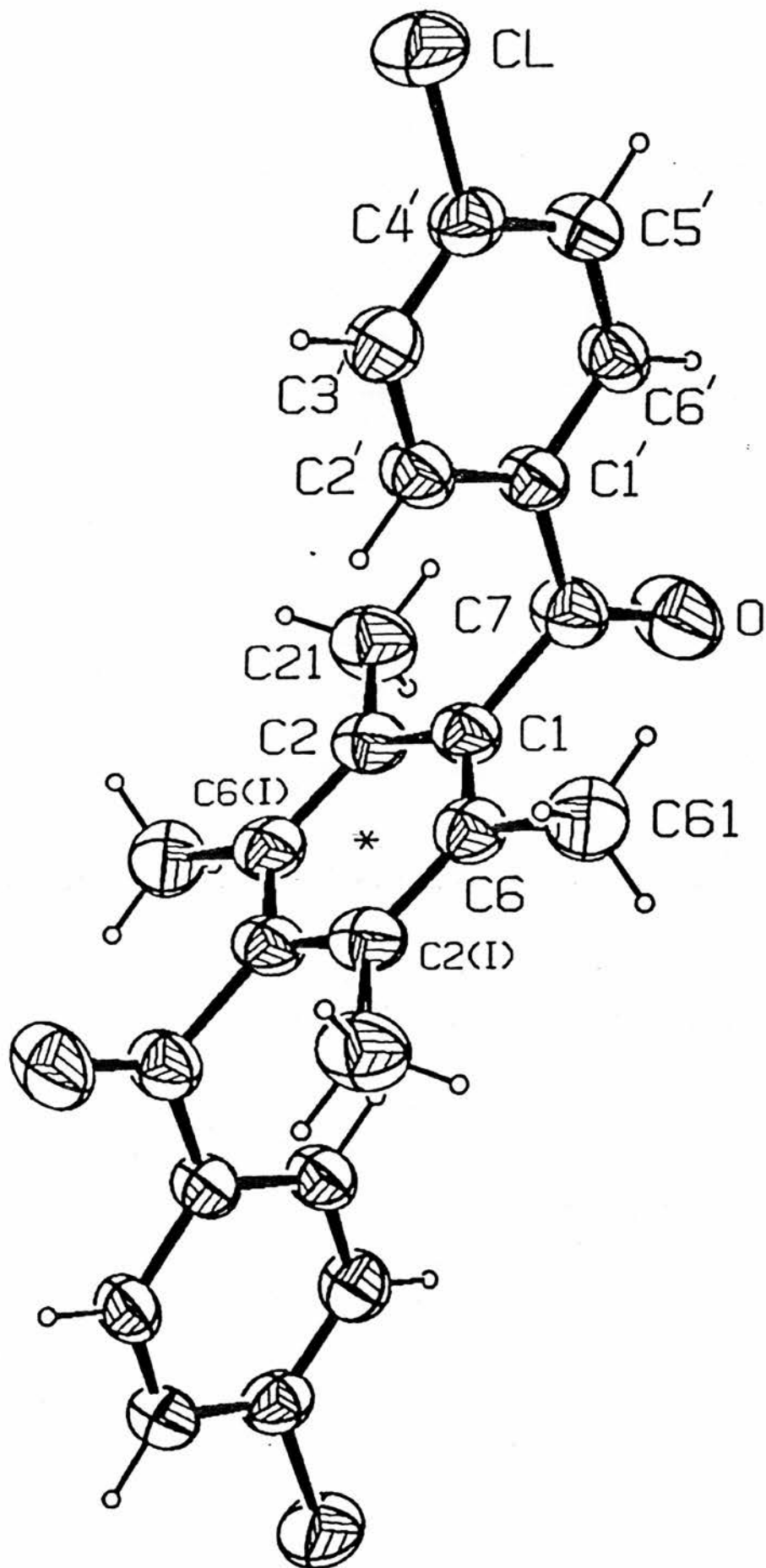
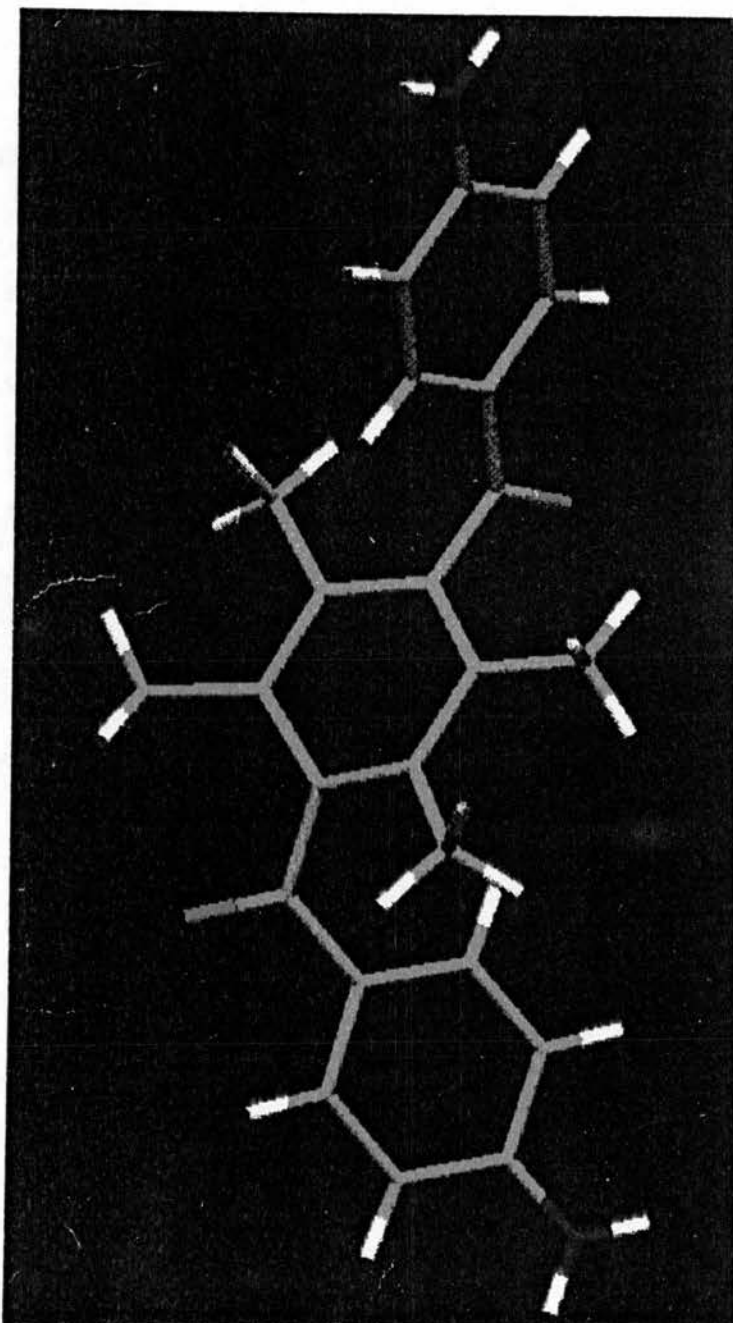
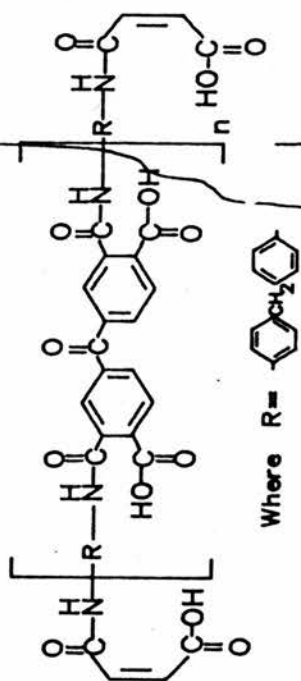


Figure B – Molecular Model illustrating
1,4-bis(4-aminobenzoyl)-2,3,5,6-tetramethylbenzene(9)



APPENDIX 2

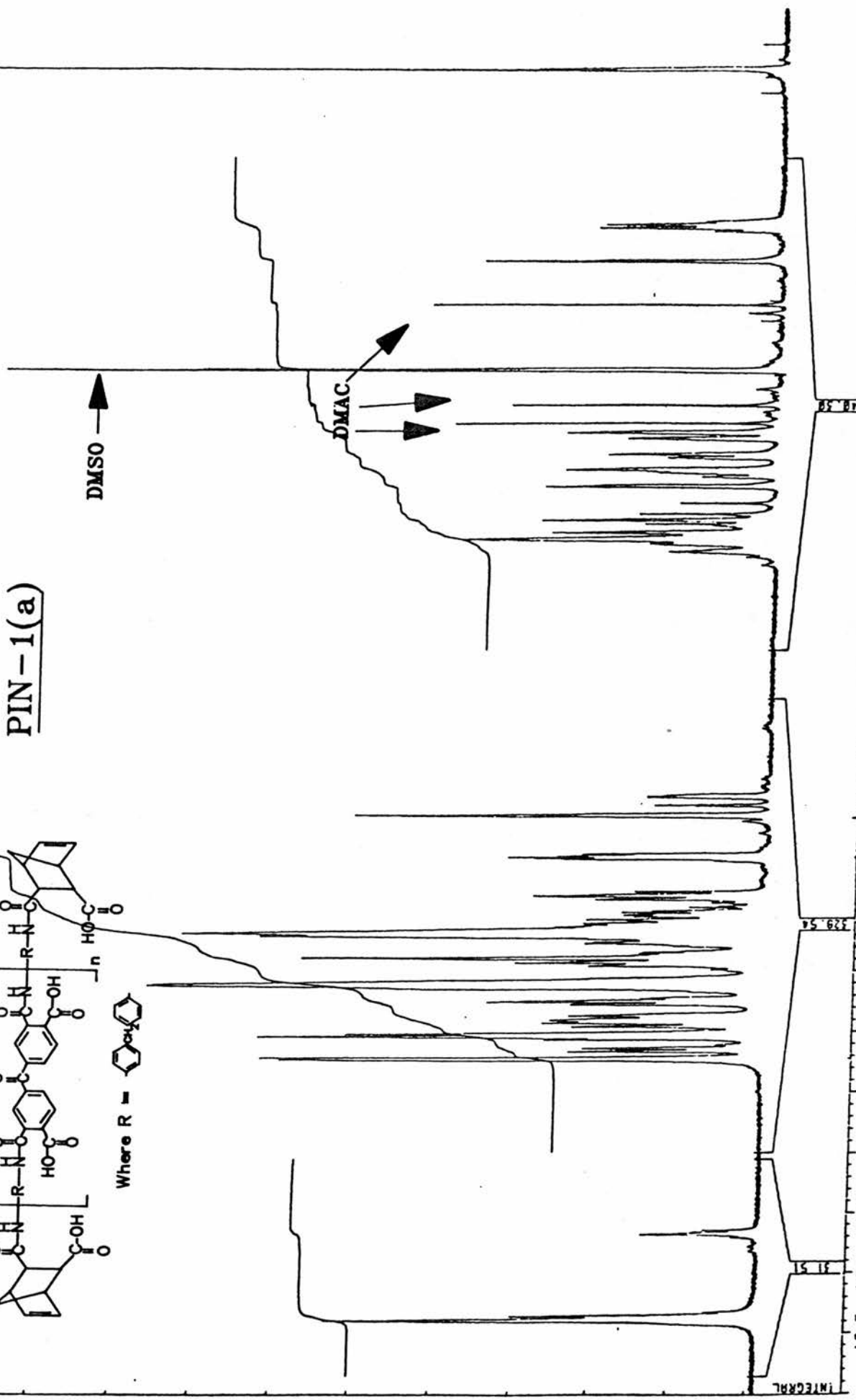
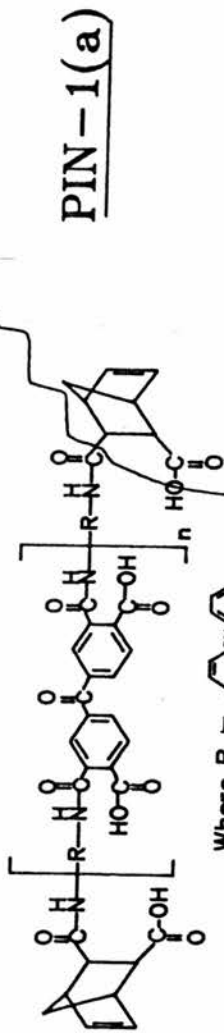
PAM-1



RUI 221
 DATE 2-2-98
 SF 328.1
 ST 128.2
 OI 6554.2
 SI 32766
 TO 32768
 SW 4865.8
 HZ/PT .2
 PW 2.5
 RD 1.5
 RC 4.6
 NS 28
 TE 72
 313
 FW 5128
 OZ 3228.8
 OP 63L PD
 LB 0.8
 CB 0.8
 CK 35.8
 CY 0.3
 F1 11.8
 F2 11.8
 HZ/CH 98.5
 PFM/CH .5
 SE 4791

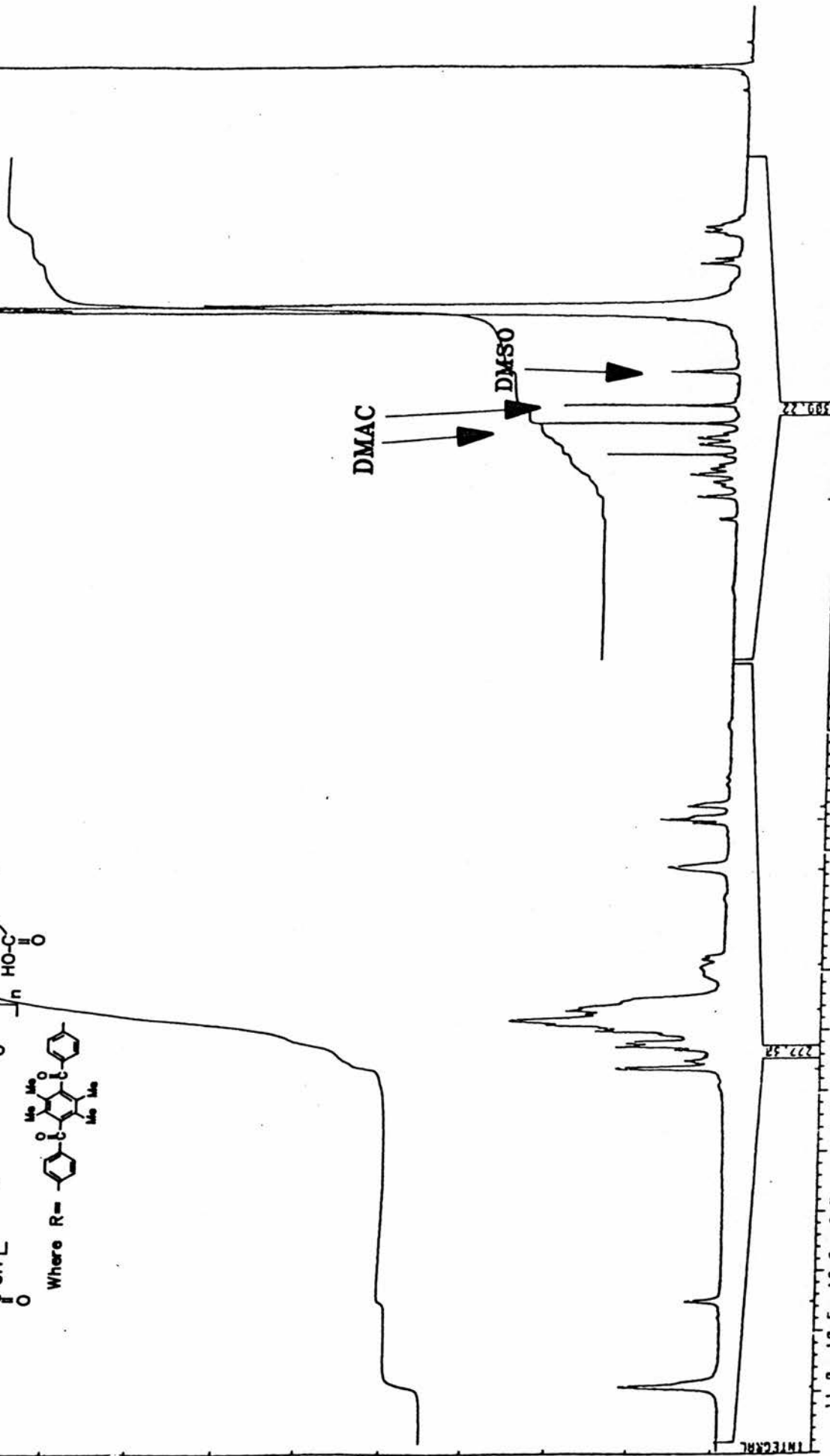
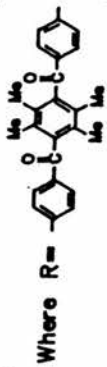
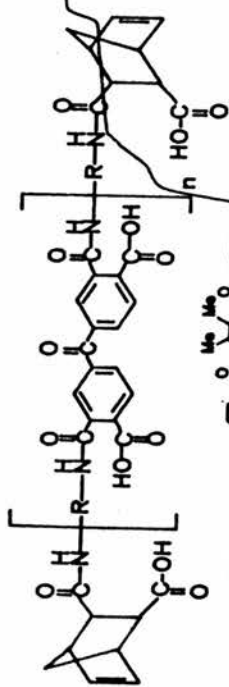
DMAC

DMSO

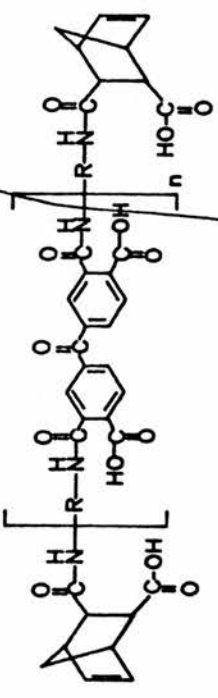


JPM
 DATE 6-2-90
 SF 322.1
 ST 122.8
 OI 6554.2
 SI 37766
 TO 37268
 SA 4265.8
 HZ 41.2
 PK 2.5
 RD 1.5
 RC 4.8
 NS 20
 TE 48
 313
 FX 5128
 OZ 3228.8
 DF 630P0
 LP 8.8
 GB 8.8
 CX 35.8
 CY 2.8
 F1 11.8
 F2 1.8
 WZ 98.8
 SE 1.8
 1.8

PIN-2(a)

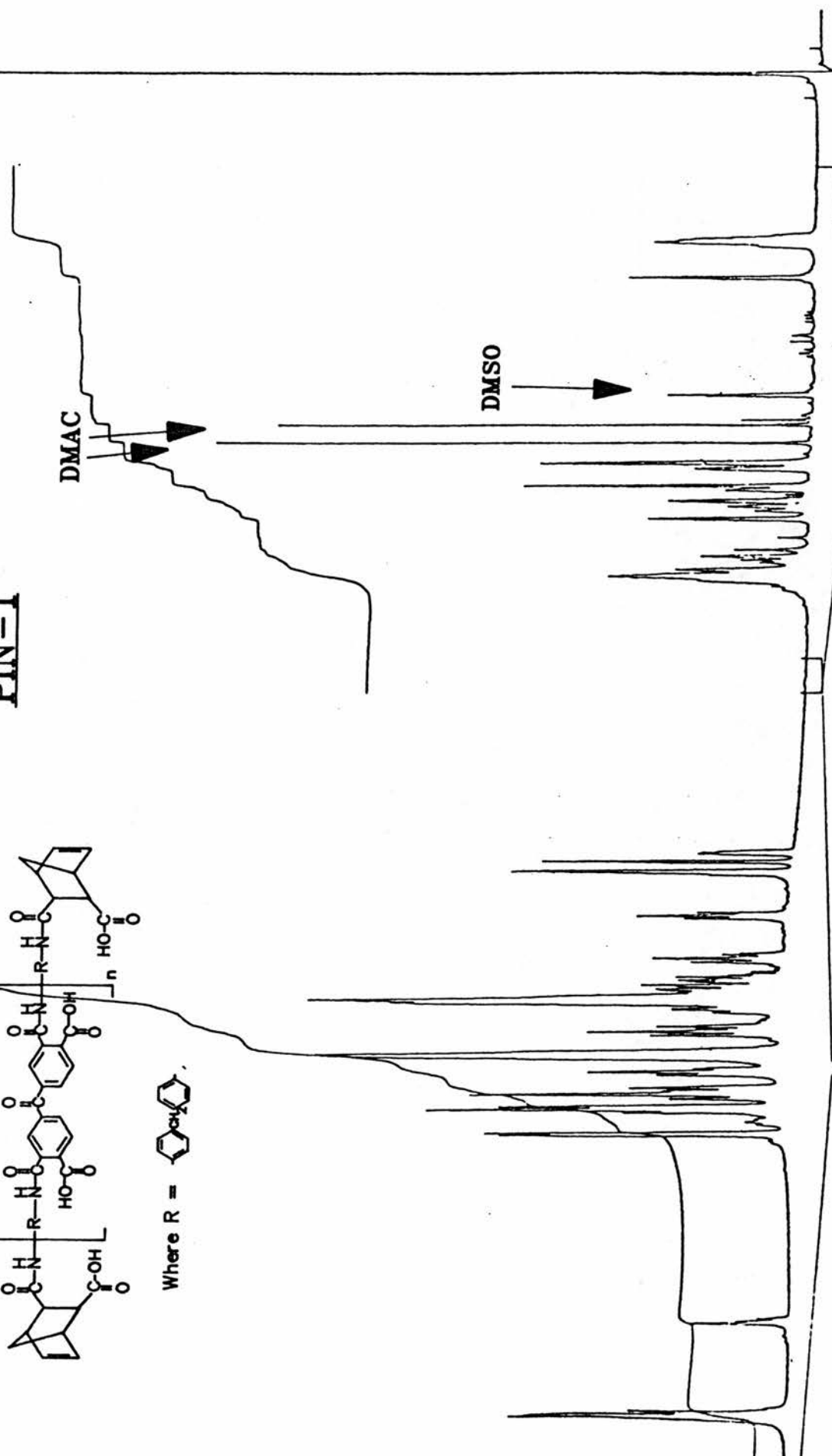


MS	303.1
SI	1.0
DI	63.2
SI	2.63
TD	32.63
SV	125.2
HL	125.2
PW	2.5
RD	1.5
R2	4.0
R3	10
MS	43
TE	315
FA	51.0
OZ	5.0
DF	65.0
LB	0.0
CP	0.0
CT	30.0
CT	30.0
F1	11.5
F2	11.5
PE	11.5
SP	1.5



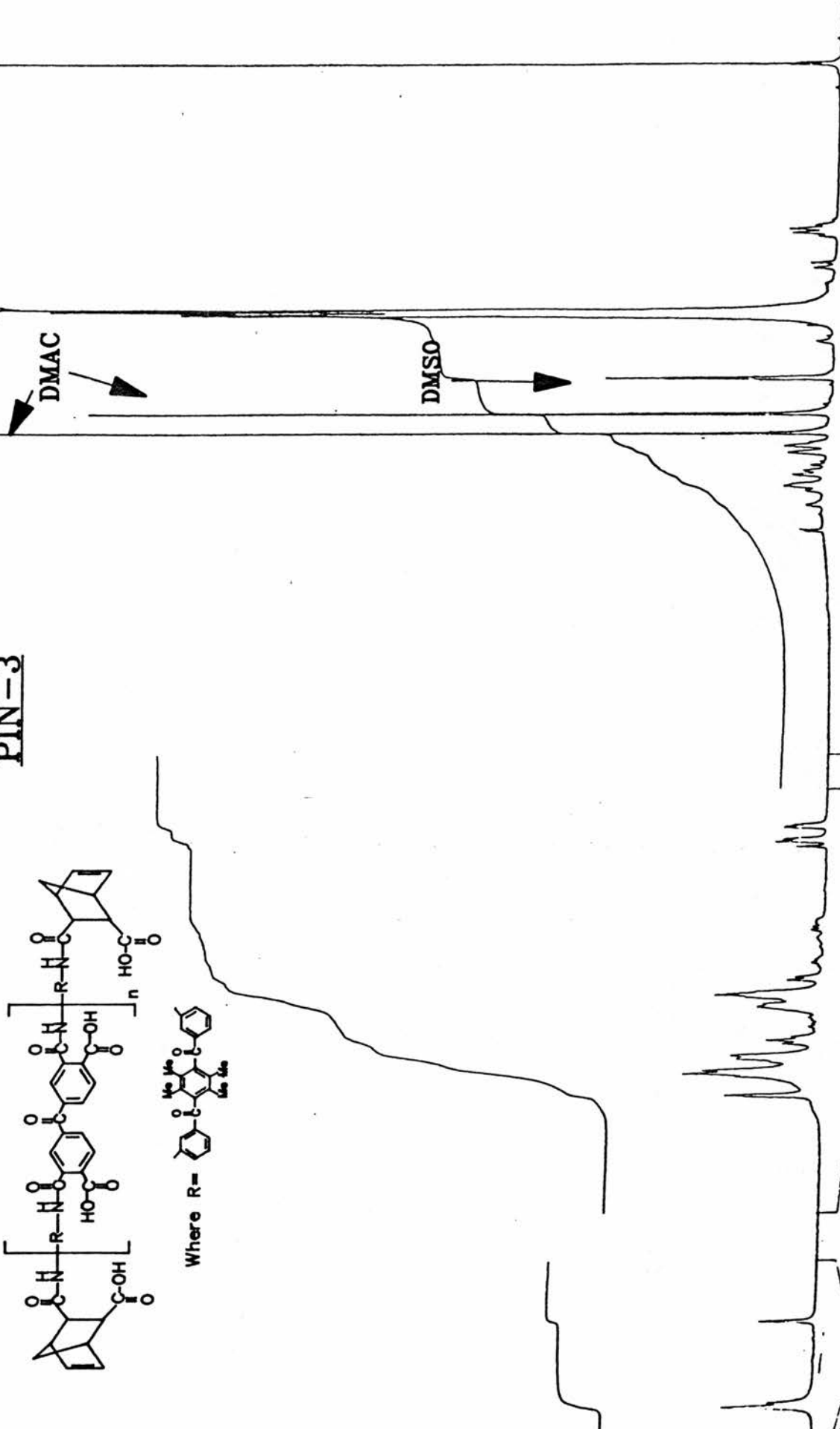
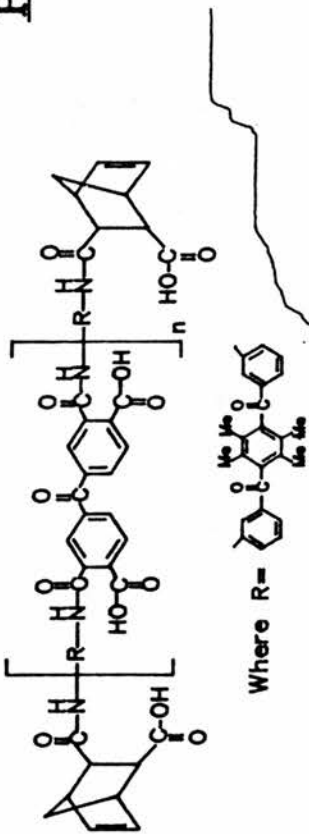
Where R = C1=CC=C(C=C1)C2=CC=CC=C2

PIN-1



SF 300.135
 ST 100.0
 SI 6534.241
 TO 32768
 SW 4065.041
 HZ/PT 220
 PW 2.5
 RD 1.500
 RC 2.03A
 RG 10
 NS 14
 TE 3.3
 FM 5102
 OZ 3202.000
 OP 63L PC
 LB 0.0
 GB 0.0
 CY 50.000
 CF 10.000
 F2 10.000
 HZ 10.000
 PC 10.000
 SF 300.135

PIN-3



SF 320.135
 SY 122.3
 OI 4334.241
 SI 32269
 TD 32265
 SV 4265.241
 HZ/PI .248
 PW 2.5
 PD 1.502
 PC 4.831
 NS 22
 TE 313
 FW 5.22
 OZ 3220.20
 DF 55. PD
 LB 0.0
 CB 0.2
 CY 0.2
 F1 11.00
 F2 0.00
 F3 0.50
 F4 0.00
 SB 0.00

APPENDIX 3

Figure C - Solid state ^{13}C NMR of
 1,4-bis(4-amino)-2,3,5,6-tetramethyl-
 benzene

